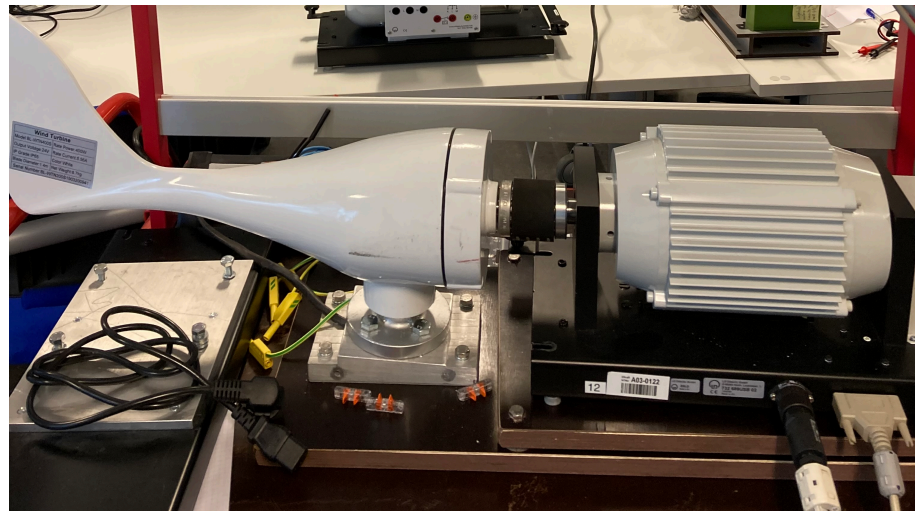


Henrik Lund Finsås
Torbjørn Løvik Mjåtveit

Wind power for cooking

Small scale wind power to heat storage

Master's thesis in Energy and environmental engineering
Supervisor: Ole Jørgen Nydal
Co-supervisor: Mulu Bayray Kahsay
June 2023



Henrik Lund Finsås
Torbjørn Løvik Mjåtveit

Wind power for cooking

Small scale wind power to heat storage

Master's thesis in Energy and environmental engineering
Supervisor: Ole Jørgen Nydal
Co-supervisor: Mulu Bayray Kahsay
June 2023

Norwegian University of Science and Technology
Faculty of Engineering
Department of Energy and Process Engineering



Preface

This master thesis was written as part of an ongoing collaboration between the Norwegian University of Science and Technology (NTNU) and University of Dar es Salaam (UDSM). The project is one of several included in the Norpart project, which has been ongoing for a few years. The thesis is written as a collaboration between two students from Energy and Environmental studies at NTNU, spring of 2023.

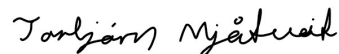
We would first like to thank our supervisor professor Ole Jørgen Nydal, and our co-supervisor, associate professor Mulu Bayray Kahsay for excellent help during this whole period. Their support and innovative thinking have been of great value for our work, as well as their ever encouraging ideas to take us further. A big thanks must also be given Stein Kristian Skånøy, Paul Svendsen and Marius Østnor Døllner for great help with the setup and lab work at the Thermal laboratory at NTNU. During the semester, we have been lucky enough to be accompanied by four students from UDSM, all in which have been a great pleasure to get to know. Of these students, a special thanks to Seleman Mayanjo, who has worked alongside us this whole time doing similar research for his own thesis, for always staying positive and motivative, and always looking for new ideas and possibilities.

Lastly, we must direct a huge thanks to Trond Leiv Toftevaag, dosent Emeritus from the institute for electrical energy. We are grateful for his dedication and belief in our abilities. He has from the very beginning shown great interest in our work, lecturing us on relevant topics, and guided us on the experimental work.

As a part of the project, we were given the opportunity to visit Tanzania and UDSM during the semester with three fellow students, in which we are very grateful. The trip offered visits to both universities and a hydro power plant, in addition to befriending several of the students and professors from UDSM, whom we will remember for their hospitality and support whilst there.



Henrik Lund Finsås
Trondheim, june 11, 2023



Torbjørn Mjåtveit
Trondheim, june 11, 2023

Abstract

Tanzania has experienced one of the fastest growing access rates to electricity in Sub-Saharan countries for the past decade, with access increasing from 7% to 37.7% between 2011 and 2020. Although electricity access in urban areas has reached 73.2% in recent years, only 24.5% in rural areas have access to electricity in their daily life. This causes challenges and health hazards, as charcoal and wood are used for daily activities such as cooking. The government of Tanzania have set a goal by 2030 to achieve electricity access to the entire county, 75% of which through national and mini-grids, and the remaining 25% from off-grid solutions.

As a step towards this goal, this project aims to offer an off-grid hybrid system, combining wind and solar power for both electricity production and cooking. By the use of a controller, diversion mode can be achieved, both charging a battery for electrical devices, and diverting excess current to a dump load working as a heat storage. This is done to demonstrate thermal storage of small scale wind power, both direct and indirect, via the use of batteries.

Using a small scale wind turbine, these concepts on wind to heat have been demonstrated to see how an off-grid solution based on wind power can be used for cooking. Originally, the turbine was placed at the roof of the Thermal laboratory at NTNU, but due to poor and intermittent wind conditions it was dismantled. Further testing were thus conducted in the lab, where the turbine was driven by an asynchronous machine, where torque and RPM could be set manually. Temperatures for heat storage are desired to reach 220°C, which would be sufficient for boiling water and such, but for the purpose of demonstrating heating using a wind turbine, temperatures were stopped at 100°C for the relevant tests. The dump load used is a small, insulated cylinder filled with Duratherm 630 oil, used mainly for demonstrative purposes.

It was found from a series of testing that with a power of up to 200W from the wind turbine a resistance of around 6Ω for the dump load was optimal for maximum power to the heat storage. These experiments were performed with the use of a Tristar controller and a small heat storage. From demonstration of direct heating from wind it was found that an optimal resistance would be between 5 and 20Ω, depending on incoming wind speed. By having a system automatically switching the resistance configuration depending on the torque shaft on the turbine, nearly optimal power could be achieved for the dump load in most operation conditions.

For a final implementation of the system as an off-grid solution, a proper controller is of great importance, enabling both wind and solar power as energy sources, as well as protecting the turbine itself and possible batteries. An MPPT controller is a reliable solution for this, optimizing the performance of a wind turbine. Several controllers offer this, but don't necessarily offer the same functioning for the PV panels, so this must be kept in mind. A buck-boost converter can also be added in the system, enabling a stable output voltage with a large range of input voltages. This would be especially practical for

the wind, as this is a more fluctuating and intermittent energy source than solar power. For the time being, however, a Tristar controller is currently used in the setup, allowing for both battery charging and heating of a dump load.

Sammendrag

Tilgangen på elektrisitet i Tanzania har det siste tiåret vært av de raskest voksende i subsahariske Afrika, med en økende tilgang fra 7% til 37.7% mellom 2011 og 2020. Selv om tilgangen i urbane områder har nådd 73.2%, har kun 24.5% tilgang utenom storbyene. Dette skaper utfordringer og helserisikoer for daglige gjøremål, ettersom det i stor grad benyttes kull og vedfyring til blant annet matlaging. Regjeringen i landet har satt et mål om at det innen 2030 skal være tilgang på elektrisitet for hele befolkningen, hvorav 75% skal være fra landets strømnnett eller småskala strømnnett, og de resterende 25% fra off-grid løsninger.

Som et steg nærmere dette målet har dette prosjektet tatt for seg en hybrid off-grid løsning, som kombinerer sol- og vindkraft til både elektrisitetsproduksjon og matlaging. Ved bruk av en kontroller kan energien både gå til lading av et batteri, samt tillate overskuddsstrøm å videreføres til et varmelager til bruk for matlaging. Dette gjøres for å demonstrere termisk lagring av småskala vindkraft, både direkte og gjennom elektrisitet ved bruk av batterier.

Ved å bruke en småskala vindturbin i prosjektet har disse konseptene blitt demonstrert for å se hvordan en slik off-grid løsning kan anvendes for varmelagring. Opprinnelig var turbinen plassert på taket av varmetekniske laboratorier ved NTNU, men grunnet dårlige og intermitterende vindforhold ble den demontert. Videre testing ble dermed gjennomført i laboratoriet ved varmeteknisk, hvor turbinen ble drevet ved bruk av en asynkronmaskin, hvor dreiemoment og rotasjonshastighet kunne bli manuelt justert. Ønsket temperatur for varmelageret ligger omkring 220°C, som vil kunne være tilstrekkelig for matlaging, men temperaturer ble stoppet ved 100°C under testing for å demonstrere konseptet. Selve varmelageret er en liten, isolert sylinder fylt med Duratherm 630 olje, hovedsakelig brukt for demonstrasjon.

Det ble funnet fra en rekke tester at ved en effekt på 200W ut fra generatoren, ville en motstand på 6Ω gi optimal effekt til varmelageret. Disse forsøkene ble gjennomført ved bruk av en Tristar-kontroller og et lite varmelager. Ved forsøk gjort på direkte vind til varme ble det observert at en optimal motstand ville ligge mellom 5 og 20Ω, avhengig av vindhastighet. Ved å implementere et system som automatisk endrer motstanden blant flere ulike settinger basert på dreiemomentet på turbinen kan nær optimal effekt oppnås over varmelageret i de fleste driftsscenarioer.

Contents

Preface	i
Abstract	ii
Sammendrag	iv
List of symbols	vii
List of abbreviations	viii
List of figures	ix
List of tables	x
1 Introduction	1
1.1 Citation	2
1.2 Background	2
1.3 Objective and scope	3
2 Theory	5
2.1 Synchronous generator	5
2.2 Permanent magnet synchronous generator	6
2.2.1 Losses in PMSG	7
2.2.2 Rectifier	8
2.3 One-dimensional momentum theory	9
2.4 Small scale wind turbine	10
2.5 Wind turbine controllers	11
2.5.1 Maximum power point tracking (MPPT)	12
2.5.2 Battery charge controller	14
2.5.3 Dump load dimensioning and PWM diversion charging	14
2.6 Energy storage	15
2.6.1 Battery storage	15
2.6.2 Thermal energy storage (TES)	16
3 Literature review	18
3.1 Direct conversion of wind energy to heat	18
3.2 Conversion of wind energy to heat through electricity	22
4 Experimental setup	24
4.1 Data processing	34
5 Experimental work	35
5.1 Preliminary testing (1)	36
5.2 Regulator battery charging (2)	38
5.3 Wind to dump load (3)	41
5.4 Diversion with DC source	45
5.5 Diversion testing with wind turbine	48
5.6 Sources of error	55
6 Conclusion	57
7 Further work	59

References	60
A Python code	I
B Duratherm 630 info brochure	II
C Tristar controller operation manual	VI
D Power meter manual	XLV

List of symbols

Symbol	Description
a	Axial induction factor [-]
c	Specific heat capacity [$\frac{J}{kg \cdot K}$]
C_P	Power coefficient [-]
E_A	Induced voltage [V]
f_{el}	Electrical frequency [s^{-1}]
f_m	Mechanical frequency [s^{-1}]
I_A	Armature current [A]
n	Rotational speed [RPM]
P	Number of poles [-]
Q	Thermal energy [J]
R_A	Stator resistance [Ω]
R_L	External load [Ω]
T	Temperature [$^{\circ}C$]
T_0	Initial temperature [$^{\circ}C$]
u_w	Wake velocity [m/s]
u_{∞}	Free stream velocity [m/s]
V_{ϕ}	Terminal voltage [V]
X_S	Stator reactance [Ω]
η	Efficiency [-]
λ_{opt}	Optimal torque [Nm]
ω_m	Mechanical rotational speed [rad/s]
ω_{el}	Electrical rotational speed [rad/s]
ϕ_F	Magnetic rotor flux [Wb]
τ_{shaft}	Shaft torque [Nm]
θ	Power factor [-]

List of abbreviations

AC	Alternating current
DC	Direct current
FESS	Flywheel energy storage system
HAWT	Horizontal axis wind turbine
HTF	Heat transfer fluid
LPG	Liquid petroleum gas
MPPT	Maximum power point tracking
OECD	Organization for Economic Co-operation and Development
P&B	Perturbation and observation
PMSG	Permanent magnet synchronous generator
PV	Photovoltaic
PWM	Pulse with modulation
RMS	Root mean square
RPM	Revolutions per minute
SOC	State of charge
TES	Thermal energy storage
TSR	Tip speed ratio
VAWT	Vertical axis wind turbine

List of figures

- 1.1 Schematic overview of small scale wind turbine system with diversion of excess power to heat storage. 4
- 2.1 Equivalent circuit per phase for round rotor PMSG. Figure based on [12]. . . 5
- 2.2 The per phase phasor diagram of synchronous generator with resistive load. 5
- 2.3 Electrical system design for the setup used in this project. 6
- 2.4 Illustration of power flowing through a three phase AC generator. Figure taken from [11]. 8
- 2.5 Diodes used for rectifying a three-phase AC supply. Figure taken from [24]. 9
- 2.6 Illustration of phase displacement for a three-phase waveform. Figure taken from [24]. 9
- 2.7 Ideal power curve for wind turbines.[31] 12
- 2.8 Wind turbine output power and torque characteristics with P&O MPPT process[31] 13
- 2.9 Torque-Generator speed curve for different wind speeds[31] 13
- 2.10 Pulse width modulation signal[38] 15
- 3.1 Schematic representation of proposed system by Chakirov and Vagapov. Figure taken from [47]. 19
- 3.2 Results from a 50 hour test period by Chakirov and Vagapov. Figures taken from [47]. 19
- 3.3 Structure of a magnetic converter in the axial (A) and radial (B) direction. Figure taken from [49]. 20
- 3.4 Efficiency at different RPM for a thermal converter. Figure taken from [49]. 20
- 3.5 Hybrid solar and wind solution combining heat and power. Figure taken from [61]. 23
- 4.1 Experimental setup used for testing. The numbering for the devices are explained in table 4.1 25
- 4.2 RPM controlled asynchronous machine with control unit. 26
- 4.3 Original location of the wind turbine on the roof at NTNU. 27
- 4.4 Wind turbine specifications. 27
- 4.5 Digital power meter used for reading values for current, voltage and power. 27
- 4.6 Electronic load used for discharging the batteries. Figure taken from [66]. . 28
- 4.7 Original wind turbine regulator. 29
- 4.8 Three phase rectifier bridge with cooling ribs. 30
- 4.9 Original 12V batteries used for electrical storage in the system. 30
- 4.10 New 12V batteries used for electrical storage in the system. 30
- 4.11 The Tristar controller used for diversion mode. 31
- 4.12 Three-phased rheostat used for varying the resistance in the system circuit. 32
- 4.13 Three variable resistances used for demonstrating wind to heat. 32
- 4.14 DC bench power supply used to test the system in diversion mode. 33
- 4.15 The dump load used for diversion during experimental work. 34
- 5.1 Circuit board for the digital power meter for a 3-phase, 3-wire connection. 37
- 5.2 Circuit board for the digital power meter for a 3-phase, 4-wire connection. 37
- 5.3 Idle test of the generator for the three different phases. 38

5.4	Power to battery with original wind turbine controller.	39
5.5	Depiction of battery power, mechanical power from the wind and power output from the generator against torque.	40
5.6	Phase current and DC power from the turbine, while placed on the roof.	41
5.7	Power to dump load with three different resistances, with the use of original controller	42
5.8	Power directly to dump load with different dump load resistances and RPM.	43
5.9	Power directly to dump load with different dump load resistances and torque.	44
5.10	Comparison of diversion with DC source, using old batteries, with diversion voltage set to 27.6V. For plots marked '*', diversion voltage was set to 28.8V. Power plotted against current to the batteries.	47
5.11	Diversion test with DC source with new batteries, with diversion voltage set to 27.6V. Power plotted against current to the batteries.	48
5.12	Diversion test with new batteries with and without the turbine controller, plotted against torque on the wind turbine. Power marked with * are measurements done without the turbine controller.	49
5.13	Temperature increase and power to dump load over time at 2Ω	50
5.14	Temperature increase and power to dump load over time at 6Ω . Power is plotted for currents both measured by Tristar logging program and the actual current measured by the Fluke clamp meter.	51
5.15	Diversion test with variable resistance and torque	53
5.16	Load and battery voltage plotted against duty cycle.	54
5.17	Load voltage and duty cycle increase towards battery voltage over time.	54

List of tables

1.1	Modified or recited sections [7]	2
2.1	Overview of wind turbine sizes with respective ratings. Adapted from [30]	11
4.1	Serial and identification number for equipment used in experimental setup. Numbering according to figure 4.1.	24
5.1	Overview of the different tests conducted in the lab.	35
5.2	Tabular depiction of equipment used in the different experiments.	35

1 Introduction

As the global community strives to mitigate its carbon dioxide emissions, Sub-Saharan countries exhibit relatively low CO₂-emissions in comparison. Nonetheless, in the approaching decades, these nations are expected to undergo a profound overhaul of their infrastructure. In Tanzania, access to electricity is limited, with only 39.9% of the population having access as of 2020[1]. Multiconsult has completed an energy transition report for Tanzania, which sets a 2050 goal for the expansion of the electricity grid through the utilization of renewable energy sources[2]. To achieve a green future it is essential that third world countries have a sustainable energy transition.

Due to the absence of electricity in Tanzania, routine activities such as cooking is mainly done by fire, which makes it more laborious and time consuming. According to the Rural Energy Agency, a vast majority (90%) of Tanzania's primary energy consumption in 2020 was derived from biomass, leading to widespread deforestation[3]. Deforestation, which accounts for about 10% of global warming, poses a severe threat to the natural habitat and wildlife while also disrupting rainfall patterns. In Tanzania, reforestation efforts after cutting down forests have been inadequate, with only a quarter of the cleared forest being replanted[4].

In Tanzania, biomass serves as the primary source of energy for cooking. As per the Rural Energy Agency's 2020 report, firewood accounted for 65% of households cooking fuel, while coal represented 26%. Indoor burning of these fuels can pose significant health risks if proper ventilation is not ensured. The World Health Organization reported 3.2 million deaths in 2020 due to indoor cooking, with women and children bearing the brunt of these hazards as they are primarily responsible for such tasks. 7.4% of these casualties are from children under the age of five[5]. Other energy sources are also used for cooking, like liquid petroleum gas (LPG) and electricity, but these only constitute 5.1% and 3%, respectively[3].

Given the poor state of the electrical grid infrastructure in Tanzania, off-grid solutions based on renewable energy sources, such as solar and wind power can be a viable alternative to ensure energy for clean cooking. In recent years, there has been a notable decline in the cost of photovoltaic (PV) panels, making them more cost-effective and efficient than in previous decades. Specifically, between 2010 and 2020, PV prices experienced a tenfold reduction[6]. Nonetheless, solar energy does possess certain limitations, including its dependence on daylight and lower efficiency under cloudy conditions. However, the integration of both solar and wind technologies can be a promising approach to generate off-grid energy in Tanzania. Since both solar and wind energy can be highly intermittent there is a need for storage options. By storing energy as heat, it can be utilized later for cooking purposes, thereby mitigating the issue of clean cooking in the region.

1.1 Citation

This thesis is a continuation of the project work ”Small scale wind power to heat storage” by Finsås & Mjåtveit, and accordingly, parts of the thesis will be reused and modified for academic purposes.[7] Parts that have been reused or modified are listed in table 1.1.

Section	Modification
1	Modified
1.2	Minor modifications
1.3	Modified
2.2.2	larger modifications
2.4	Modified
2.6.2	Minor modifications
3	Modified

Table 1.1: *Modified or recited sections [7]*

1.2 Background

The Norwegian Agency for Development Cooperation (NORAD) is primarily responsible for distributing the Norwegian development aid funds. In pursuit of this goal, the agency launched the Norhed program in 2012, which prioritizes development in research and higher education. One of the projects is a cooperation between NTNU and universities in six Sub-Saharan countries. The focus of the research in this project includes utilization of power generated by solar and wind sources, which is stored as heat for later use for cooking. Over the years, various projects and prototypes have been developed and refined to improve heat storage capabilities. The idea is to implement these cookers for cafeterias in for example schools and hospitals or in small communities, so that cheap and clean energy can be used for cooking.

The three tank system is one of the solar cookers previously built. This system has one tank for hot oil, one for cold oil and one for used oil. Different valves controls the flow of oil in this system. Even simpler systems have been built without the need for valves to control the flow of oil. All consisting of one or more tanks used for heat storage with oil as storage medium, and a cooker. One of them is the single tank system where the cooker and the oil storage is in one single unit. To separate hot and cold oil, such that the cooker can be used both during charge and discharge, a funnel is installed. Even simpler versions of this system have been built previously, but challenges were encountered with cooking during charging and discharging of the thermal storage. One of the final prototypes that has been built is the two tank system. This cooker has shown promising results and is planned to be implemented in Africa. The previous versions of the cooking device has been tested with solar power but none has been tested with wind power.[8, 9]

In the spring of 2022, a wind turbine was mounted at the rooftop above the thermal laboratory at NTNU, and connected to batteries in the lab. A turbine controller was

installed to regulate the wind turbine and prevent it from overcharging the batteries. Wind conditions and power production from the wind turbine were measured and logged during the autumn of 2022 as a preliminary project to this master thesis. This concluded in too turbulent flow at the roof and that the wind conditions was too intermittent to perform experiments. This resulted in dismantling of the wind turbine and that the rest of the experiments were decided to be carried out at the lab.

1.3 Objective and scope

With solar power only being available during the day, wind power can be implemented alongside solar power to secure a robust energy flow for off-grid solutions. The first task of this master thesis is to test a commercial small scale wind turbine at EPT, using a few different setups. This includes diversion mode, where power is diverted to a thermal energy storage when the batteries are fully charged, as illustrated in figure 1.1. The wind turbine will also be tested with the heat storage directly connected without the use of batteries. During testing an adjustable resistance is used as the "heat storage" for simplification. The second part of this master thesis is to explore methods for wind to heat solutions both direct mechanically or via electricity.

1. Experimental testing of a commercial small scale wind turbine to heat storage
2. Literature review on methods for wind to heat solutions (mechanical and electrical)

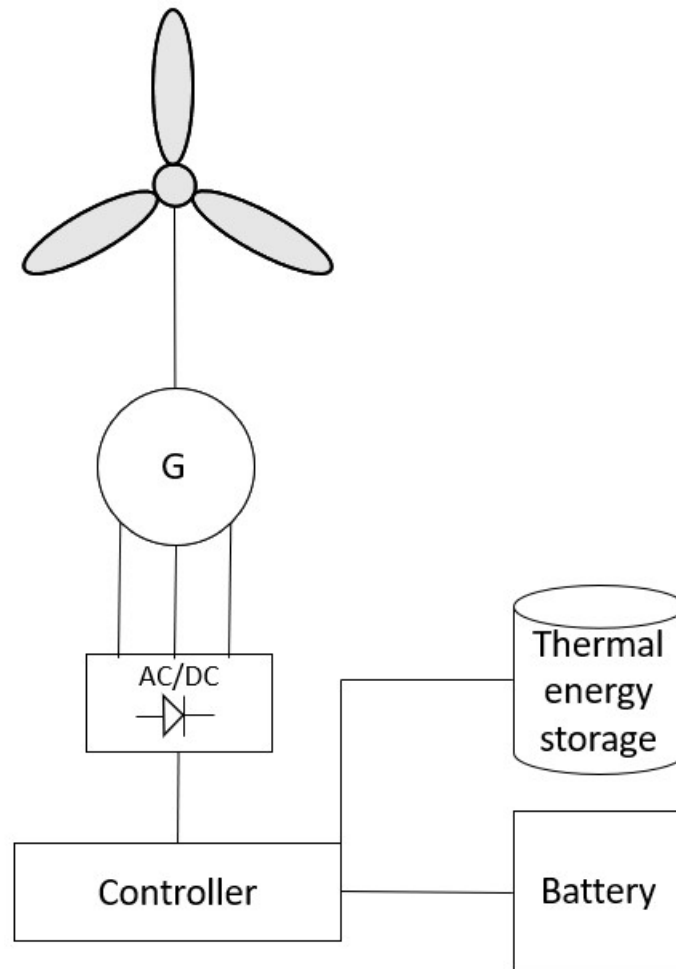


Figure 1.1: *Schematic overview of small scale wind turbine system with diversion of excess power to heat storage.*

PV systems to heat storage are already designed and tested. This master thesis will be based upon wind energy to heat storage, which can be implemented together with solar systems as a hybrid solution. Solar power can only be produced during the day, but wind power can be available both day and night. For charging of a thermal based storage used for cooking, a hybrid solution can therefore be appropriate.

2 Theory

In this chapter essential knowledge of the power extraction from the wind, general electrical engineering theory and energy storage are included to give an introduction to the topic at hand.

2.1 Synchronous generator

To represent a PMSG, an equivalent circuit can be applied per phase, as shown in figure 2.1. ω_m is the mechanical rotational speed of the permanent magnet, and ϕ represents the magnetic flux of the rotor. The different parameters in the circuit can be expressed by equation 2.1. E_A and V_ϕ are induced voltage and terminal voltage, respectively. R_A and X_S represents the resistance and reactance of the stator, while I_A is the armature current flowing through the circuit into the load. If an external load, R_L , is connected between the terminals, the current is expressed based on the geometric of figure 2.2, given that V_ϕ is the product of R_L and I_A , and that the power factor, θ , is 1.[10, 11]

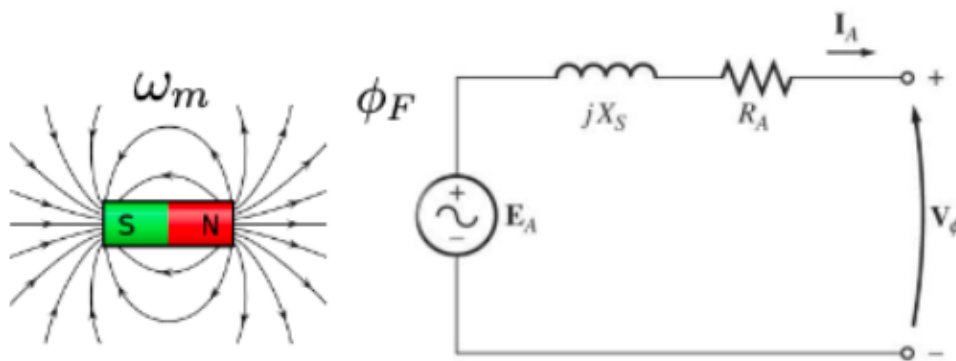


Figure 2.1: Equivalent circuit per phase for round rotor PMSG. Figure based on [12].

$$\overline{E_A} = R_L \overline{I_A} + (R_A + jX_S) \overline{I_A} \Rightarrow |\overline{I_A}| = \frac{|\overline{E_A}|}{\sqrt{(R_A + R_L)^2 + (X_S)^2}} \quad (2.1)$$

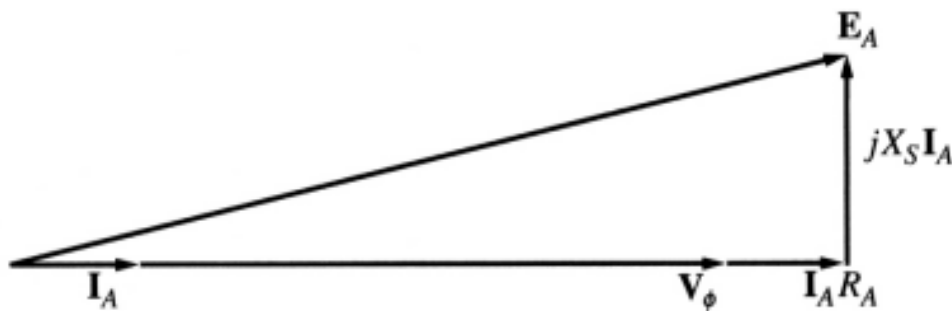


Figure 2.2: The per phase phasor diagram of synchronous generator with resistive load.

Similarly, the reactance, X_S , of the stator can be found from the geometry of figure 2.2, expressed as in equation 2.2. The phase voltage is measured at one of the three phases, while the induced voltage, E_A , is measured during no-load operation at different rotational speeds.[10].

$$X_S = \sqrt{\frac{E_A^2 - (V_\phi + I_a R_a)^2}{I_a^2}} \quad (2.2)$$

The internal generated voltage of the stator can also be expressed by equation 2.3, where K is a constant given by the construction of the machine, ϕ_F is the rotor flux, and ω_m is the rotational speed in rad/s.[11]

$$E_A = K\phi_F\omega_m \quad (2.3)$$

2.2 Permanent magnet synchronous generator

The working principle behind the permanent magnet synchronous generator(PMSG) is based upon two parts, a rotor and a stator. The rotor is a rotating part consisting of a permanent magnet, driven by an external propulsion unit. Through the concept of magnetic induction, the rotor inside the stator will generate a magnetic field, inducing a voltage in the stator windings. The stator, being the stationary part, will have sets of windings deciding the amount of phases in the generator. The electric system design for the generator for this project is shown in figure 2.3.

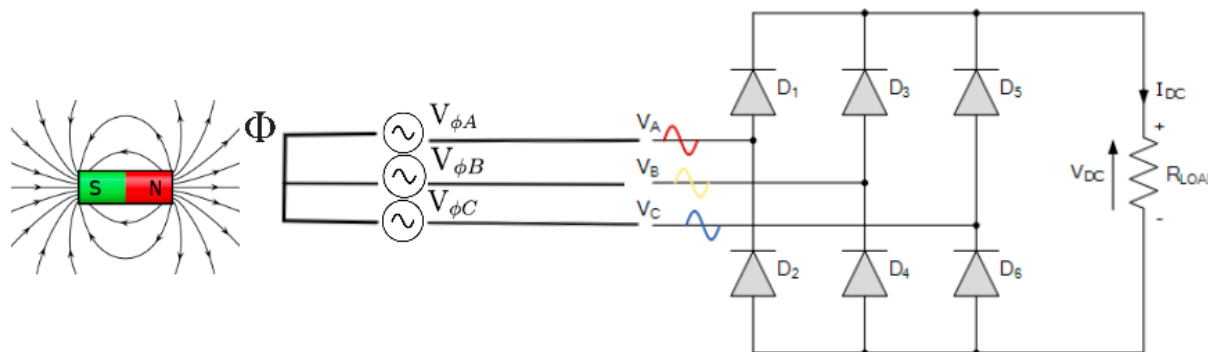


Figure 2.3: *Electrical system design for the setup used in this project.*

The generator itself can be either single-phase or poly-phased, where a three-phased construction is commonly used for a poly-phased generator. In a synchronous generator sine wave alternating current (AC) is produced. The generator has to be designed such that voltage and current waves are produced with high accuracy, avoiding ripples in the sine waves. The number of poles in a synchronous generator, P , is related to the mechanical rotational speed, n , and the electrical frequency, f_{el} , by equation 2.4.[10, 13, 14]

$$P = \frac{120f_{el}}{n} \quad (2.4)$$

In modern small scale wind turbines a PMSG is most common. In such generators a permanent magnet, a so called ferromagnet, is used, which has a magnetic field around it given as an intensive property. Typical ferromagnets are nickel, cobalt and iron. Such magnetic materials are mounted on the rotor body surface in the generator, producing electricity in the stator winding as the shaft rotates. As reliable as they are, permanent magnets do not offer any way of controlling the output voltage, so sudden variations in voltage must be tolerated by the system. Permanent magnets are exposed by the risk of demagnetization, in which magnetic properties are reduced or removed from a magnet. Such an occurrence can happen with increased temperatures, physical damage or interference with other magnetic fields.[13–15]

The electrical frequency has a direct influence on the reactance, according to equation 2.5, where ω_{el} is electrical rotational speed in rad/s and L is the inductance, measured in Henry. The reactance in a circuit is present only when the current is alternating, and for short periods in direct current (DC) at the turn of a switch.[16, 17]

$$X = 2\pi f_{el}L = \omega_{el}L \quad (2.5)$$

Frequency can be separated into electrical and mechanical frequency. The mechanical frequency, f_m , is found from the rotational speed and can be calculated from equation 2.6 with the factor 60 being the number of seconds per minute, as the rotational speed is given in RPM.

$$f_m = n/60 \quad (2.6)$$

Electrical frequency on the other hand is measured as the rate of oscillation in the current and voltage. The relationship between mechanical and electrical rotational speed can be expressed by equation 2.7, where ω_m is given from equation 2.8.[16, 17]

$$\omega_{el} = \frac{P}{2}\omega_m \quad (2.7)$$

$$\omega_m = \frac{2\pi n}{60} \quad (2.8)$$

2.2.1 Losses in PMSG

The power flow for a three phase AC generator is shown in figure 2.4, and depicts the different losses in the machine. The power, P_{in} , supplied to the generator from the turbine, is given by equation 2.9, where τ_{app} is the apparent shaft torque. The losses can be grouped in four categories; mechanical losses, core losses, copper losses and stray losses. Mechanical losses include frictional and windage losses. Moving parts such as the bearings make up the frictional losses, while windage losses is due to ventilation in the generator. The core losses consists of hysteresis loss and eddy current loss, both related to the changing magnetic field, and overcoming magnetic friction in the iron parts in the

core of the generator. Stray losses are those related either to an non-uniform field flux distribution in the machine, or by wear and tear of the slip rings.[18, 19]

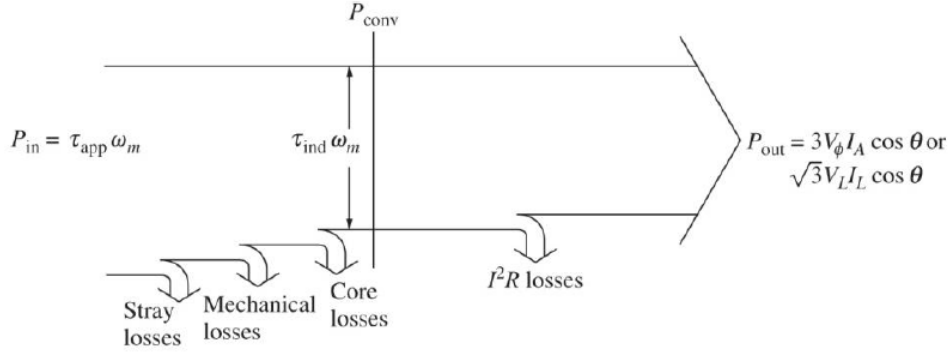


Figure 2.4: Illustration of power flowing through a three phase AC generator. Figure taken from [11].

$$P_{in} = \tau_{app} \omega_m \quad (2.9)$$

The wiring inside the turbine generator is commonly made out of copper, which will have a loss, P_{cu} . These losses are increasing with the current squared according to equation 2.10, where R_{Cu} is the resistance of the copper winding. In addition to iron losses, these contribute to most of the losses in an AC machine, though frictional forces and ventilation also will have some minor losses. Additionally, copper have a temperature coefficient of 0.00393, meaning the resistance of copper increases by 0.393% with 1°C temperature increase.[20–22].

$$P_{Cu} = R_{Cu} I^2 \quad (2.10)$$

Most of these losses will be converted into heat, further decreasing the efficiency of the generator. The power output, P_{out} , from the generator is expressed by equation 2.11, where $\cos \theta$ is the previously mentioned power factor between V_{ϕ} and I_A . This will together with the total losses, from equation 2.12, give an overall percentage efficiency of the generator, given by equation 2.13.

$$P_{out} = 3V_{\phi} I_A \cos \theta \quad (2.11)$$

$$P_{losses} = P_{stray} + P_{mec} + P_{core} + P_{cu} \quad (2.12)$$

$$\eta = \frac{P_{out}}{P_{in}} 100\% = \frac{P_{out}}{P_{out} + P_{losses}} 100\% \quad (2.13)$$

2.2.2 Rectifier

The main task of a rectifier is to convert the current from AC to DC. This is done by utilizing one or more P-N junction diodes that allow the current to only flow in one

direction, hence being rectified. The design of a rectifier depends on the characteristics of the incoming current, such as whether it is single-phase or three-phase, and whether it has low or high voltage.[23]

The schematics of a three-phased rectifier is shown in figure 2.5. The figure clearly illustrates how voltages from three phases are rectified, producing a current, I_{DC} , with an output voltage V_{DC} . The phases are out of phase from each other with an electrical degree of 120° , corresponding to a phase rotation of $360^\circ/3$. This "rotation" is illustrated in figure 2.6.[24]

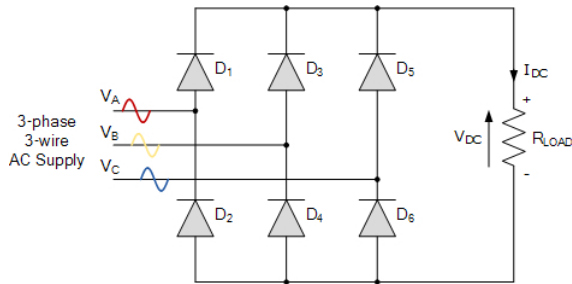


Figure 2.5: Diodes used for rectifying a three-phase AC supply. Figure taken from [24].

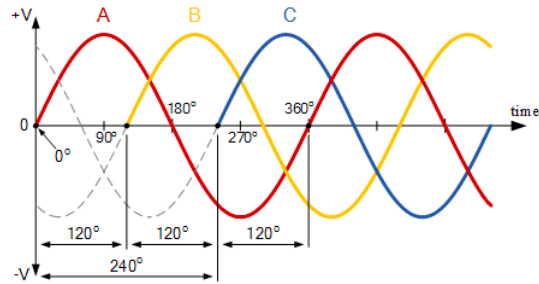


Figure 2.6: Illustration of phase displacement for a three-phase waveform. Figure taken from [24].

The quality of the output signal depends on the complexity of the rectifier.[23] A rectifier can for example be designed with a capacitor to smooth the output DC voltage, acting as a filter to reduce ripple but this is not necessary for a three phase bridge rectifier which only has about 4.2% ripple[25].

A bridge rectifier, which typically requires four diodes for single-phase or six diodes for three-phase rectification, is commonly used for rectifying AC signals. The rectified voltage V_{DC} out of a three phase bridge rectifier can be calculated using equation 2.14, where V_{LL} is the line-to-line voltage of the three-phase AC input.[26]

$$V_{DC} = 1.35V_{LL} \quad (2.14)$$

2.3 One-dimensional momentum theory

To understand how kinetic energy is extracted from the wind it is fundamental to understand the one-dimensional momentum theory. Firstly, there are some simplifications in this theory that need to be mentioned. It is assumed no skin friction and that maximum power is extracted from the wind. This is because the rotor is assumed to be an inviscid, ideal disc and incompressible and axisymmetric flow is assumed. Consider an incoming flow with a velocity u_∞ . In front of the rotor the velocity slows down to u_r . According to the Bernoulli principle, when the velocity of a fluid decreases, the pressure within the fluid must correspondingly increase. Downstream of the rotor in the wake, the velocity

decreases to u_w . How this flow develops both in front and in the wake of the rotor can be explained by equations 2.15 and 2.16, respectively.

$$P_0 + \frac{1}{2}\rho u_0^2 = p_r^+ + \frac{1}{2}\rho u_r^2 \quad (2.15)$$

$$P_r^- + \frac{1}{2}\rho u_r^2 = p_0 + \frac{1}{2}\rho u_w^2 \quad (2.16)$$

The total pressure difference ΔP can be derived from equations 2.15 and 2.16 to equation 2.17

$$\Delta P = \frac{1}{2}\rho(u_0^2 - u_w^2) \quad (2.17)$$

To find the velocity at the rotor plane, combining equation 2.17 with mass and momentum conservation leads to equation 2.18. The axial induction factor a is the ratio of the free stream velocity reduction, to the velocity at the rotor plane, shown in equation 2.19

$$u_r = \frac{1}{2}(u_0 + u_w) = (1 - a)u_0 \quad (2.18)$$

$$a = \frac{u_\infty - u_r}{u_\infty} \quad (2.19)$$

The axial induction factor is used to express the power coefficient, C_P , which is shown in equation 2.20. C_P is the ratio of the energy captured from the wind, to the actual kinetic energy in the wind.

$$C_P = 4a(1 - a)^2 \quad (2.20)$$

C_P is limited by a factor of 0.593, known as the Betz limit which is the upper limit for power extraction from the wind. Considering other losses like friction and wake losses C_P usually lays around 0.4 for a horizontal axis wind turbine (HAWT). C_P is used in the power equation showed in equation 2.21 which can be used to calculate the energy extracted from the wind. Where A is the swept area of the turbine blades and ρ is the density of air. The total power produced by a wind turbine is significantly influenced by the velocity of the incoming wind speed, being of cubic relation.[27]

$$P = \frac{1}{2}\rho A u_0^3 C_P \quad (2.21)$$

2.4 Small scale wind turbine

Wind turbines are devices that transform the kinetic energy in wind into mechanical energy using turbine blades. The primary function of these turbines is to capture the maximum amount of energy from the wind, with the specific design varying based on the intended application, location, and cost. The most common type is the three bladed HAWT. HAWTs function by converting the wind's energy into rotational energy due to lift force. This rotation powers a shaft connected to a generator, previously described in chapter 2.2.[28]

Wind turbines can also have a vertical axis (VAWT). VAWT blades move in the same direction as the incoming wind and are driven by a pressure differential causing it to spin.

The highest efficiency achievable for a VAWT is up to 37%. Even though the efficiency is lower than a HAWT there are some advantages to it. It is suitable in turbulent wind conditions as it can produce energy independent of wind direction.[28, 29]

Table 2.1 shows an overview of different wind turbine sizes and their respective power ratings. Small scale wind turbines are mostly used in off-grid solutions, and turbines in the commercial scale are almost always grid connected. The size of small scale wind turbines makes them more manageable to transport and mount. There are some distinctive differences on small scale and larger wind turbines. A large scale wind turbine has a yaw mechanism which directs the turbine against the wind. Wind turbines of smaller scale have a tail vane that controls the direction. Another difference is that the angle of the blades on larger wind turbines are usually controlled by a pitch regulation. This makes it easier for the turbine to spin at desired speed causing it to harvest more energy. These systems are complex and unnecessary for smaller wind turbines, which usually are regulated by a controller.[30]

Table 2.1: Overview of wind turbine sizes with respective ratings. Adapted from [30]

	Rotor diameter [m]	Power rating [kW]
Small scale	0.5-10	0.004-16
Small commercial	10-20	25-100
medium commercial	20-50	100-1000
large commercial	50-150	1000-10000

2.5 Wind turbine controllers

Wind turbine systems consist of controllers that regulate different parts of the system. This could either be regulation of power, regulation of a battery or diversion of excess energy to a dump load . A controller can be manufactured in one single unit taking care of all the aforementioned functionalities or as separated units. Regarding the wind turbine, the controller needs to not only take care of the power but also the durability. This can be explained by the use of the ideal power curve for a wind turbine figure 2.7. In region 1, up to V_{cut-in} , the energy production is at such a low level that the controller brakes the turbine. This is to protect the wind turbine and generator from unnecessary degradation. Above $V_{cut-out}$ the wind turbine should be stopped to prevent damage of system components due to too high rotational speeds. The generator is dimensioned with a maximum capacity corresponding to P_{rated} , and should not exceed this.[31]

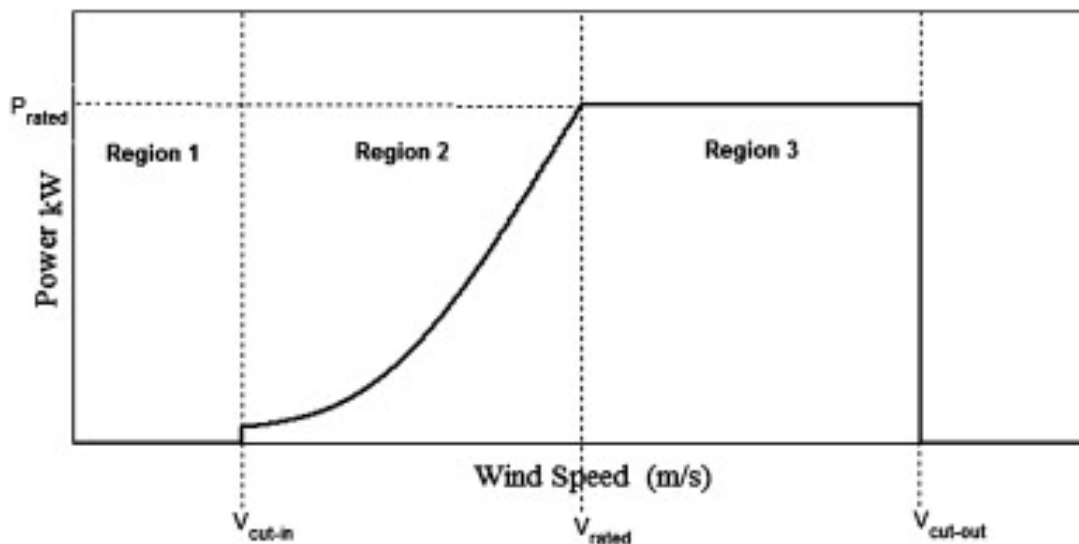


Figure 2.7: *Ideal power curve for wind turbines.*[31]

A boost-buck controller is such a device for regulating power in a wind turbine system, and can also be used for hybrid solutions in combination with PV panels. The controller, really working as a converter, can take in any voltage within a given range, and step it up or down, depending on the desired output voltage of the system. For an intermittent energy source such as wind power, this allows for a more stable power supply to both battery and dump load, as the voltage is held at a constant value.[32]

2.5.1 Maximum power point tracking (MPPT)

Small scale wind turbines are usually connected to a controller that regulates and optimizes the performance of the wind turbine system. As mentioned in chapter 2.4 larger wind turbines usually pitch the blades to ensure desired operation. Smaller wind turbines have a fixed blade position and must therefore be controlled in another way. An MPPT controller can ensure optimal power production for small scale wind turbines, where different MPPT algorithms are used. The optimal power production of a wind turbine follows the slope of region 2 in figure 2.7 and an MPPT controller is manufactured to follow this slope as closely as possible.[31]

MPPT systems are based either on or without the use of wind speed sensors. A sensor based MPPT system measures the incoming free stream velocity of the wind, usually by an anemometer. Since the anemometer is supposed to measure the undisturbed velocity it has to be placed at a certain distance from the wind turbine. If the placement of the wind turbine is in an area with fluctuating wind speeds this can become a challenge.[33] An MPPT method that require wind speed measurements is tip speed ratio (TSR) control. TSR is the ratio of the incoming wind speed and the rotational speed, at the tip of the blades and it usually has a value of 6-7. As mentioned the method is based on wind speed measurements, and the controller regulates the load on the turbine to achieve optimal TSR. It is a simple way to control the wind turbine where only the TSR needs to be known.[31]

Perturbation and observation (P&O) also known as Hill-climb searching method, uses mathematical optimization to find the local optimum point of a given function. Different functions for optimum power production are used, where the algorithms try to find the peak where the slope become zero. The P&O MPPT method is shown in figure 2.8, where the optimum power point iterative process is illustrated.[31][33]

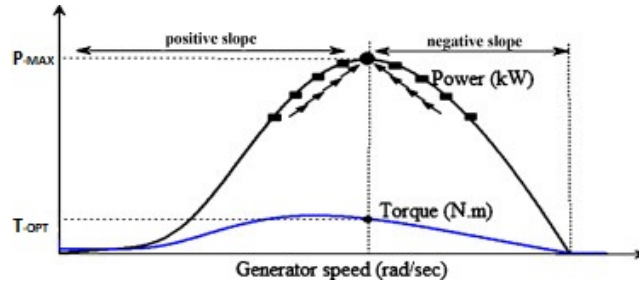


Figure 2.8: Wind turbine output power and torque characteristics with P&O MPPT process[31]

The P&O method is simple to implement on existing wind turbines since it requires no prior knowledge of the characteristics, but it is not as efficient as other MPPT methods. There is also no need for wind speed measurements.[31][33]

Optimal torque control is probably the most popular MPPT method for small scale wind turbines. Wind turbines have different optimal torque, λ_{opt} , that ensures optimal generator RPM at different wind speeds, as shown in figure 2.9. A torque controlled MPPT tries to find this optimal torque for each wind speed.

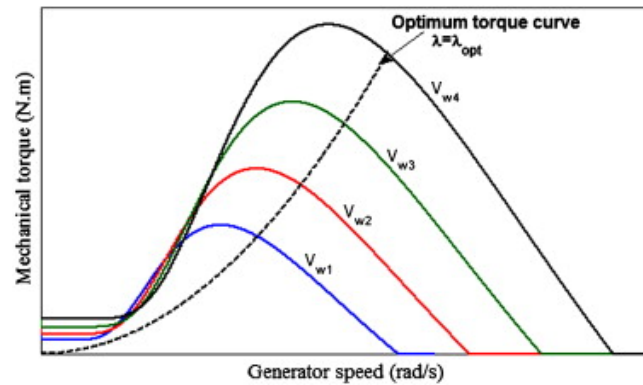


Figure 2.9: Torque-Generator speed curve for different wind speeds[31]

Due to its simplicity and effectivity, Abdullah et al.[31] found optimal torque control to be the best way of controlling wind turbine systems, based on simulation results found in the literature. It does however need prior knowledge of the wind turbine.

2.5.2 Battery charge controller

A charge controller is used to regulate the charging process of batteries. As mentioned in chapter 2.2 the current coming out of a PMSG is AC. The incoming current to a battery has to be DC and rectification is therefore necessary, which usually is done by implementing a rectifier bridge in the circuit. Furthermore, the charge controller needs to prevent the battery from overcharging or undercharging. This happens if the batteries reach a voltage too high or too low respectively. Both over- and undercharging reduce the life expectancy of the battery, additionally the battery should be charged regularly. If the batteries are left without charging for an extended period of time it can lead to sulfate crystals forming on the battery plate and stratification of the electrolyte, both reducing the lifetime of the battery. A charge controller can perform an equalization process to limit these issues. An equalization process stirs up the electrolyte by controlled overcharging of the battery. [34, 35]

The charge controller monitors the battery voltage at all times and has a set value where it cuts the power going to the batteries. For PV-controllers this is usually done by shortening the circuit. If the same procedure is used for a wind turbine when it is rotating, it can result in a high current spike that can damage both the controller and generator. The wind turbine should also not be disconnected and free wheel without any load attached, since the RPM of the wind turbine can become very high and damage both blades and generator. To address this issue a high ohmic resistor can be incorporated in the controller, or the power can be diverted to a dump load. The latter is most favorable since the energy won't be wasted.[34]

A battery goes through three stages during charge. This is done by the charge controller to ensure optimal charging. The first stage is called bulk charging and stands for approximately 80% of the charging. During this charging process batteries are fed with a constant current, causing the voltage to increase linearly. The next stage is called the absorption stage, where the current is regulated such that the battery has a constant voltage. In the absorption stage the battery is still charging, and as time passes it requires less and less current to stay at this voltage level. The last stage of the charging process is the float stage. At this stage the current almost stops flowing into the battery, as a result the voltage drops and the battery is now fully charged. There is just a tiny amount of power coming into the battery at this stage, which is done to avoid self discharge.

2.5.3 Dump load dimensioning and PWM diversion charging

A diversion controller charges the battery until they reach a voltage set point value where diversion begins. The excess power is then diverted to a dump load. The dump load is usually a heating element that should be placed in an insulated tank with a heat transfer fluid to store the energy. The dump load must be dimensioned after the system specifications, depending on the battery voltage and the amperage of the wind turbine.[36]

The working of the heating element is a current flowing through a resistance, which allows

the element to generate a certain amount of heat. The current is given from Ohm's law, presented in equation 2.22. As can be seen from the equation, a resistance too high will lead to a low current, and therefore little heat is produced. However, with a resistance too low, the current will be too high for the system components to handle. Mathematically, it can also be shown that the current will have a greater impact on the power than the resistance does. From equation 2.23, the power is proportional to the resistance, and proportional to the square of the current. The resistance in the heating element should be high enough to handle the maximum power that can be produced by the wind turbine.[37]

$$U = RI \implies I = \frac{U}{R} \quad (2.22)$$

$$P = UI = RI^2 \quad (2.23)$$

Pulse width modulation (PWM) is often used to control the power in electric circuits by switching the power on and off. Figure 2.10 shows a typical PWM signal where M is the on time and S is the off time for each period. The duty cycle tells how much the signal is on for each period. The average voltage from a PWM device can be found by multiplying the duty cycle with the source voltage, and the power delivered to the load is regulated by adjusting the duty cycle.[38]

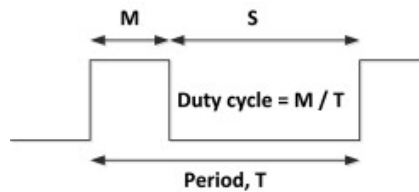


Figure 2.10: *Pulse width modulation signal*[38]

2.6 Energy storage

Energy storage is essential in off-grid systems that utilize energy from intermittent sources like solar and wind. During high energy production the energy can be stored and used later on when the production is low. Batteries and thermal storage are two options for energy storage and a combination of the two gives gives a versatile storage solution.

2.6.1 Battery storage

The main option for energy storage in an off-grid system using batteries are lead-acid batteries. This is mainly due to its low initial investment cost. Lithium-ion batteries is another more energy dense alternative, but it requires a higher investment cost. In return it has a longer lifetime. The behavior of a battery is described by its voltage. The current flows into or out of the battery when being charged or discharged, increasing or decreasing the voltage. The internal resistance in the battery varies by different factors such as capacity, temperature or amount of current while charging or discharging. By measuring the voltage level, the batteries state of charge (SOC) can be determined. The

SOC is the amount of energy that is currently available in the battery.[39] The energy efficiency of a lead acid battery is typically around 70%. Some of the energy will dissipate during charging, storing and discharging.[40]

The lifetime of a battery in a renewable energy system can be limited. Due to intermittent energy production, and discharging from electrical applications connected, the optimal charging cycle is hard to fulfill. This is an element that needs to be considered when dimensioning the battery package. If the battery is too large, it might not get fully charged. The battery should also not be discharged 100% since this also will shorten the lifetime. One option can therefore be to replace a smaller battery package more frequently.[25]

2.6.2 Thermal energy storage (TES)

TES systems have been useful to meet with the mismatch in energy supply and demand, and there are mainly two types; sensible and latent. For selection of the appropriate system, storage period, operating conditions, economic viability and season dependency will be decisive factors.[41]

The sensible heat of a material/substance equals the energy released by a reduction of temperature, or the energy absorbed by an increase in temperature. Latent heat on the other hand, represents energy demand associated with phase change of a material/substance, for example vaporization of water. Determining the sensible heat for solids and liquids is quite easily done, but for gases the volume has to be accounted for. Therefore, one has to apply the specific heat constants C_p and C_v , for constant pressure and volume, respectively.[41]

The operation of TES usually consists of three steps or more; charging, storing and discharging. Temperature range and application will decide storage medium, such as water. Water is a reasonable choice due to its high specific heat in liquid state at ambient temperature. Although its specific heat is not as high as for several solids, it can easily be pumped to transport thermal energy. A huge advantage with TES is the usage of off-peak electricity, as the energy can be stored thermally and be used during peak hours.[41]

A heat transfer fluid (HTF) is any fluid used to transfer heat from a source to its location of heat demand. It is recirculating, meaning it will return to the heat source after delivering heat where required. Water has for years been a cheap and efficient transfer fluid, but has several limitations both chemically and physically, affecting thermal performance and reliability. For operation above 100°C for example, non-aqueous HTFs are necessary. Efficient transfer and low pumping-energy will improve both system performance and return of investment. A few other characteristics are also advantageous for transfer fluids, such as minimal energy consumption for pumping, minimal environmental impact and preservation of pipework. The latter is of importance to avoid corrosion via oxidation.[42]

The HTF itself will be heated up, and by the concept of natural circulation and convection currents, it will circulate itself in a closed compartment. This is due to the density

reduction, which takes place as a fluid increases its temperature. The hot fluid with lower density will be brought up to the surface, as the cooler and denser fluid will sink to the bottom. This causes a higher temperature at the top, and as the fluid at the bottom is heated up, it will again rise to the surface, causing this convection current.[43]

A commonly used thermal oil for thermal applications requiring good temperature stability is the duratherm-630. It offers a precise temperature control and is applicable for temperatures up to 332°C. Its flash point, however, in which the fluid is at risk of being ignited, is at 229°C, so for some safety margin temperatures should be kept below 220°C. Additionally it has high performance and efficiency, and is environmentally friendly, non-toxic and non-hazardous. The HTF itself will need an external heat source to be heated up, and the amount of energy needed to heat up the fluid is given by equation 2.24. Q is the thermal energy of an incompressible liquid, m is the mass of the liquid, C_p is the specific heat capacity, and ΔT is the temperature change from final temperature (T) and initial temperature (T_0).[44, 45]

$$Q = mC_p\Delta T = mc_p(T - T_0) \tag{2.24}$$

3 Literature review

Several studies have been evaluated to avoid the challenges associated with energy loss when converting wind energy to heat. The loss is mainly due to an electric loss, which is significantly reduced if one could convert the wind energy directly to heat. Researchers have evaluated methods such as compression, induction, and friction to enable efficient energy conversion. Studies which have evaluated methods for this conversion have primarily focused on friction based methods using the Joule machine principle or a Taylor-Couette system. Conversion by induction through eddy current permanent magnets has also been used.[46]

3.1 Direct conversion of wind energy to heat

Rotational energy from a wind turbine can be converted to heat directly, without the use of a generator. This will reduce the energy loss since the process goes directly from mechanical energy to heat, rather than from mechanical energy, via electricity, to heat. Since there is no need for a generator, this will also reduce the cost. One of the methods for mechanical conversion of wind energy follows the same principles as the Joule machine. This method is as follows: The wind turbine is connected to an impeller through a shaft, and the impeller rotates in a fluid. This will cause heat generation because of the frictional forces, also known as viscous dissipation.[47]

Wind systems based on the Joule heating principle started with the oil crisis in the 1970s. At this time Denmark was dependent on imported oil for residential heating. The first windmill for this purpose had a diameter of 6 meters and was built with wooden blades. From 1993 to 2000, 34 windmills based on the Joule heating principle were commercially produced in Denmark, by a company named Westrup. They had a diameter of 5 meters and a rated power of 5kW. The largest windmill based on Joule heating that has been built was the LO-FA. This was built by Knud Berthou in the 80s and had a diameter of 12 metres and a maximum rated power of 90kW. The braking liquid for the impeller was hydraulic oil which can be heated to even higher temperatures than water.[48]

Chakirov and Vagapov proved Joule heating theoretically based on the use of a Savignon VAWT and an impeller rotating in water. The proposed system can be connected to a radiator for residential heating, as illustrated in figure 3.1. Matching the torque-speed characteristics of both the turbine and the impeller should be realized to obtain maximum power. This is achieved by testing different impeller sizes and number of blades.[47]

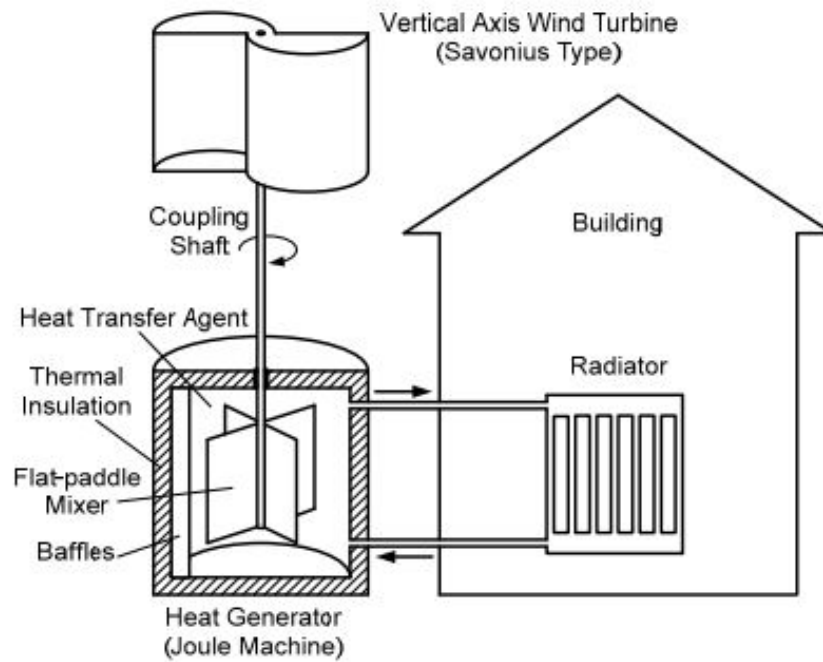


Figure 3.1: Schematic representation of proposed system by Chakirov and Vagapov. Figure taken from [47].

Figure 3.2 presents the results of Chakirov and Vagapov, evaluating the use of a wind turbine for Joule heating. Testing was conducted over the time span of 50 hours, in which power, temperature and wind speed were simulated. From the results shown in figures 3.2a and 3.2b it is clear that temperature increase is faster at the time of peak power, and this increase will stabilize as the power drops. A temperature increase of almost 50°C was achieved with an assumption of zero losses, with power ranging between 0-1200W.[47]

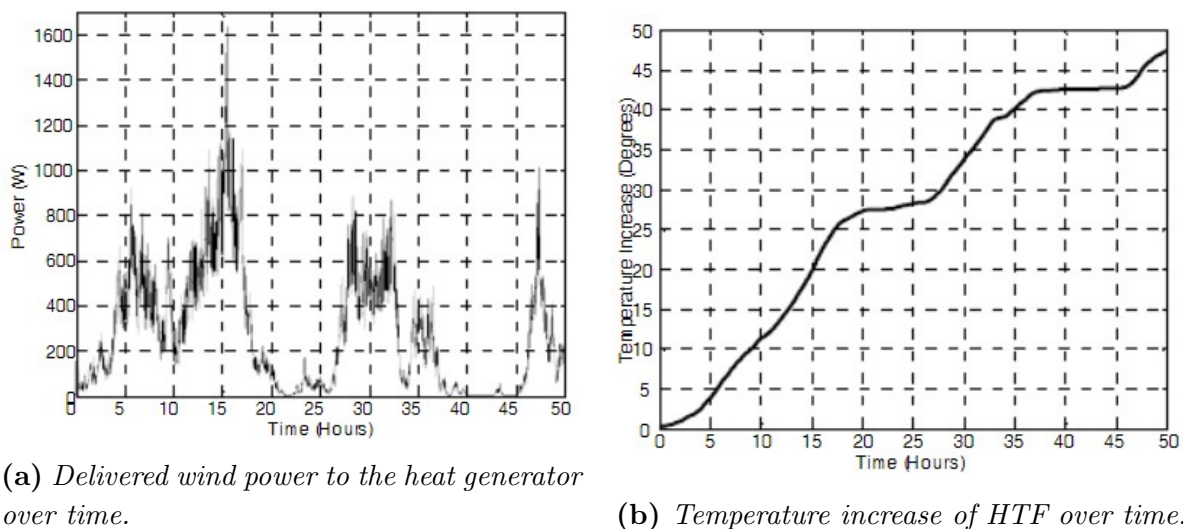


Figure 3.2: Results from a 50 hour test period by Chakirov and Vagapov. Figures taken from [47].

Chen et al. wanted to convert all input energy in an electric motor into thermal energy.

The working of the converter is shown in figure 3.3. A driving force such as wind power, produces a magnetic field in the gap, stator and rotor. As a result of the rotating magnetic field, eddy current power and hysteresis are generated in the permanent magnets, the rotor and the stator. All forms of thermal power are transmitted to the water during this process, either by the frictional forces or the rotational energy. In figure 3.4, efficiency is plotted against the rotational speed of the converter, showing a high efficiency at lower RPM, decreasing with an increase in rotational speed of the converter. From 500 to 3000RPM, efficiency goes down from 98.5% to around 96.5%, due to increased thermal power of the converter, and heat loss to the surroundings, though this reduction is minimal.[49]

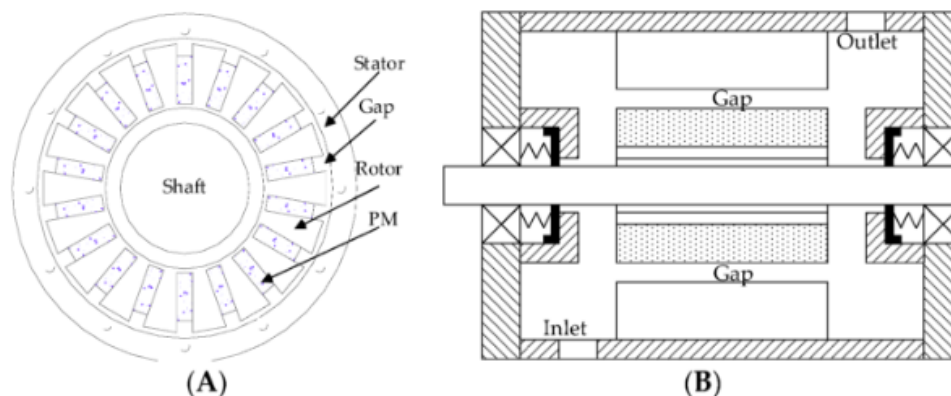


Figure 3.3: Structure of a magnetic converter in the axial (A) and radial (B) direction. Figure taken from [49].

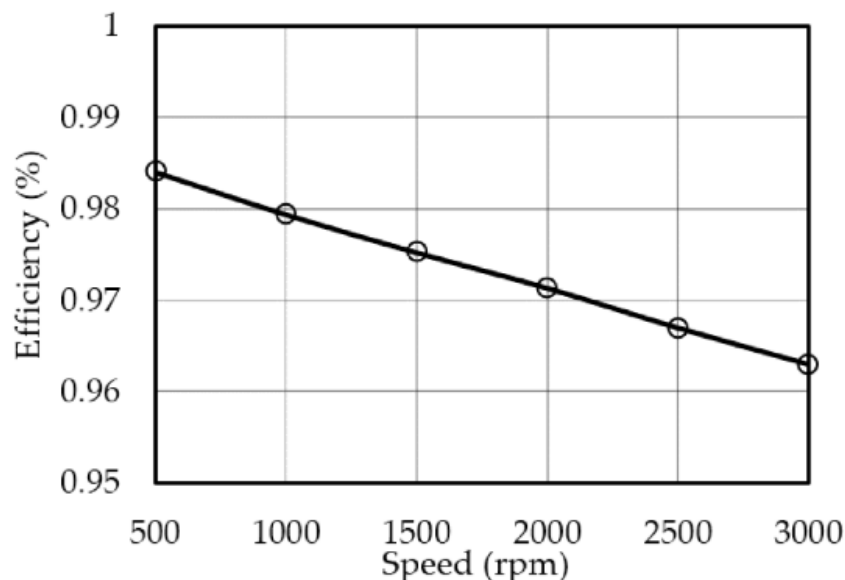


Figure 3.4: Efficiency at different RPM for a thermal converter. Figure taken from [49].

Another example of a similar system as Chen et al. using the heat generated in a permanent magnet rotor is purposed by Khanjari et al. They tested a permanent magnet

eddy current heater with different magnet arrangements to find the highest efficiency. Nine different magnet configurations were tested with RPM ranging from 100-500. In one of the simulations with a power input of 844W an efficiency of 97% was achieved. With a mass flow rate of 0.035kg/s the resulted temperature difference was 5.6°C.[50]

Mujtaba et al. made a heating system based on hydraulic energy. A pump is driven by a wind turbine which pumps oil through the system. The oil is then throttled from high pressure to low pressure, and through viscous dissipation this sudden change in pressure generates heat. A parametric study showed that the main contributors to heat generation was the space of the throttle orifice and the angle of the needle tip at the back of the throttle. Results showed that a small opening of the throttle and a small angle on the needle tip gave largest result in pressure difference.[51] Zdankus et al. performed an experimental study with the same type of setup as Mujtaba et al. It was simplified with the use of an electric motor taking the place of a wind turbine. They found that lower oil temperatures gave higher efficiency, which arguably is due to higher viscosity of oil at lower temperatures causing more frictional forces and thereby higher temperature increase. The maximum amount of generated thermal energy was 723W and the temperature increase of the oil was undisclosed in this paper.[52]

Swinfen-Styles et al. proposed a directly driven offshore wind turbine system which powers a liquid piston-air compressor. Direct drive compression of air at ambient temperature requires a lot of energy. A two stage compression is then reviewed with different types of compression techniques. One of the mentioned is a wave powered hydraulic air-compression. The energy generated from the compression is stored in two forms, either in gravel packed bed as heat or in flexible energy bags as compressed air. The system is not tested, but calculations showed promising results in cost and compared to traditional wind generating systems. The cost is expected to be around \$21/kWh compared to the cost of lead acid batteries which is about \$(65-100)/kWh[53]. The efficiency is estimated to reach up to 95%.[54]

Serov et al. tested the concept of a Taylor-Couette system, directly driven by an electric motor as a substitution for a wind turbine. Taylor-Couette flow consists of a high viscosity fluid between two rotating cylinders. Heat is generated due to viscous dissipation in the system. Counter rotating cylinders generated most heat. To effectively generate heat, rough surfaces give a higher viscous dissipation effect, leading to greater potential for generating heat. [55]

Based on this literature review of direct conversion of wind energy to heat, it is found no studies that can be applied for cooking. The temperature differences have either been undisclosed, or they are too low for cooking purposes. It can therefore seem as a necessary path is to go through electricity to achieve high enough temperature. Direct conversion of wind to heat does however ensure a high efficiency and has been proposed as a solution for residential heating.

3.2 Conversion of wind energy to heat through electricity

Chapter 3.1 gives an insight in different ways to convert wind energy directly into heat. These methods mostly give small temperature increases in the fluid and are not sufficient for high temperature storage. This part of the literature review gives an oversight over methods for converting wind energy to heat through electricity.

Senanayaka et al. made simulations of a 5kW wind turbine used to heat up water, with the generator connected to a dump load. The system is designed to heat up water to 60-70°C, and also charge a 90Ah battery bank when the power is high enough. To ensure good performance the system is regulated by a maximum power point tracking algorithm. A sliding-mode observer is modelled to estimate the rotational speed of the wind turbine. The maximum power point tracking is supposed to remove the need of wind or rotational speed sensors in the system. The simulations showed similar results as a systems using sensors for power tracking would give.[56]

Li et al. performed a feasibility study for an off-grid residential heating solution, where a heat pump is driven by the electricity generated from a wind turbine. Due to the intermittency of wind, desired thermal comfort in the house was not achieved. They found upscaling of the wind turbine to be unnecessary for solving this problem. Instead the focus should be on the energy storage. A larger battery package showed to improve the loss of load probability with 24.1%. This study was based on simulations alone, and they found that high resolution time step is of importance to evaluate dynamic behaviour of the heat development in the system.[57] A similar study is performed by Ji et al. for domestic heating in Scotland.[58]

The previous mentioned challenge regarding the intermittency of wind power has opened for new ways of storing this energy. Frequency variations and voltage sag are both results of rapid varying wind conditions, leading to strain on common storage technologies such as batteries. Rapid transitioning from charge to discharge will for instance lead to increased degradation rates in the batteries, wearing them out quicker. A solution more suitable for this challenge is the use of flywheels in a flywheel energy storage system (FESS). They are ideal for such use, given their resilience to high frequency rates. The mechanical energy from the wind turbine is stored as kinetic energy, as the flywheel will rotate at high speeds maintaining angular momentum.[59, 60]

Flywheel energy storage (FESS) was evaluated by Sebastián and Alzola, and further reviewed by Hutchinson and Gladwin. They found the technology to be 3-5 times less expensive for low speed applications (1800-3600RPM), with purchase costs of around \$100/kW, against \$300/kW for high speed storage systems. These prices and results are however found for larger systems, and a financial evaluation should be conducted to decide the profitability of a FESS in a smaller scale system. Conclusions from the simulations tell that efficient sizing of the system is of importance for its economic merit. Targeted power should also be further evaluated against sizing, to find an optimal compromise for the FESS.[59, 60]

Kavian et al. investigated a hybrid solar and wind system for co-generation of heat and power. Depending on the mirror coefficient, defined as the relation between solar heat with and without side mirrors, the system generates a significant amount of both heat and power. For mirror coefficient, $n=1$, the system annually generates 239.41kWh/year of electricity, and recover 3675.42kWh of heat. For $n=3$, those numbers are 799.4kWh and 22844.35kWh, respectively. The setup is shown in figure 3.5, and works in the following way; [61]

The double-glazed window (1) and the copper absorber plate(2) collect the sun rays, between which is a vacuumed gap to reduce losses due to natural convection. Side mirrors (9) are attached to increase solar irradiation and heating of the absorber plate. The inlet air (4) will follow a duct through the heated plate, in which the air is heated from the thermoelectric generator (3). This generator is driven by a temperature difference between the absorber plate and the air. The warm air rises up through the solar chimney (6) due to lower density, and exits the chimney (5), going into a vertical axis savonius wind turbine (7), with a sufficient speed to run the turbine blades. Electricity is produced, and can be stored by traditional methods, while the outgoing air (8) still possesses heat, and can be used for heating, drying and other similar purposes.[61].

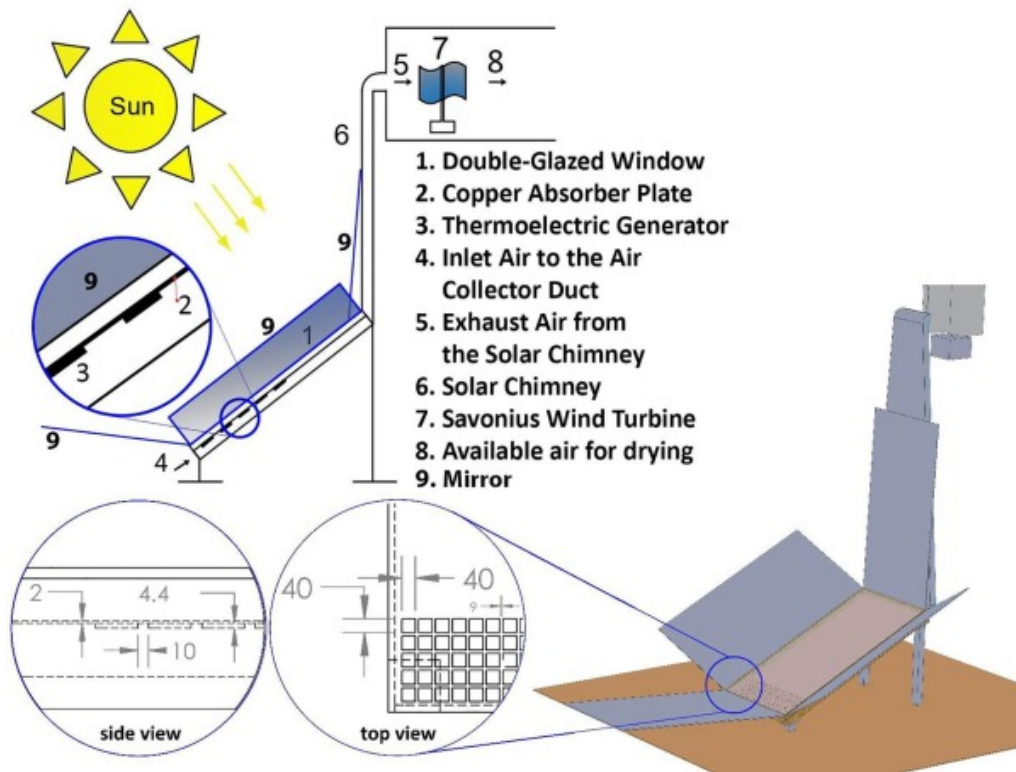


Figure 3.5: Hybrid solar and wind solution combining heat and power. Figure taken from [61].

4 Experimental setup

The two main objectives of this thesis are to examine direct conversion of wind energy to heat, and conversion through electricity to heat by the use of a small scale wind turbine. For testing of the generator and its controller in different working operations, several setups were used in order to better understand the working principals and limitations of different parts of the system. As the turbine was removed from its original location at the roof to be tested in the lab, a detailed description of the equipment used is of importance for further work, and for the tests do be repeated. The specifications of the different equipment used for the setup are listed in table 4.1, and an overview of the entire system is presented in figure 4.1

Number	Device	Specification/serial number	NTNU number
1	Asynchronous machine	732 689USB 02	A03-0122
1	Control unit	732 689USB 01, 1000W	B03-0504
-	Multimeter	Fluke	S03-0416
2	Turbine	BL-WTN200S1903200941	-
3	Digital power meter	53BU0764	E02-0003
4	DC electronic load	Kel103300W	-
5	Turbine controller	-	-
6	Rectifier bridge	-	-
7	2*Battery	SR550	-
8	Tristar controller	TS-45	-
9	3-phase rheostat	MFPR 6000W25R-W	-
-	3*Variable resistance	-	K01-0366/0367/0368
-	Current clamp	Fluke 336	I04-0486
-	Bench power supply	EA-PSI 5200-10A	B02-0729

Table 4.1: *Serial and identification number for equipment used in experimental setup. Numbering according to figure 4.1.*



Figure 4.1: *Experimental setup used for testing. The numbering for the devices are explained in table 4.1*

Asynchronous machine & control unit

The electric machine used is a three-phased cradle type asynchronous machine with a squirrel cage rotor. It measures RPM as well as torque, with the use of stainless steel bars with strain gauge. The control unit, seen as the upper part in figure 4.2, displays both RPM and torque during operation, and is equipped with micro-controllers and an integrated frequency converter.[62]



Figure 4.2: *RPM controlled asynchronous machine with control unit.*

Wind turbine

The wind turbine used in the project, shown in figure 4.3, can deliver up to 400W out from its generator. It operates between a cut-in wind speed of $2\frac{m}{s}$ up to $50\frac{m}{s}$, while its optimum lies around $13\frac{m}{s}$. Further specifications for the turbine can be seen in figure 4.4. It automatically adjusts its positioning according to wind direction by the mechanism of a tail vane explained in chapter 2.4. The turbine has a built-in permanent magnet synchronous generator, explained in chapter 2.2, generating the power harnessed from the wind.[63]



Figure 4.3: *Original location of the wind turbine on the roof at NTNU.*

Wind Turbine	
Model: BL-WTN400S	Rate Power: 400W
Output Voltage: 24V	Rate Current: 5.56A
IP Grade: IP65	Color: White
Blade Diameter: 1.4m	Net Weight: 6.7kg
Serial Number: BL-WTN200S1903200941	

Figure 4.4: *Wind turbine specifications.*

Digital power meter

The digital power meter has three input terminals, allowing for readings from three phases simultaneously. It gives the RMS values for current, voltage and power with high precision. Figure 4.5 shows the power meter with its three displays for reading values from three phases. By the use of an analog output, these display readings can be logged continuously on a computer program to get more accurate readings. Its operation manual can be found in appendix D.[64, 65]



Figure 4.5: *Digital power meter used for reading values for current, voltage and power.*

DC electronic load

The DC electronic load shown in figure 4.6 is a device enabling short circuit testing and battery testing, in addition to discharging of batteries. With a rated discharging power of 300W, and currents up to 30A, it allows for an efficient discharge of batteries of up to 120V.[66]



Figure 4.6: *Electronic load used for discharging the batteries. Figure taken from [66].*

Turbine controller

The turbine controller is meant to automatically charge the battery in the system, and will brake the turbine when the battery voltage reaches a certain value of around 29V, as seen in figure 4.7. When the battery voltage has dropped to a recovery voltage of around 26.4V, the controller will stop braking the turbine, and the battery is charged back up. The alternating current inputted from the generator is rectified in the controller, sending DC into the batteries.[67]

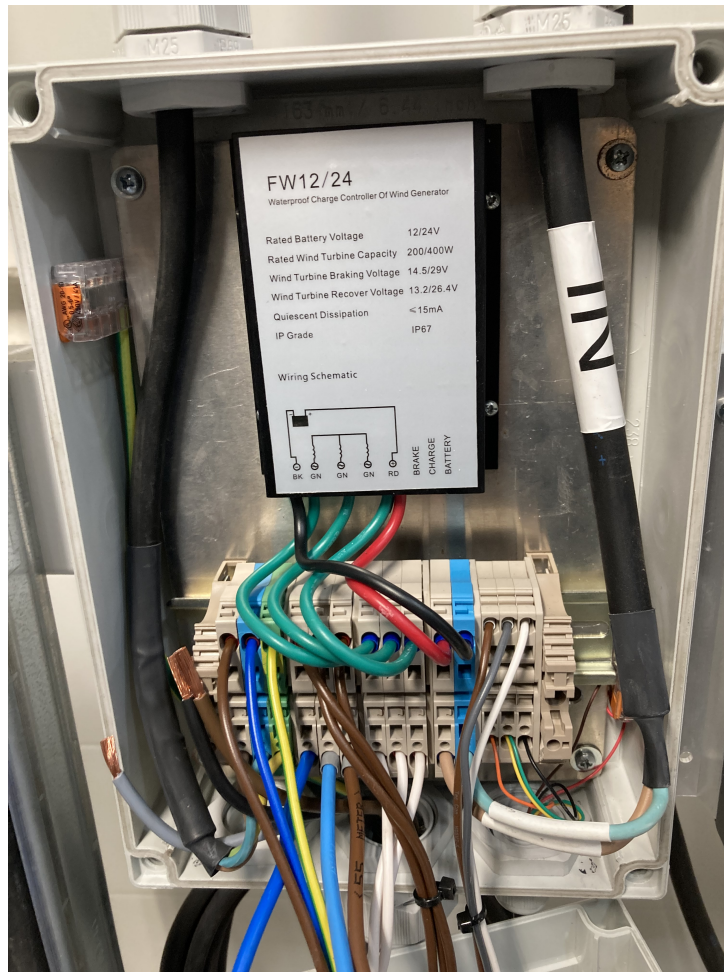


Figure 4.7: *Original wind turbine regulator.*

Rectifier bridge

A three phase rectifier bridge is used to rectify a three phased alternating current, such that it outputs a single phased DC current. It is widely used in instrumental applications, being both efficient and reliable during operation. In addition to their high power/volume ratio, they can withstand high currents for their size. Figure 4.8 shows the rectifier bridge used for the setup, with a cooling rib attached to avoid too high temperatures in the device.[68]

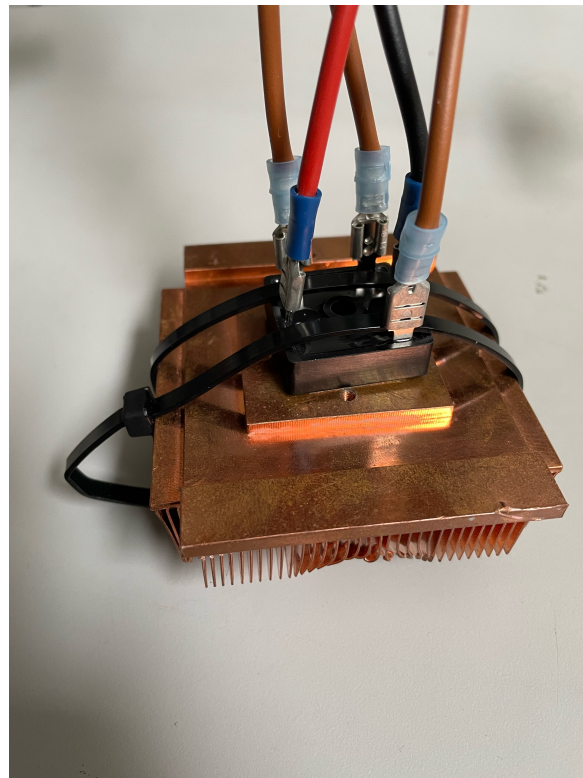


Figure 4.8: *Three phase rectifier bridge with cooling ribs.*

Battery

The old and new batteries in the system, shown in figure 4.9 and 4.10, respectively, are all 12V lead-acid batteries used as a first hand storage for the power produced in the system. The batteries are used to run smaller electrical devices, and are in themselves not used for heating of the thermal storage.



Figure 4.9: *Original 12V batteries used for electrical storage in the system.*



Figure 4.10: *New 12V batteries used for electrical storage in the system.*

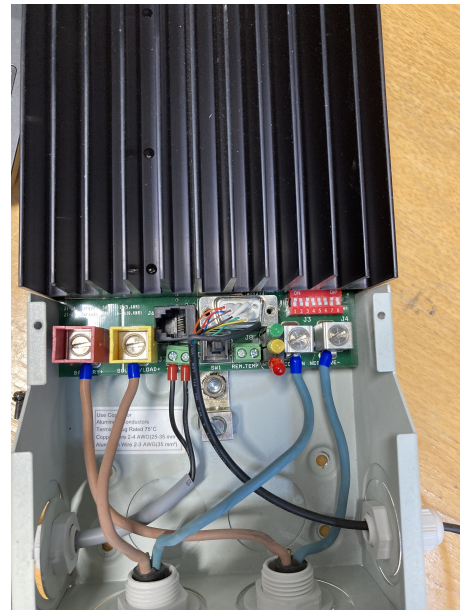
Tristar controller

The Tristar controller is designed to offer several operation modes used in power applications, with usage for both wind and solar systems. By the flip of eight DIP switches, different operation modes can be set, depending on the system setup and parameters. In addition to its reliable operation, the controller has built-in LED lights that will inform about any error occurring in the system. All light configurations are explained in the operation manual, seen in appendix C, making it user friendly for small scale applications.[69]

The controller is made to operate either with a 12V or a 24V battery system. Sizing of the dump load must be done accordingly, accounting for the maximum current of the energy source, such that it is able to divert all the incoming current. There are two main voltages that are decided by the aforementioned switches, found in the operation manual, denoted PWM absorption voltage and float voltage. The PWM voltage is the voltage at which diversion takes place, where battery voltage is kept constant. Float voltage is the voltage at which charging voltage will be set to when the battery is fully charged.[69]



(a) *Tristar controller.*



(b) *Tristar LED lights and DIP switches.*

Figure 4.11: *The Tristar controller used for diversion mode.*

Variable resistance

The three phased rheostat, shown in figure 4.12, was used to represent the heating elements in the thermal heat storage. Having three phases, the rheostat offers great flexibility for the resistance set for the system. By the use of an electrical drill, the resistance can be varied between its upper and lower limits. As the resistance is three phased, it can be set either inn series or parallel with one to three phases, enabling several configurations.

The three variable resistances shown in figure 4.13 were used for the final test demonstrating wind to heat. With each element enabling resistances from 0.2 to 19.6 Ω , they too offered great flexibility for the dump load. They were used due to minor inaccuracies in the rheostat in the final stages of the project.



Figure 4.12: *Three-phased rheostat used for varying the resistance in the system circuit.*



Figure 4.13: *Three variable resistances used for demonstrating wind to heat.*

Bench power supply

The bench power supply serves as a power source, replacing the turbine during parts of the testing. The wind turbine used in the setup is rated for 400W, while the bench power supply can deliver up to 640W, with a limit of 10A and 200V. It is a DC power supply, erasing the need for a rectifier, and is solely used for efficient testing of the Tristar controller during diversion mode.



Figure 4.14: *DC bench power supply used to test the system in diversion mode.*

Dump load/heat storage

The heat storage used for the project was a small cylinder filled with 3.97 liters of duratherm-630 oil, isolated with 2.75cm insulation covered with aluminium foil. The cylinder is shown in figure 4.15, with four temperature sensors enabling temperature logging using a Pico data logger, which can be seen in the same figure. In the event of the battery being fully charged, the system will need somewhere to dump excess power, to prevent it from going into the battery, leading to overcharging. The energy dumped to the heat storage can later be used for cooking.



Figure 4.15: *The dump load used for diversion during experimental work.*

4.1 Data processing

To enable proper and accurate measurements of current, power and voltage, several data logging programs were used in varying extend. With the turbine controller, a DC power meter was included, allowing for continuous logging of the DC variables at any given point in the setup. This was useful to track the DC voltage and current to the batteries, to see how much power was lost in the system. Also, by connecting the digital power meter to a computer, all AC readings were stored in a Labview program made by the help of a lab-technician at the institute. In addition to this, the Tristar controller has its own logging program, allowing for reliable readings during diversion mode. This was shown to be especially helpful when evaluating power to the dump load during diversion, as the current read from the clamp meter and the Tristar logging program deviated from one another by a significant amount. Lastly, the temperatures of the oil storage were closely monitored using a program called PicoLog.

The data collected were either written down manually from measurements by multimeters and power meters or by logging. This data was sorted in Excel and plotted in Python, in which an example of the code can be found in appendix A. Some of the testing is done with logging from power meters in different parts of the electrical circuit. This data is sorted to ensure measurements are corresponding with respect to time. For this purpose, certain data points have been excluded, in order to evaluate relevant data.

5 Experimental work

As the wind turbine was removed from its original location at the roof in the initial stages of the project, alternative methods had to be used in order to properly demonstrate the concepts of the thesis. Therefore, testing in the lab was done in several steps, where different equipment and setups were used, to obtain the required data for dimensioning the system optimally. An overview over the different test modes and their purpose can be seen in table 5.1.

Test	Purpose
Preliminary testing (1)	Power output, losses and efficiency of the turbine
Regulator battery charging (2)	Examine behaviour of turbine regulator without external load
Wind to dump load (3)	Examine behaviour of wind turbine without batteries
Diversion mode with DC source (4)	Diversion mode using a DC source and Tristar controller.
Wind turbine diversion (5)	Diversion using Tristar controller with wind turbine

Table 5.1: Overview of the different tests conducted in the lab.

To enable desired test results, the setup was altered somewhat between tests. An overview over equipment used for the different tests is shown in table 5.2, where the numbering corresponds to the subsections of chapter 5.

Equipment \ Test number	1	2	3	4	5
Asynchronous machine w/control unit	✓	✓	✓		✓
Wind turbine	✓	✓	✓		✓
Digital power meter	✓	✓	✓		✓
DC electronic load		✓			✓
Turbine controller		✓	✓		✓
Rectifier bridge					✓
Batteries		✓		✓	✓
Tristar controller				✓	✓
Rheostat	✓		✓	✓	✓
Variable resistances			✓		
Bench power supply				✓	
Heat storage					✓

Table 5.2: Tabular depiction of equipment used in the different experiments.

During operation, a wind turbine will usually be cooled down by the airflow, such that

the generator doesn't overheat. The coils in the generator will have current limitations to prevent them from burning up. Cooling is therefore necessary for the generator to operate under rated conditions. For the tests done in this project, the generator has been kept in the lab, driven by an asynchronous machine, removing the natural cooling that follows with the incoming air. Therefore, current limitations have been met with extra care in order to avoid possible overheating of the generator. As a result the generator has not been run to the same power as it would in real life, giving less power to both dump load and batteries. The power will, however, be far more stable than in an outside scenario, this is something that needs to be taken into account when observing the results. With the rated phase current of 5.56A, the power is limited to around 200W for tests that include batteries, and even lower for testing over longer periods with constant power.

5.1 Preliminary testing (1)

Method

Due to intermittent and poor wind conditions, an experimental setup for the turbine was built in the lab at the institute for electrical energy at NTNU. To simulate the intermittency of the wind, the asynchronous machine was used. By varying the torque and rotational speed of the turbine, several output parameters could be observed to see the behaviour of the turbine at given input parameters. The motor is in turn supplied directly from the grid at 230V. To represent the heating element in the system, an external variable resistance was used, seen in figure 4.12. By using a variable resistance, an optimal resistance can be chosen empirically to optimize power output.

Preliminary testing was done using the two wattmeter method for the power meter, with the setup listed in table 5.2 and the corresponding circuit connection as in 5.1, with readings from the control unit in figure 4.2. Using a digital power meter, shown in figure 4.5, current, voltage and power could be read off for two of the phases. As the turbine itself does not have a neutral point, this method was first applied to measure the parameters of the circuit. For further and more accurate testing, the three wattmeter method was applied. For this, a neutral point is needed, so the neutral point of the 3-phase rheostat was used, and connected corresponding to the circuit board for the power meter in figure 5.2. Using this method, voltage, current and power could be read off for all three phases. During testing, an important note was to make sure the phase current did not exceed the rated current of 5.56A given for the turbine, shown in figure 4.4. The measurements start at 300RPM due to vibrations in the setup at lower frequencies. Measurements at rotational speeds lower than this are also likely unnecessary since the wind turbine has a cut-in wind speed of about $2m/s$.

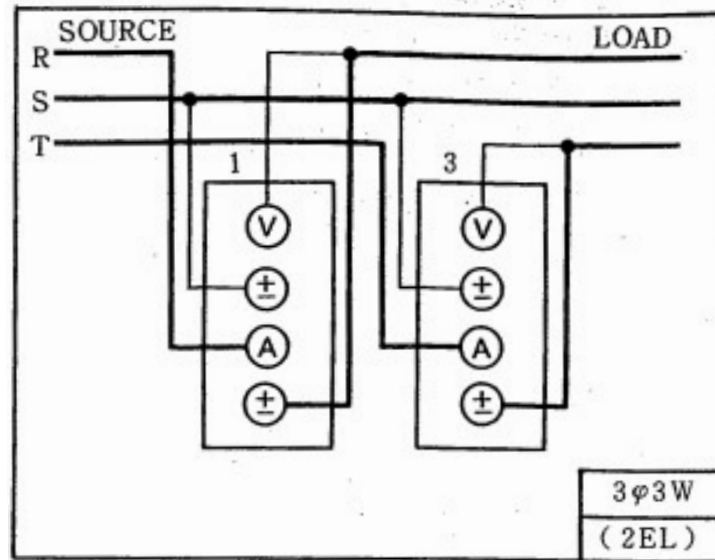


Figure 5.1: *Circuit board for the digital power meter for a 3-phase, 3-wire connection.*

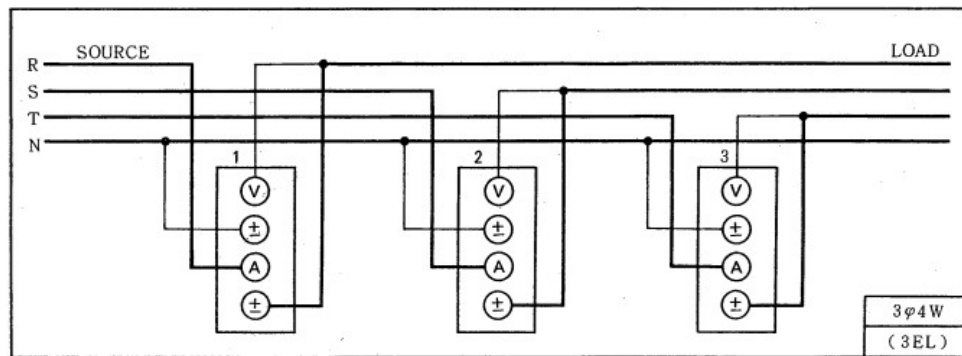


Figure 5.2: *Circuit board for the digital power meter for a 3-phase, 4-wire connection.*

An important factor for the induced voltage, and power produced in the generator is the number of poles, which can be calculated from equation 2.4. From measurements done during preliminary testing, an electric frequency of 100Hz and 150Hz was measured at 1000RPM and 1500RPM, respectively, giving a number of 12 poles in the generator.

Results and discussion

An idle test was performed to show the proper functioning of the generator. The proper functioning of the generator was questioned due to its low performance when it was placed outside. This test was performed without any load connected, to show how the induced voltage varies with RPM. As can be seen from figure 5.3 the induced voltage increases proportionally with the RPM. The induced voltage per phase differs a bit for one of the three phases. Whereas EA1 and EA2 are nearly the same, EA3 is somewhat higher. This is likely due to small physical differences inside the generator that can lead to some variations in the measured output. Given the similarity of the three phases and the linear increase of voltage with frequency, the generator can be assumed to function properly.

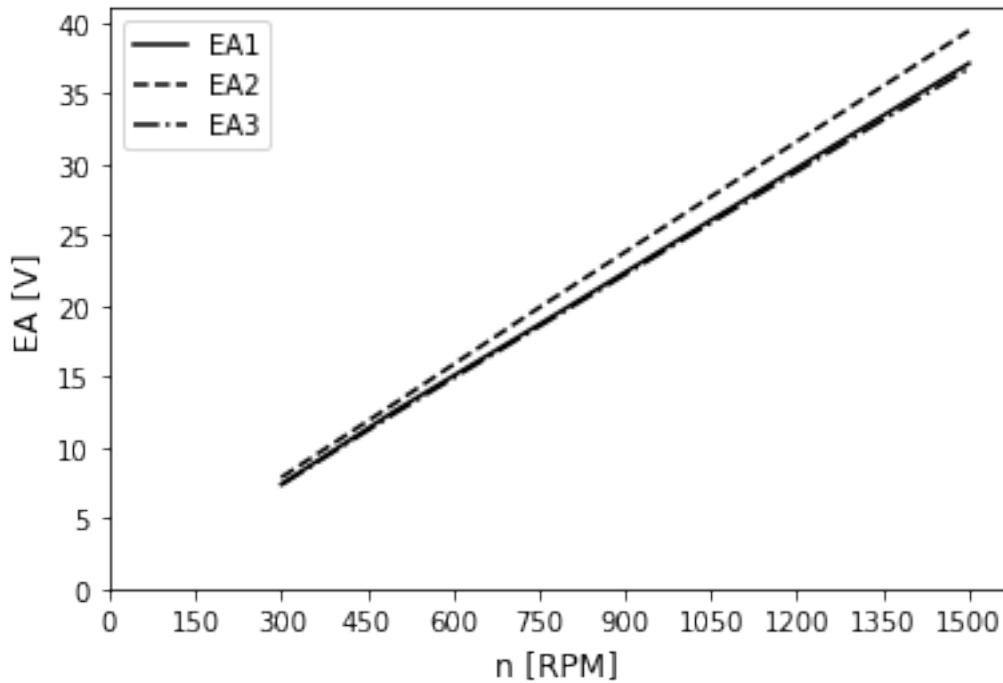


Figure 5.3: Idle test of the generator for the three different phases.

5.2 Regulator battery charging (2)

Method

Although this was not the main scope of the project, it was found useful to run the turbine regulator solely with the battery, to see how the controller behaves in different operation scenarios. The test was done in the thermal laboratory at NTNU, using parts of the setup shown in figure 4.1. By running the asynchronous motor under controlled conditions given a certain torque, behaviour of the turbine controller was far more evident. The limitations within the controller regarding both current and voltage could then be isolated and evaluated more easily, knowing how much power the turbine could output with the controller in the system.

Results and discussion

Figure 5.4 shows the power delivered to the batteries with corresponding RPM. It can be observed that the cut-in RPM is approximately 450. This should correspond to the cut-in wind speed of $2 \frac{m}{s}$ stated by the manufacturer[63]. Then the power increases almost linearly up to a power of 210W. The measurements are stopped at this point because the rated current of 5.56A is reached. To start the charging of a battery system the induced voltage in the generator has to be larger than the battery voltage, to create a voltage differential for power flow. This is the cause for the cut-in wind speed, which is normal for wind turbines because it limits wear and tear on the system. It also explains why there is no torque when starting the turbine, as this promotes higher rotor acceleration and increased power output for low wind speed. The slope of the curve is almost linear, and it

is unsure how it will develop up to its rated power of 400W. During testing the batteries became nearly fully charged. A battery discharger was then connected to continue the experiments without having the regulator braking the wind turbine. This happened at the end of the experiments and did not seem to have any visible impact on the results.

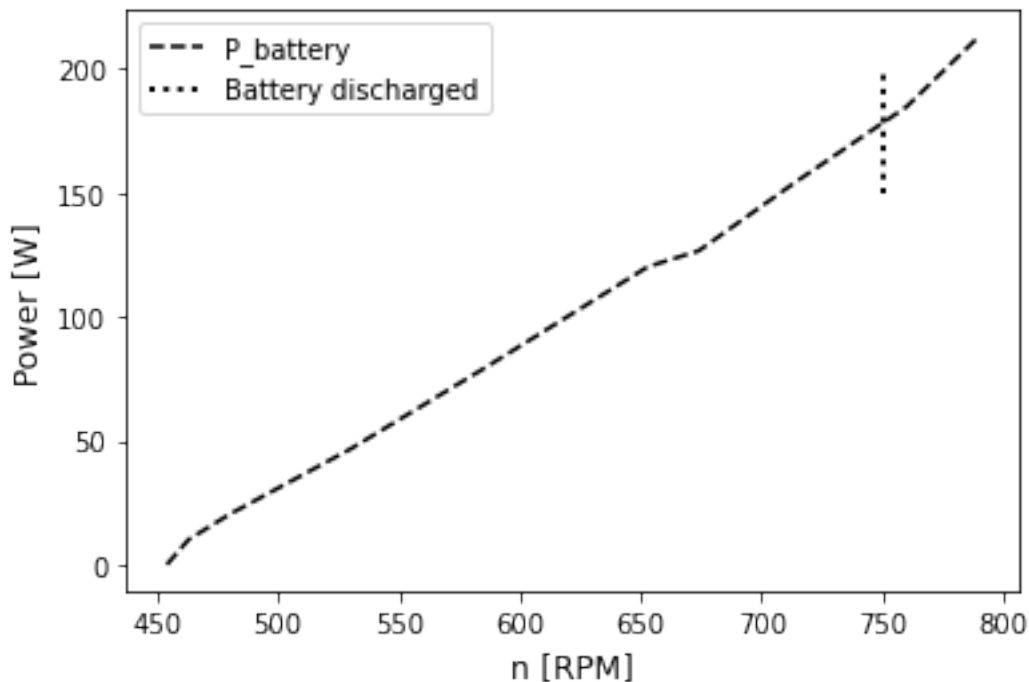


Figure 5.4: *Power to battery with original wind turbine controller.*

Evaluating the same test plotted against torque, it was seen during operation that lower torque made the turbine controller take longer to stabilize at a certain RPM, and that this happened much faster at higher torque. This was clearly observed by manually varying the torque, as both RPM and torque were displayed underway. After a while the batteries were nearly fully charged. To continue testing a battery discharger of 300W was connected, and was discovered to have a minor impact on the results. The test was done with the old batteries, but was decided not to be repeated as it was mainly meant for demonstrating the limitations and workings of the turbine controller.

For this test, power from the wind, the generator and to the battery were measured in order to calculate losses. The losses in the system were increasing at a higher rate at higher torque, as can be seen as the difference between P_{wind} and P_{gen} in figure 5.5. Results revealed an average generator efficiency of around 72%, and a peak efficiency of 78.7% at a torque of 1.64Nm, equivalent to 586RPM for the given conditions. The figure shows a input power of 360W to the turbine from the asynchronous machine at a torque around 4.36Nm. What can also be seen from figure 5.5 are the rectifier losses. Rectifier losses has a very small impact at low power, and increases up to 10% loss at the maximum generator power. These losses are mainly due to heat loss in the rectifier. The rectifier is mounted with cooling ribs as shown in figure 4.8 to limit these losses. With further increase in power the rectifier losses will also increase. To limit these losses a possibility

is to mount a small cooling fan.

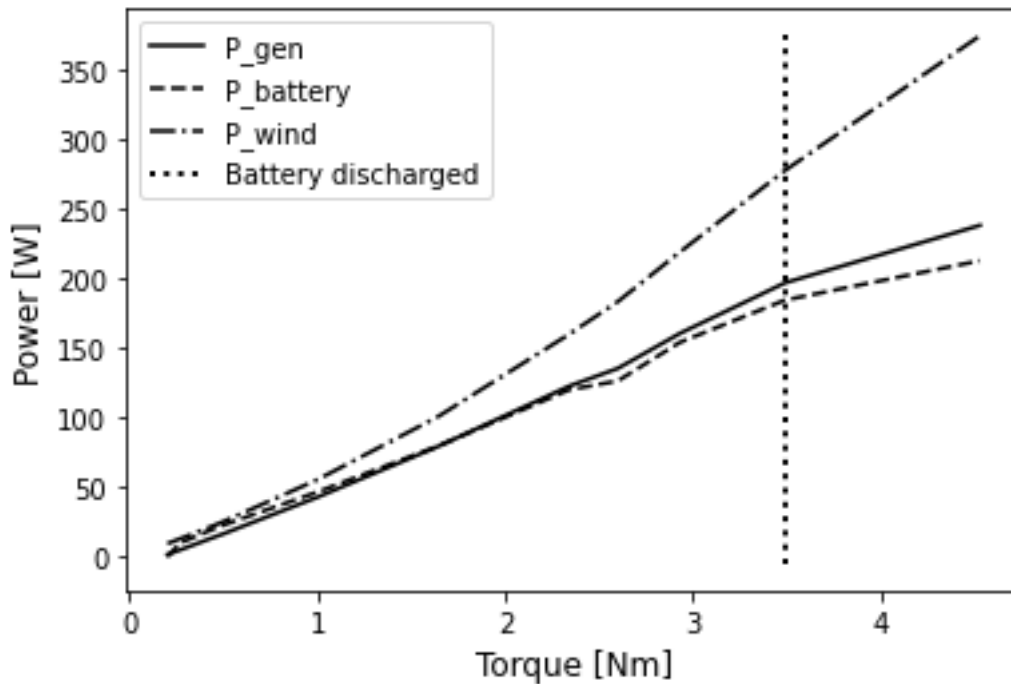


Figure 5.5: *Depiction of battery power, mechanical power from the wind and power output from the generator against torque.*

Although the turbine was taken down from its location at the roof, some testing was conducted in the beginning of the project while it was still outside. As have been mentioned previously, the rated phase current is limited to 5.56A. Wind conditions were over all poor due to the placement of the turbine, leading to hardly any power outputted, yet some days offered sufficient winds. Figure 5.6 shows the phase current from the generator and the DC power to the battery while located on the roof. This figure shows a time interval of two hours during a particularly windy day, but as can be seen from the figure, currents were overall higher than the rated current, upwards of 10A.

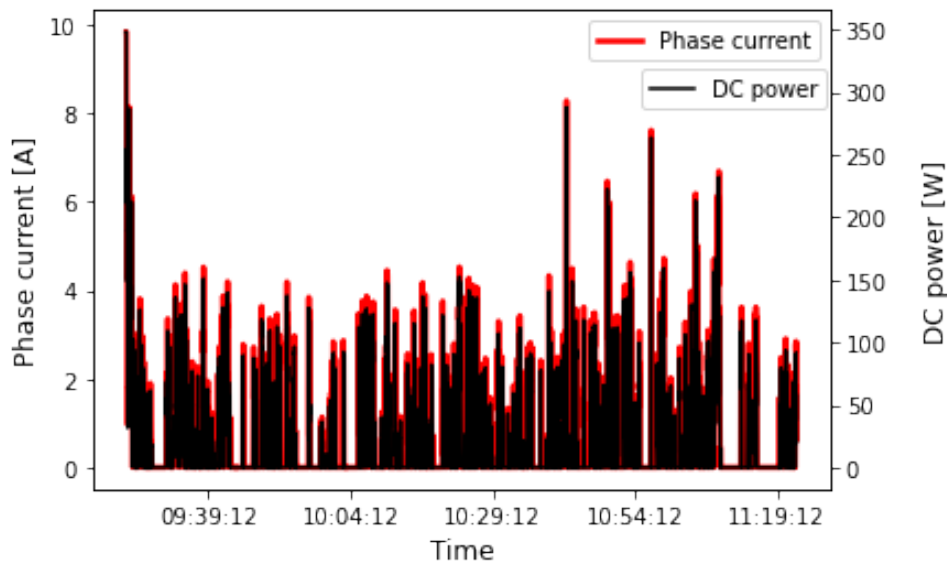


Figure 5.6: *Phase current and DC power from the turbine, while placed on the roof.*

The current values from the roof measurements are given as the DC current to the batteries, and has been calculated back to the phase current through a few steps based on the presented theory in chapter 2. By firstly dividing the DC power by the DC current we get the DC voltage to the batteries after the rectifier. Using equation 2.14, we can then get the line-line voltage, which is then divided by the square root of three to obtain the phase voltage. The rectifier will only have minor losses, which are assumed negligible in this case, meaning that the generator delivers the same amount as the DC power to the battery. By dividing this power by three to get power per phase, and further dividing by the phase voltage, we are left with the phase current, which is plotted in figure 5.6.

5.3 Wind to dump load (3)

Method

To demonstrate the principle of wind directly to heat, an external load was again used, both with and without the turbine controller. By keeping an eye on the turbine controller, it could easily be observed at which point the controller started braking, indicated by a braking light on the turbine controller. It was of interest to see how much mechanical power from the turbine could be transferred to thermal power in the external load. The original controller following the turbine is designed to charge batteries. A test to see how the controller acts when only a resistance is connected was performed with three different resistances connected, at 1.8, 3.5 and 6.6 Ω .

A few tests were also done directly from the turbine to the dump load without the controller, to obtain a power curve plotted against the torque. As there are no batteries in the system there are no need for rectifying the current from the turbine, reducing losses and amount of electrical components for this setup. For the last test, three separate

variable resistances were used, shown in figure 4.13, as the rheostat was unavailable for testing.

Results and discussion

Results from testing with three resistances are shown in figure 5.7. The test yields almost the same result in power to dump load for 3.5 and 1.8Ω, slightly in favor of the 3.5Ω resistance. It can be observed that the experiments are performed at low RPM, hence lower power. This is due to the behavior of the regulator and the limiting factor of the rated current. When not having a battery connected, the controller observes the resistance as a 12V battery system. The controller is designed to charge a 12V/24V battery package. When having a 1.8Ω resistance connected, the regulator starts braking the wind turbine at a voltage corresponding to the maximum charging voltage of a 12V battery system, around 14.7V. The controller behaves in a similar manner when a resistance of 3.5Ω is connected but the rated current is also reached in this test. For the 6.6Ω test, the controller started braking at much lower RPM, around 350. This indicates too high of a resistance, and it was observed that once torque was adjusted down, the braking lights went out and the power went up again. Both braking and recovery voltage are given by the controller itself, and is meant to protect the batteries from overcharging. After evaluating this test it can point towards that the original regulator sets the load itself, and that by adding an external load with a different resistance than a battery does not function properly with the regulator since it is designed to charge batteries.

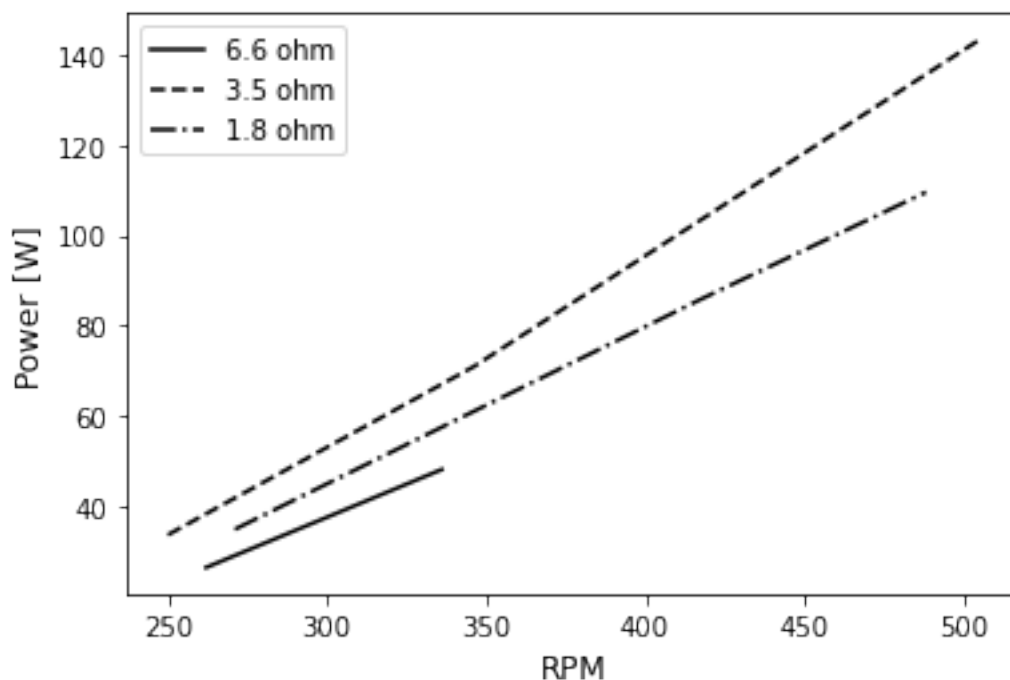


Figure 5.7: Power to dump load with three different resistances, with the use of original controller

A test was performed with different resistances directly connected to each phase of the generator which was run on low to high RPM. The purpose of this experiment was to find the optimal resistance for each rotational speed. From figure 5.8 it can be observed that the highest resistance value of around 20Ω gives the lowest power for each rotational speed. The power increases exponentially with decreasing resistance, where the maximum power is limited by the rated current of 5.56A . The resistance providing maximum power varies from 0.5Ω at an RPM of 300 up to 4.4Ω and an RPM of 1200.

At an RPM of 300, 500, 1000 and 1200, control measurements are performed using the three watt method, explained in chapter 5.1, which allows for measuring of all the three phases. The control measurements are done with slightly different resistances but they follow the same trend as the original measurements. The original measures are plotted with a straight line in between the measuring points, and this can also explain why the control points differs a bit, especially at an RPM of 1200. A weakness with this test is that the torque is not controlled but the RPM. From measurements during testing it became apparent that the torque was low with high resistance and increased with lower resistance. This is also the reason for highest power at low resistance. Since this test can be a bit misleading, another test was performed where the asynchronous motor is controlled by torque, with results shown in figure 5.9.

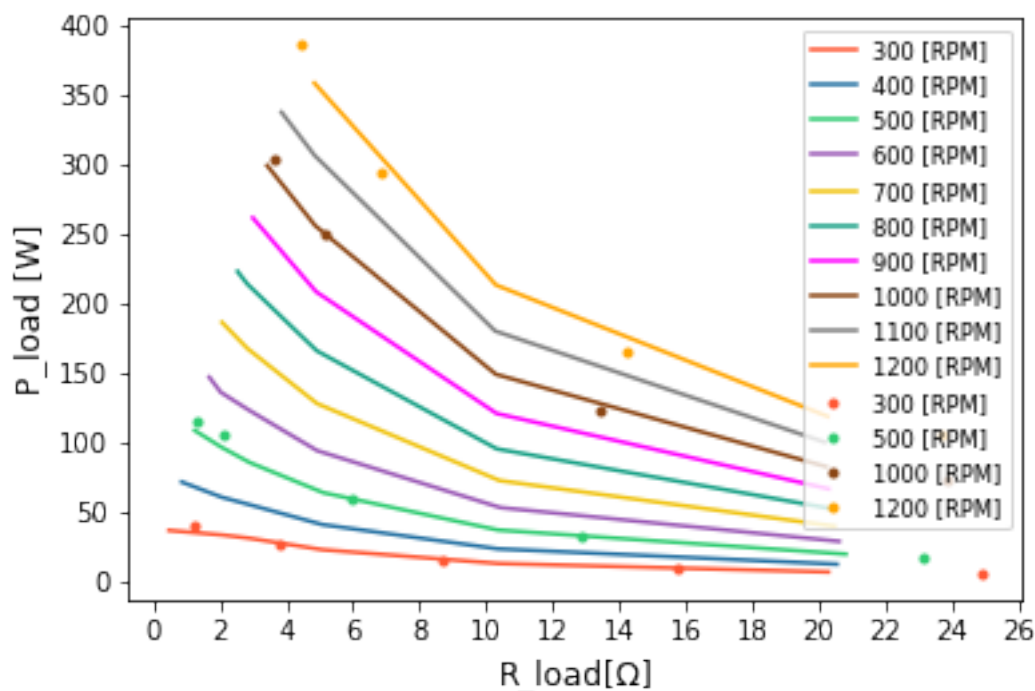


Figure 5.8: Power directly to dump load with different dump load resistances and RPM.

A test was also done with different resistances for increasing torque, yielding somewhat different results. This test gave a power curve, showcasing at which resistance the generator provides the optimal power to the dump load. The results can be seen in figure 5.9, showing that with increasing torque, lower resistance for the dump load will give a higher power to the dump load. The test were again conducted under the constrains

of the assumed phase current of 5.56A, meaning that the upper points of the power curves in figure 5.9 represent the point at which this current is reached, except for the 20, 10 and 8Ω resistance which had to be stopped due to high rotational speeds.

It is clear from these results that the power to the dump load is highly dependent on the resistance and shaft torque, which is again related to the wind speed. Therefore, in order to optimize power output, a variable set of resistances would make for the best solution to cover the operation scenarios for the turbine. For instance, a resistance of 20Ω should be used for a torque in the range 0.5-1.5Nm, while from 1.5-3Nm a resistance of 8-10Ω would be optimal. Finally, at torque higher than 3Nm, the resistance would have its optimum somewhere in between 6-8Ω.

As torque and current are directly proportional, low shaft torque will lead to low currents out of the generator, and a relatively low induced voltage. According to Ohms law saying $U = RI$, the resistance must be quite high in order to reach the voltage drop over the load. As the resistance is the only source drawing current in this circuit, all voltage drop besides losses will take place there. This also means that for high torque, inducing high voltages, leading to high currents, the resistance must be reduced. This explains the somewhat counter intuitive reason why high resistance leads to higher power output at low torque.

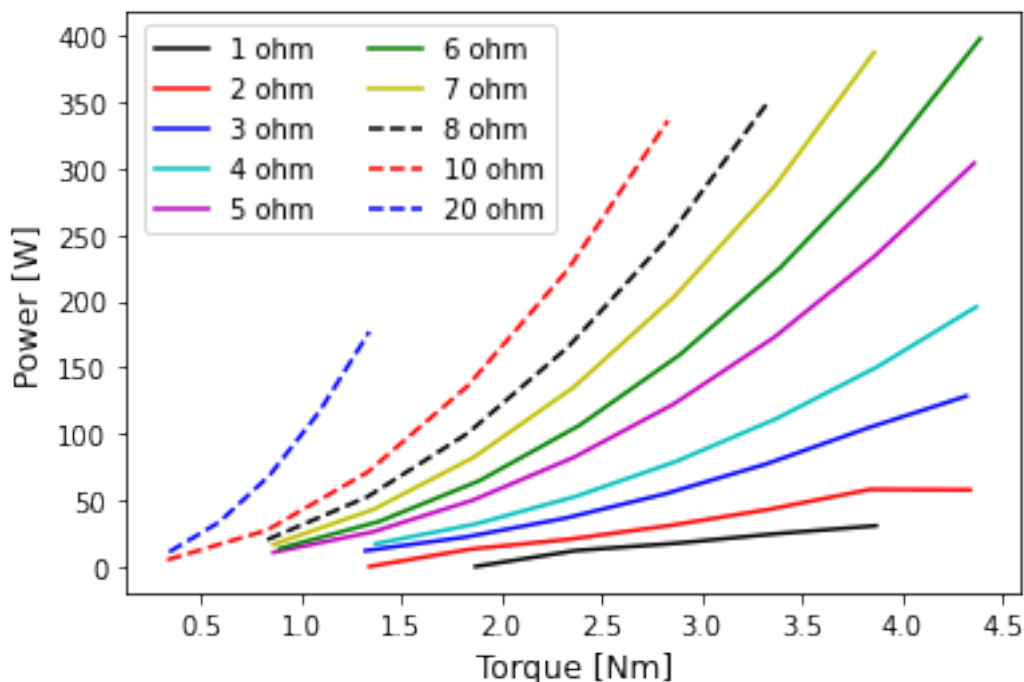


Figure 5.9: Power directly to dump load with different dump load resistances and torque.

Observing the results from figure 5.9 and figure 5.4, the original regulator following the wind turbine must have some sort of electronic load control. Hence it should be an MPPT algorithm embedded in the controller. The information from the producer is very limiting both regarding the wind turbine and the following regulator. Since the regulator does

not require wind measurements it is not TSR controlled. The regulator can possibly be a P&O controller but the most popular MPPT control option for small scale wind turbines is optimal torque control.

The results plotted in figure 5.8 indicates that a low resistance for the dump load gives highest power for each rotational speed. By performing the same test and plotting against torque as in figure 5.9, it became clear that the opposite was favorable for high power. As can be observed in figure 5.9, the highest power is given with high resistance at low torque. To control the wind turbine in a smooth way the electronic load set by the controller should be adjusted smoothly. If the load is set to for example 20Ω up to a torque of 1, and then changed to a load of 10Ω , the turbine will experience a huge change in rotational speed. Both for battery charging and to ensure a long lifetime of the wind turbine this is of importance. If it were to be made a system without batteries, were the power goes directly to the dump load, it could be a possibility to connect several smaller heating elements either in parallel or series by changing the connection of the wires with a switch, to adjust the load depending on the incoming wind speed. To avoid sudden changes in the rotational speed it is important to gradually change the resistance for the dump load in such a system.

5.4 Diversion with DC source

Method

Using the DC source for diversion was the first test done with the Tristar controller, in which correct dimensioning of the dump load is crucial. Using a dump load too small will not enable it to divert enough power from the energy source, leading to overcharging of the battery. Choose a load too large, and currents will exceed the rating of the Tristar, causing the Tristar to disconnect from the dump load. This will lead to all the source current going to the battery. To avoid such errors, a safety margin for the system current is given as two thirds of the rating of the Tristar, which equals 30A for the TS-45 controller. Additionally, current sizing of the dump load must be set to 150% of the rated Tristar current as a diversion load margin.

The rating of the dump load was done with help from a employee at Morningstar, the producer of the Tristar controller. With a rated wind turbine current of 5.56A, combined with a maximum battery voltage of 27.6V, an approximate power to the dump load can be estimated to find the maximum value for the resistance.[70]

The minimum resistance can be found by dividing the maximum voltage by the current limit of the Tristar controller. Assuming maximum voltage equals the battery charging voltage, we get that

$$R_{min} \geq \frac{V_{max}}{I_{limit}} = \frac{27.6V}{45A} = 0.61\Omega \quad (5.1)$$

A calculation of maximum power given the phase current limitation gave a power output from the generator of about 200W. As this limit has shown to be well surpassed from actual measurements, shown in figure 5.6, this power is far too low. Therefore, no maximum resistance was initially set, but rather found from testing with different resistances under controlled conditions. The resistance was initially set to 2Ω for the diversion tests, both with the DC source and with the turbine.

Testing with the DC source first was a good way of confirming that the Tristar controller diverted excess power according to its operation principle. Previous tests with batteries of poor quality had built up an uncertainty as to whether the Tristar worked properly. By using a DC source rather than the turbine it was easier to isolate different parts of the experimental setup, to see where any possible errors might occur. Two rounds of testing with this setup were performed, both with old and new batteries. As the first tests with old batteries did not give expected results, new batteries were bought and the testing redone.

Results and discussion

During testing with old batteries, it was of interest to see how the PWM absorption voltage in the Tristar affected the power to the dump load. Therefore, testing was done with this diversion voltage set to both 27.6V and 28.8V, with results presented in figure 5.10. The current, I_{in} is the current going into the batteries, which normally would be the current after the rectifier when not using a DC source. The power measured at 28.8V is marked with '*' in the figure.

An important note to make is that current and voltage measurements were done using a multimeter, instead of the Tristar data logging program, leading to a certain deviation in both current and voltage readings. This is due to the PWM signal, explained in chapter 2.5.3, which causes the signal from the Tristar to be turned on and off during duty cycles, reducing the overall current going to the dump load. The Fluke clamp meter, however, cannot reach the same frequency of the current, and will not read the signal fast enough, leading to inaccuracies in the readings. It is, however, a good way of illustrating inaccuracies and limitations with the experimental equipment used. The Fluke clamp meter measurements were pretty close to the logging from the Tristar, hence this test is therefore not repeated with the use of the logging program

As can be seen from the figure, power to battery is decreasing while power going to the dump load is steadily increasing for both voltages. At the far left of the figure, the Tristar has just begun diverting, and thus most of the current is still going to the battery to charge it. This is to be expected as the battery will get power until it's fully charged, at which point the battery power will be reduced to the amount required to maintain battery voltage. It is worthwhile to note that the power from the wind in these cases is a

”fictive” value, as it is a pure DC source, exceeding the phase current limit of 5.56A used in other tests. For the DC supply, current was varied all the way up to 10.2A, which gave a maximum power output of 283.8W and 293W for the two tests. It was observed that a higher diversion voltage led to more power going to the battery, which is to be expected as the battery needs to reach a higher voltage before diverting. As the battery diversion voltage is increased from 27.6V to 28.8V, it takes somewhat longer to reach target voltage, leading to lower voltage on the dump load as well, giving less power to the dump load for the same current.

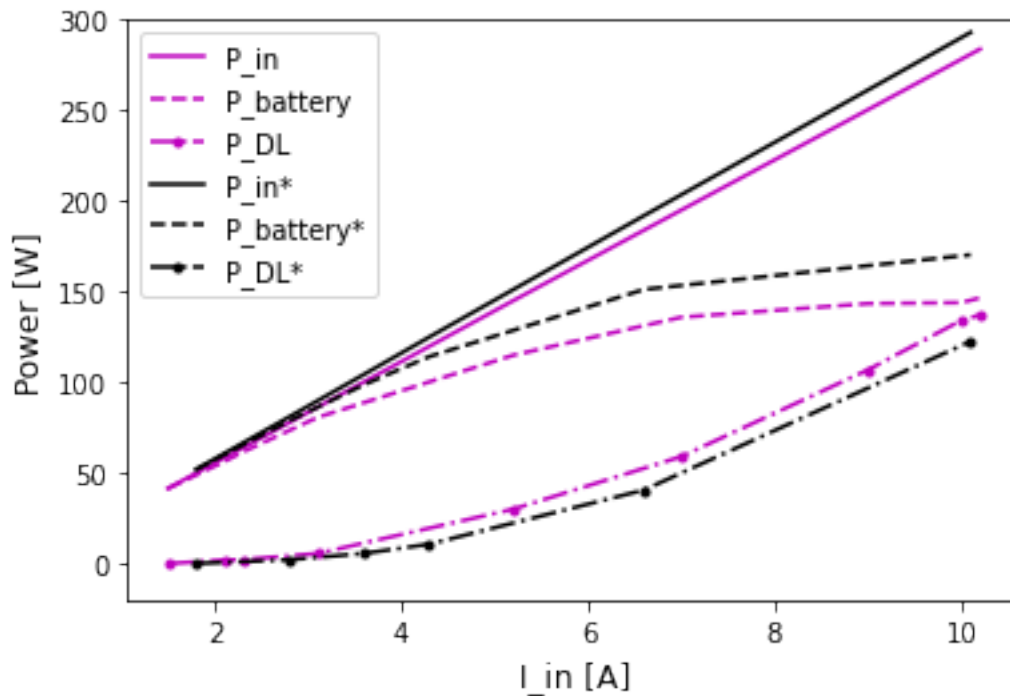


Figure 5.10: Comparison of diversion with DC source, using old batteries, with diversion voltage set to 27.6V. For plots marked ’*’, diversion voltage was set to 28.8V. Power plotted against current to the batteries.

The same test was repeated with new batteries, with a diversion voltage of 27.6V, to illustrate how battery condition impacts the power distribution, as well as testing the quality of the original batteries in the system. Results presented in figure 5.11 showed that with an increasing current to the batteries, the rate of power to the dump load is significantly higher than to the batteries. This is as to be expected, as the new batteries won’t demand much power to maintain battery voltage, meaning most of the power will go to the dump load. For this test, power and current measurements were done using the Tristar data logging program, accounting for PWM signals. Although the data from testing of new and old batteries cannot be compared directly due to different measuring methods, it gave an indication that the batteries were due for an upgrade in order to get the desired results.

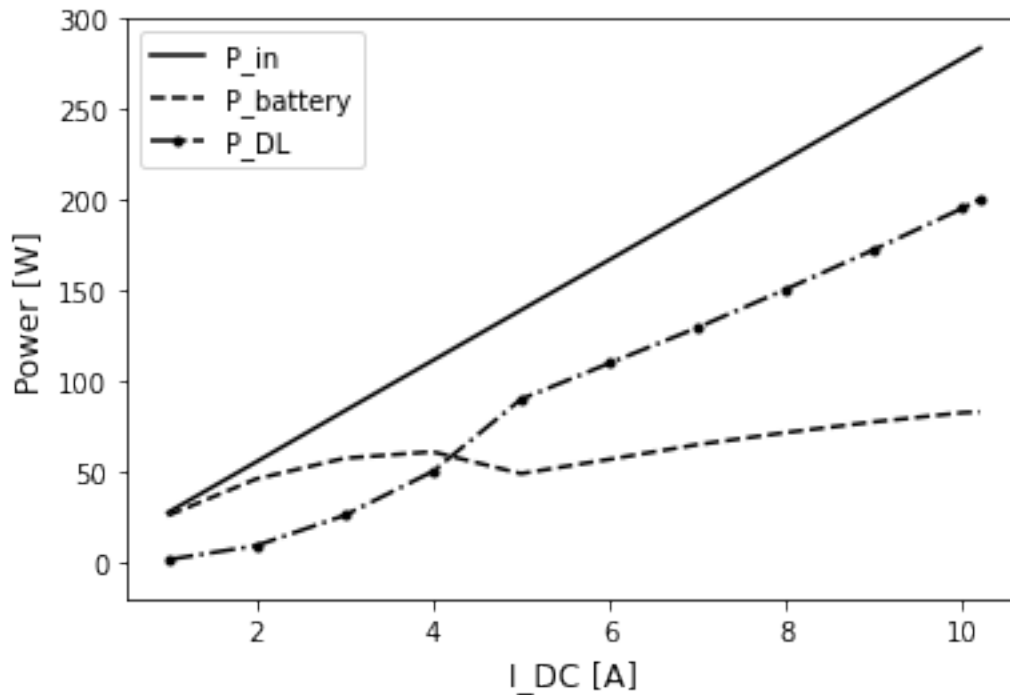


Figure 5.11: Diversion test with DC source with new batteries, with diversion voltage set to 27.6V. Power plotted against current to the batteries.

5.5 Diversion testing with wind turbine

Method

One of the to assess main tasks to assess was the performance of the Tristar controller during operation. Having both the batteries and the dump load in the system allowed us to see how voltage and power were distributed during diversion mode, and how the battery voltage inflicted the diversion voltage. To observe the diversion more clearly, an oscilloscope was used for early stage testing. During operation with the battery charging, it was clearly observed that diversion took place just around the voltage of 27.6V set on the Tristar, at which point it began diverting to the dump load.

After first doing the diversion test with a DC source, the actual diversion test could be conducted, with the certainty that the experimental setup worked according to expectations. In order to see if the Tristar and the turbine controller would work together, testing under the same conditions were done, both with and without the turbine controller in the setup.

Results and discussion

By using the same resistance for the dump load, at 2Ω , and adding a bridge rectifier, results for both tests were as shown in figure 5.12. Power from the wind, into the batteries and into the dump load; P_{wind} , $P_{battery}$ and P_{DL} , respectively, are plotted against torque,

which was manually varied using the asynchronous machine. Results revealed that the power to both the dump load and the battery was close to equal in both scenarios. This showed that the two controllers had no issues being used in the same system, and did not interfere with one another during diversion. As the Tristar is made for protecting the battery, the turbine controller is also meant for protecting the turbine itself, the two of them could potentially limit operation voltage. As this was not the case, the turbine controller was later left out for simplicity, but power and current were held under their rated values in order to avoid equipment failure. During testing, a significant temperature increase was felt with the rectifier, further increasing losses.

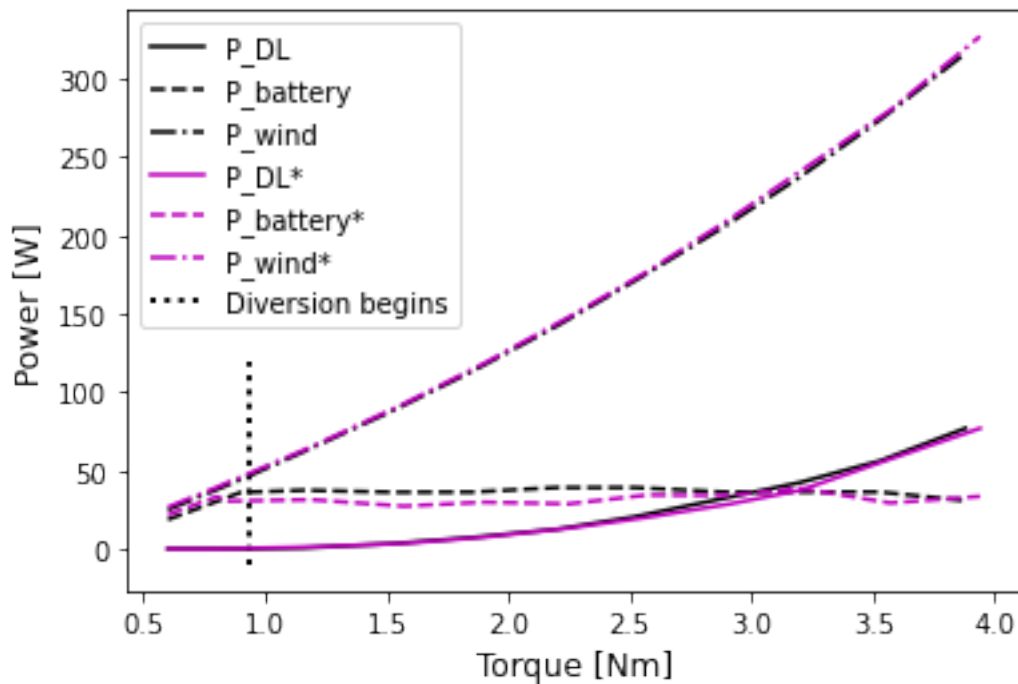


Figure 5.12: *Diversion test with new batteries with and without the turbine controller, plotted against torque on the wind turbine. Power marked with * are measurements done without the turbine controller.*

As the main objective of the thesis is experimental testing of a commercial small scale wind turbine to heat storage, an actual heat storage was later used as dump load rather than just the variable resistance. It was decided to use an oil based heat storage, as this had already been built for use in similar previous projects. This heat storage unit is shown in figure 4.15 and is filled with duratherm oil. By the use of temperature sensors and PicoLog, a computer program for data logging, the temperature development in the cylinder could be measured as the power from the turbine increased.

As a resistance of 2Ω had been used in previous stages for testing, this was also firstly used in the diversion test with a heat storage. Two heating elements of 1Ω in series, each with a rated power of 170W, were used in the heat storage for heating the oil. Three temperature sensors were used for logging the temperature increase, which can be seen in

figure 5.13. Over a time span of about two hours, the power to the dump load heated up the oil to a temperature of 100°C in the upper part of the heat storage. The bottom part had then reached a temperature of 67°C , giving an average temperature in the cylinder of about 85°C . A thermocouple were also added at the outside of the tank to observe the heat loss. It reached a maximum temperature of around 35°C .

The power input from the generator was increased slowly to begin with, giving a minor temperature increase, but was then kept constant at around 120W for the duration of the test, leading to an almost linearly curve. The AC power measured from the generator was held constant at 120W for the duration of the test, as previous testing had given quite a large temperature increase on the generator. To prevent the wiring inside from overheating from continuous running for two hours, the power was therefore held at a lower value. For demonstration purposes the test is stopped at a temperature of 100°C in the heat storage.

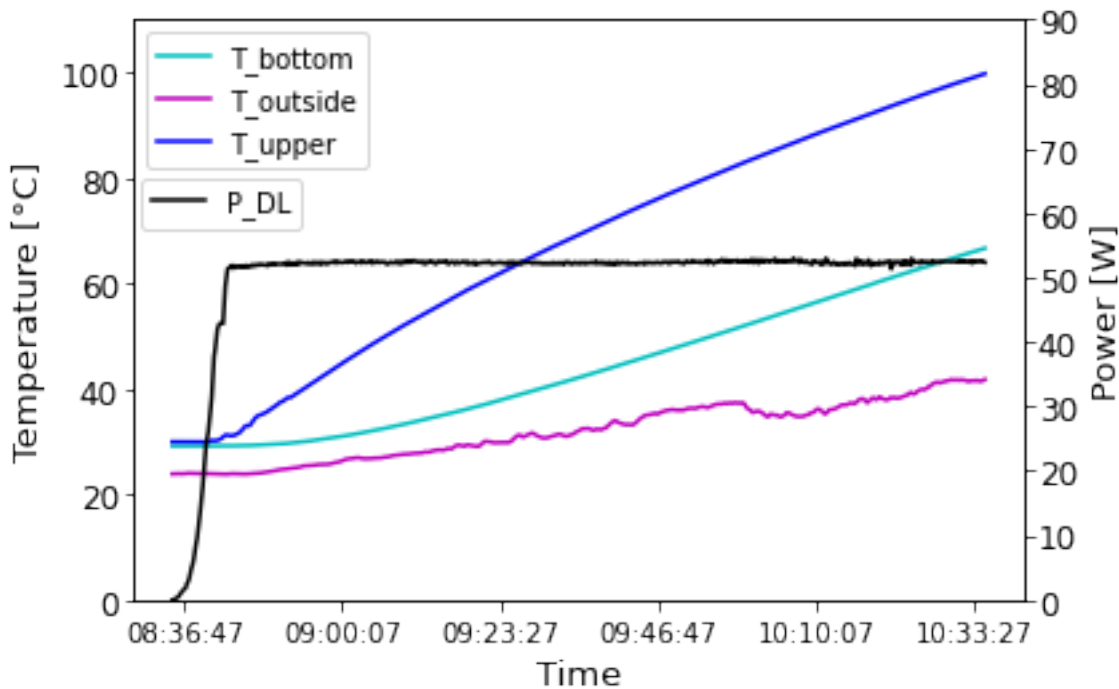


Figure 5.13: *Temperature increase and power to dump load over time at 2Ω .*

Testing of different resistances varying from 1Ω to 10Ω presented in figure 5.15, using the three-phase rheostat revealed a higher power output using a higher resistance. Heating of the dump load was therefore repeated with a few more heating elements, giving a total resistance of 6Ω . The total of five heating elements is not ideal for the low power used in the test since the heating elements are rated for higher power. This will result in lower surface temperature of the heating elements compared to what is ideal. Due to limited access to heating elements during the time of testing, the test were performed with the five of them to get the desired total resistance of 6Ω . A few more temperature sensors were also included for this test, all in which can be seen with their temperature increase

in figure 5.14. Again, the oil was heated until the upper part reached 110°C , at which point the average temperature in the cylinder was 103.4°C . Since five heating elements were used in the cylinder for this test, the heat is more evenly distributed in the cylinder, causing a higher average temperature. The power from the generator was for this test held constant at around 140W , slightly above that for the 2Ω test. The reason was again the previous testing, revealing that a 6Ω resistance was better suited for high input power operation. To avoid overheating of the generator it was not of interest to go any higher in power for an extended period of time.

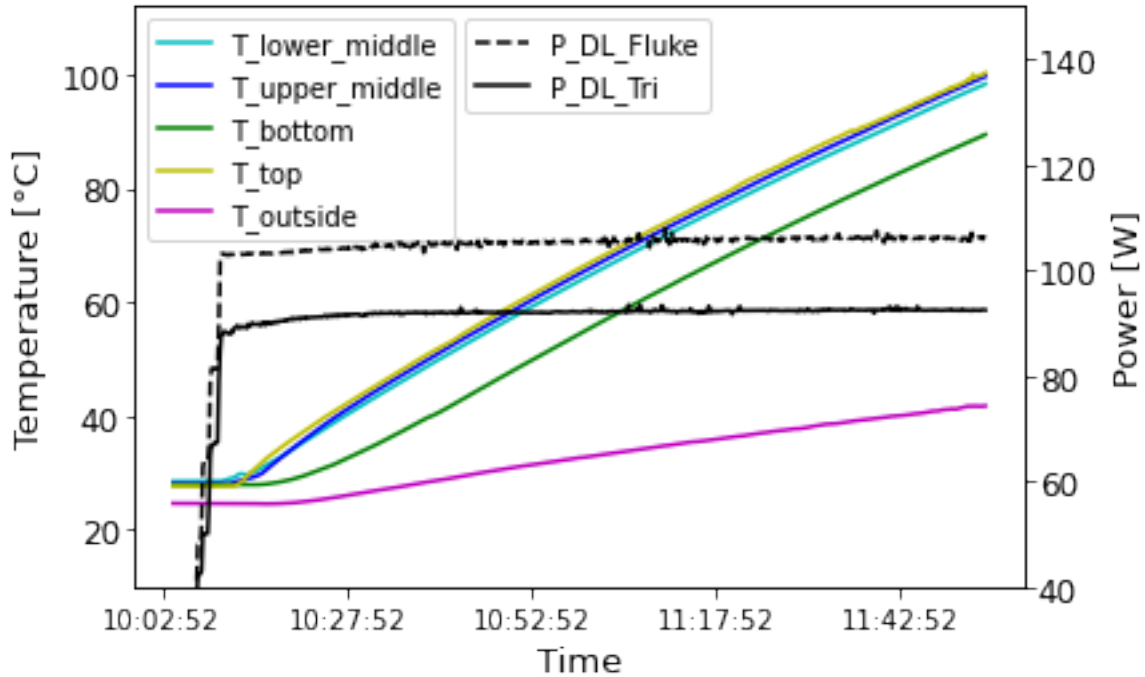


Figure 5.14: Temperature increase and power to dump load over time at 6Ω . Power is plotted for currents both measured by Tristar logging program and the actual current measured by the Fluke clamp meter.

The two power measurements presented in figure 5.14 are based on two different current measurements; using the Tristar data logging program and the Fluke clamp meter. During testing, the current to the dump load was measured manually at different RPM, which revealed a significant deviation from the Tristar logging. This is due to the PWM signal discussed in chapter 5.4. This means that the power P_{DL_Tri} shows the correct measurements, and should be used rather than a multimeter or clamp meter presented as P_{DL_actual} in figure 5.14.

To compare the theoretical concepts with the practical work, a heat calculation was done in order to see how much power is needed for the dump load to reach its desired temperature. This was done using the intensive properties of the duratherm oil found in appendix B, and a oil volume of 3.97L . With an initial temperature of 28.06°C at 6Ω , and a time frame of two hours, it was found from the results that the temperature in the tank

reached 103.4°C. Using the average temperature at around 65°C to find density and heat capacity, these values were found to be $\rho = 835 \frac{kg}{m^3}$ and $c = 2.08 \frac{kJ}{kgK}$, respectively. With the use of equation 2.24, the energy, Q , needed to heat the oil was found to be;

$$Q = 3.97L * 835 \frac{kg}{m^3} * 10^{-3} m^3 * 2.08 \frac{kJ}{kgK} * (103.4 - 28.06)K = 519.48kJ \quad (5.2)$$

This was further calculated to an average power input, P_{DL} , as there are 3600 seconds per hour, and 1kJ=1kWs;

$$P_{DL-theoretical} = \frac{519.48kWs}{2 * 3600s} = 0.072kW = 72W \quad (5.3)$$

This power calculation was done for the 6Ω test, which had five heating elements evenly distributed in the cylinder. The same calculation for a resistance of 2Ω was not found as it was too inaccurate to assume the average temperature with only two temperature sensors. The average power to the dump load for the same time frame given from the results for the 6Ω and 2Ω test gave an actual power input of 92W and 50W, respectively. For the 6Ω cylinder, this means that losses would be around 20W, as this corresponds to the difference in actual and theoretical power to heat the oil.

A diversion test with different resistances as dump load was performed to see how this influences Tristar diversion. The test is done with different torque, starting at 0.3Nm increasing up to 3.8Nm, with different resistances ranging from R_{min} to R_{max} connected as dump load, as shown in figure 5.15. Figure 5.15a shows the power going to the batteries, figure 5.15b shows the power going to the dump load and figure 5.15c shows the sum of the power going to both the batteries and dump load.

From figure 5.15c it can be observed that the total incoming power ranges between approximately 10-200W for corresponding dump load resistance of 1, 2, 4 and 6Ω. When the torque is set to 2Nm or higher the power for dump load resistance 8 and 10Ω deviates from the others. This is because they are outside the R_{min} - R_{max} range for the corresponding power. However, they are included in the result to show how overdimensioning of the dump load resistance affects the system. From testing it could be observed that the battery voltage started to increase at 2Nm, hence the increase in power. If this is continued for a long period of time it will overcharge the batteries.

It can be observed from figure 5.15a and 5.15b that dump load resistance has a great influence on Tristar diversion. A resistance of 1Ω results in a low power to the dump load and a high power to battery charging since the dump load won't handle all the power, which over time will overcharge the batteries. The resistance of 1Ω is within R_{min} of the Tristar manual but this limit only takes into account the current limit of the controller at 45A. The manual also states that if the dump load resistance is too small the batteries will overcharge [69]. A resistance of 1Ω is therefore too small for the system. A resistance of around 6Ω gives highest power to the dump load for almost all power up to 200W. For all the resistances some power goes to the batteries. Some of this power has to go to the

battery to remain the diversion voltage set at the Tristar but this power will get lower and lower as the battery gets fully charged. Considering these results, proper dump load dimensioning is of importance when designing a diversion system.

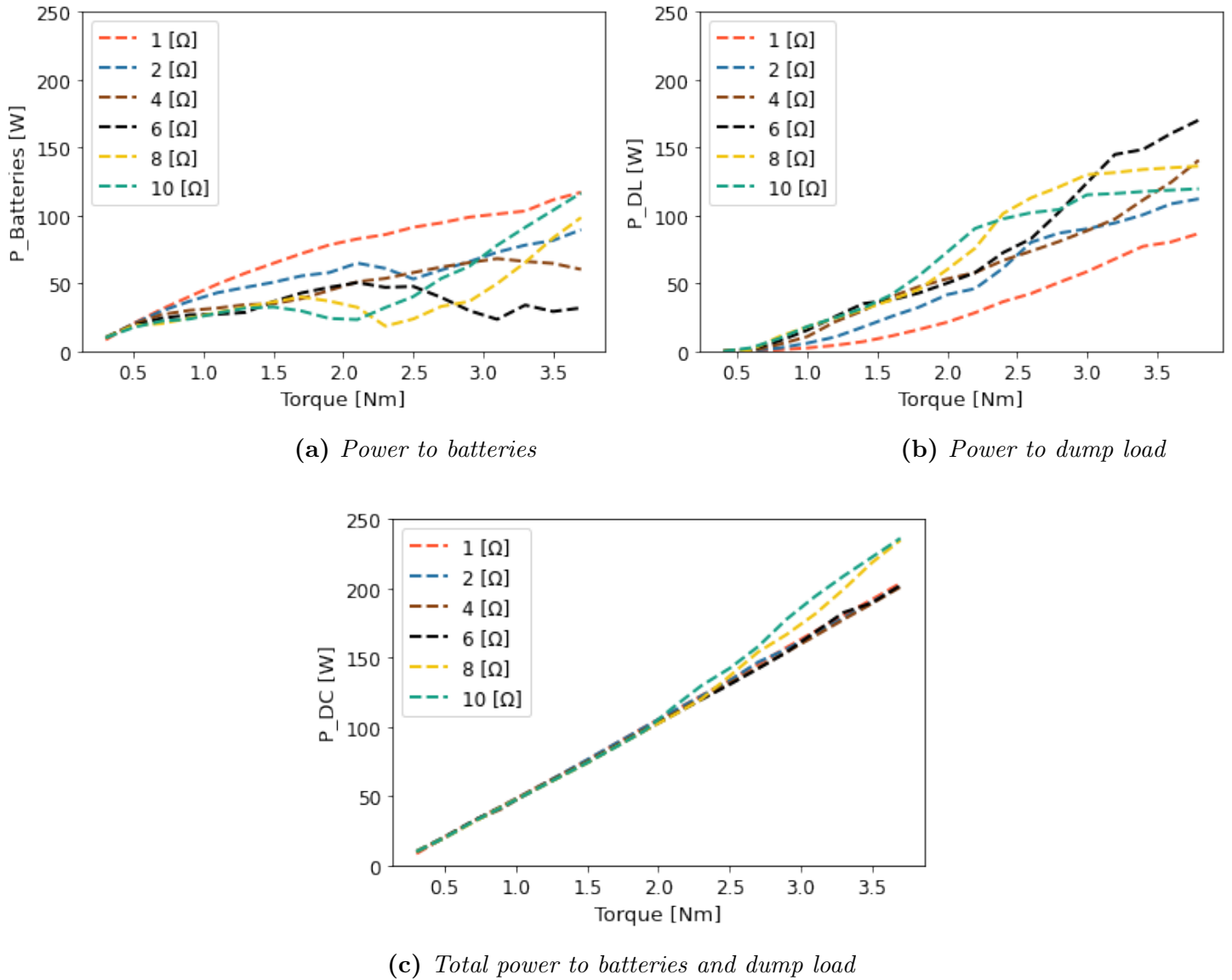


Figure 5.15: *Diversion test with variable resistance and torque*

During diversion testing with a 6 Ω dump load it was observed that the load voltage would start at zero, slowly approaching battery voltage, while the battery voltage was held somewhat constant for the most part. The battery voltage is independent of the duty cycle and will only vary with the incoming current and voltage from the generator. The load voltage, however, follows the duty cycle and is shown in figure 5.16 for the 6 Ω dump load used in the experimental setup. Figure 5.17 shows how duty cycle increases over a time span of two hours, as the load voltage approaches battery voltage, and will give an indication of how much of the power is being diverted to the dump load.

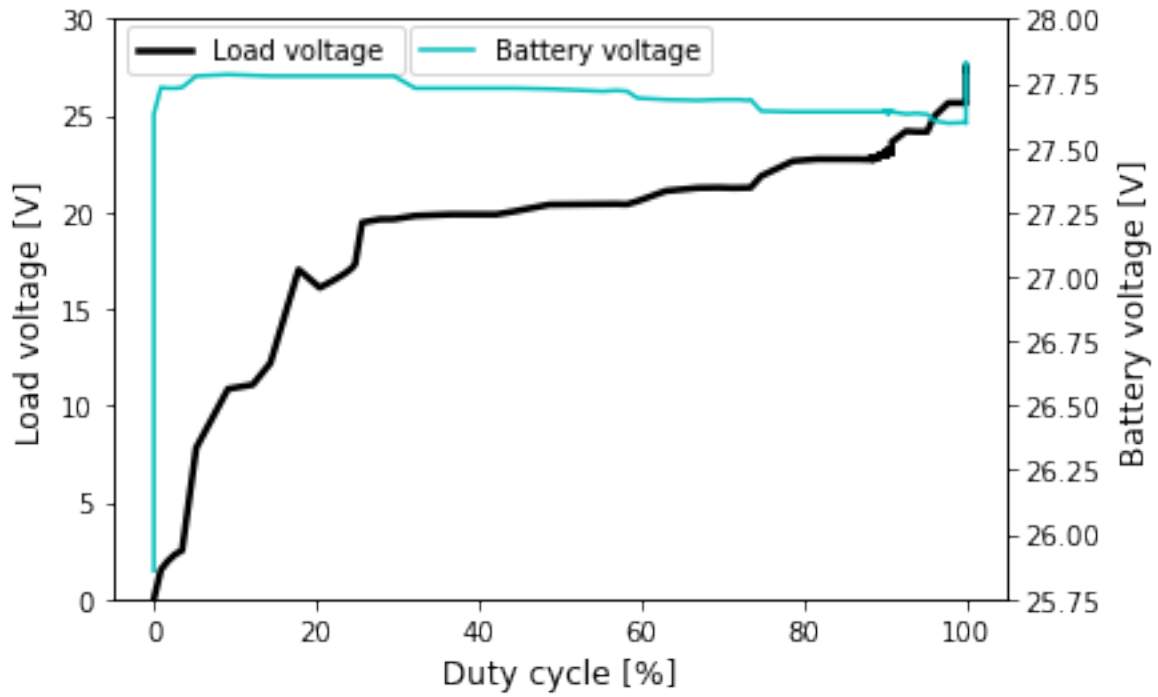


Figure 5.16: Load and battery voltage plotted against duty cycle.

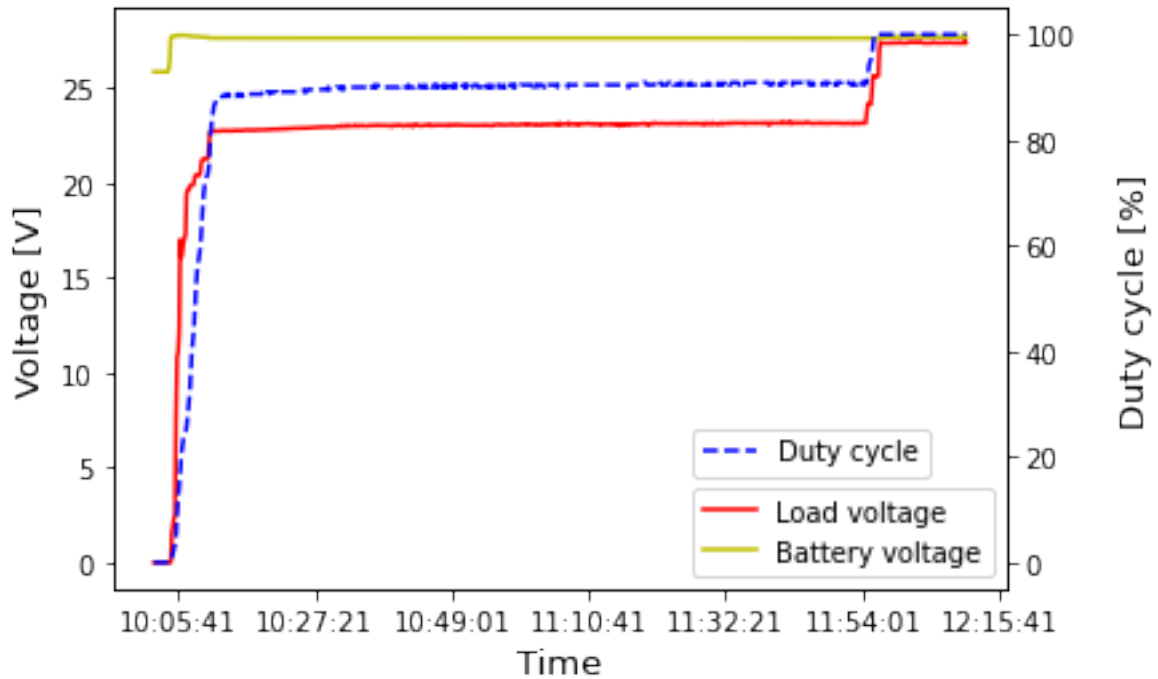


Figure 5.17: Load voltage and duty cycle increase towards battery voltage over time.

This duty cycle is based on the concept of PWM explained in chapter 2.5.3. For a duty cycle of 100%, the "on time" of the voltage signal is 100%, giving the maximum voltage, which should be equal to the battery voltage. At the point in which duty cycle reaches 100%, the battery is fully charged, and ideally all power will flow to the dump load. In 5.15a It can be observed that with a correctly dimensioned dump load, as with the 6Ω

resistance the power to the batteries decreases from a torque of around 2.5-3.8Nm. At this point the duty cycle is close to 100% and the batteries are nearly fully charged. If this power would have been maintained for a longer period of time it is expected that the power to the batteries would decrease towards zero, if not they will get overcharged.

5.6 Sources of error

Although not a source of error itself, large heat losses and other losses in the system have been assumed equal to those present in an actual wind turbine driven system outside. Results should therefore be evaluated with a margin of error regarding such losses, to account for differences that appear in tests such as those conducted in this thesis. Testing has, however, been done in a manner to represent the conditions of varying outdoor wind speeds. During testing, the air running the turbine has been simulated by a machine, creating a steady and laminar flow. In a real operating scenario, the air flow is often more turbulent close to the ground, creating unstable and frequently varying wind conditions. Thus, the power generated in the conducted tests will be far more consistent than that of an outside turbine. By using a DC-DC converter, however, power output will be far more consistent, as a large interval of voltages is taken in and stepped up or down maintaining a steady output voltage.

In an effort to simulate the wind conditions in a more controller manner, the wind tunnel at NTNU was meant to be used. That way, the experimental setup could be brought to the wind tunnel to repeat tests there, to get a clear indications on how representative the lab tests actually were. It turned out, however, that the wind turbine, with a blade diameter of 1.4m, had too big of a sweeping area for the wind tunnel. As the height of the tunnel is just about 1.8m, it wouldn't nearly be able to properly simulate real wind conditions, due to turbulence, and a large blockage of the tunnel at about 30%. Testing in the wind tunnel would also be of great value in order to see which wind speeds corresponds to which rotational speed, as all tests done with the asynchronous machine were done in torque control, displaying the rotational speed.

Several tests done on diversion revealed issues regarding the working of the Tristar controller. While it was informed by the manufacturer of the controller that dump load voltage would equal the battery voltage during diversion, this was not the case for the most part. It was evident from tests done on diversion that the dump load voltage increased gradually upwards of the battery voltage, and for a resistance around 5-8ohm managed to reach a duty cycle of almost 100%. For the remaining tests, however, the voltage remained quite a bit lower, leading to some power loss from the battery to the dump load.

With several heating elements placed in the cylinder, an accurate estimation of temperature development is difficult to obtain. This is due to uneven temperature increase as a result of stratification in the cylinder. Therefore, deciding on an average temperature for certain calculations can deviate somewhat, also due to uncertainty in the Pico logger

provided as the sum of $\pm 0.2\%$ of the reading, and $\pm 0.5^\circ\text{C}$. [71]

Human error will always be a potential source of error in cases where manual measurements and work is done. During a few of the tests, readings on the asynchronous machine and the power meter were written down by hand. Combined with inaccurate calibration of the experimental equipment, this allows for some deviation from actual measurements, although measures were taken in order to minimize these errors. As testing was mostly done within short time periods, the turbine generator did not have time to cool down properly, enabling small errors as the coils in the generator heat up over time.

6 Conclusion

This thesis is a continuing work of a literature study done on small scale wind power to heat storage. The objective of this work is experimental testing of a commercial small scale wind turbine to a heat storage, and a further literature review on small scale wind power to heat.

An already existing 400W wind turbine placed on the roof of NTNU was meant to be used for the experimental work in this thesis, but was early on revealed to be poorly placed, barely giving any power output due to poor wind conditions. It was therefore decided to take the turbine down from its original location outside, and rather be mounted in the lab under controlled conditions. This was done using an asynchronous machine, which could be operated in either RPM or torque control, controlling the power from the "wind".

The wind turbine used for testing was stapled with a rated current limit. Preliminary testing from the roof revealed that this current limit of 5.56A given for the generator was well surpassed under several occasions when winds were particularly high. It was unclear as to what this value meant, but was assumed to be the maximum phase current in the three phase generator. Under operation in the lab, however, the turbine generator went hot when exposed for currents around the limit. This led to all testing being done under restricted power input, to prevent the coils in the generator from burning up. It was concluded that the turbine will be naturally cooled down from the air when placed outside, which allows for the current limit to be surpassed and still avoiding the coils from overheating. For all tests, the current limit of 5.56A was still complied with, which gave a power input from the wind at about half of its rated power of 400W, when being connected to a battery.

An experimental setup was mounted in the lab, consisting of the generator, two 12V batteries, a dump load and a controller. The controller used for the diversion was a Tristar, meant to divert excess power from the energy source to a dump load after charging up the batteries. A variable resistance was used in order to find an optimal resistance for the dump load. Based on several tests both with diversion mode using the Tristar controller, an optimal resistance was found to be around $4-6\Omega$ when the generator produces a power up to 200W. This was applied for further tests with a heat storage, where a small cylinder filled with Duratherm oil was heated up to 100°C in order to see how much power would be diverted under normal operation. It was found that an insulated tank of oil would require about 185Wh to heat four litres of oil to the desired temperature, compared to a theoretical amount of 144Wh. Based on the theoretical amount, this gives a heating efficiency of 77.8% in the dump load, which can be further improved by better insulation of the cylinder.

Testing done on direct wind to heat with the use of the original wind turbine controller was found to be uncompliant, since the original controller was designed for battery charging. The wind turbine controller was designed to charge a 12V or 24V battery package, and when being connected to a dump load directly it observed the dump load as a 12V

battery. The wind turbine could therefore only generate half its potential power and braked the turbine when the voltage exceeded the controllers limit for charging of a 12V battery system, which is set to prevent overcharging of the batteries. Without the use of the turbine controller, however, the turbine was allowed to operate beyond these values, giving an optimum dependent upon the applied shaft torque. A solution with dump load resistance varying with wind speed can be designed from the given results such that a resistance configuration would be set after wind conditions, easily implemented by an automatic system utilizing switches. Several heating elements can be connected as dump loads in either series or parallel to change the resistance. Such a controller can be made if it is not desired to implement batteries in the system.

Choosing the right controller is an essential part of a hybrid off-grid system consisting of a wind turbine and PV panels. As the wind is an intermittent energy source, offering frequently varying power, harvesting this energy in an efficient way can be challenging. A MPPT controller is highly applicable for wind powered systems, and can be designed in different ways, including torque control, perturbation and observation or TSR control utilizing wind speed sensors. Where torque control is the most popular MPPT control design for wind turbines. A buck-boost converter can also be implemented in a controller if batteries are included in the circuit, since battery charging needs to take place within a certain range of voltages. This enables a stable power output to a battery or dump load, also protecting the battery from overcharging at high voltages.

7 Further work

As all tests were done in the lab due to poor wind conditions at the original test cite, actual wind conditions have been attempted simulated as best as possible. It was, however, not possible to test the wind turbine in a wind tunnel as planed, leading to uncertainties as to which RPM corresponded to what wind speed. For further work it would therefore be of great value to repeat the testing in an environment more suited, with better and more stable wind conditions. Alternatively, a smaller wind turbine could be used and tested in the wind tunnel.

It is still somehow uncertain as to whether the turbine controller is in fact an MPPT controller. It would therefore be of interest to look into this, so that the power in to the battery and dump load is optimized. A way of doing this could be based on lab testing done in this thesis, preferably repeated for more reliable results. By setting different configurations of the resistances in the dump load, intervals for the power from the generator could be defined, so that the dump load resistance would vary with the wind speed. This would enable an optimized power tracking system, similar to that of an MPPT controller.

A combined controller should be considered for the purpose of this project, enabling both diversion and maximum power point tracking. As the Tristar is not an MPPT controller, a new controller is advised. A new controller should also be able to convert DC voltage within a certain range to a constant voltage, i.e. a DC-DC converter.

A final hybrid system should be tested utilizing both solar and wind power. This system needs MPPT control units designed for optimal PV and wind turbine performance. A single heat storage unit should be used for both solar and wind.

References

- [1] Worldbank. *Tanzania — Data*. URL: <https://data.worldbank.org/country/tanzania?view=chart> (visited on 09/09/2022).
- [2] Multiconsult. *Clean Energy Transition in Tanzania*. Tech. rep. Apr. 2022. URL: <https://www.norway.no/contentassets/00c56b3642e5429fbc917d5fa42ff869/clean-energy-transition-in-tanzania-report.pdf>.
- [3] Rural energy agency. *ENERGY ACCESS AND USE SITUATION SURVEY IN TANZANIA MAINLAND*. Tech. rep. Apr. 2020. URL: <https://rea.go.tz/News-Center/energy-access-and-use-situation-survey-in-tanzania-mainland-april-2020-2>.
- [4] WWF. *Learn the effects of deforestation*. en. URL: <https://www.wwf.org.uk/learn/effects-of/deforestation> (visited on 09/09/2022).
- [5] WHO. *Household air pollution and health*. en. URL: <https://www.who.int/news-room/fact-sheets/detail/household-air-pollution-and-health> (visited on 09/09/2022).
- [6] *Evolution of solar PV module cost by data source, 1970-2020 – Charts – Data & Statistics*. en-GB. URL: <https://www.iea.org/data-and-statistics/charts/evolution-of-solar-pv-module-cost-by-data-source-1970-2020> (visited on 03/13/2023).
- [7] Henrik Finsås and Torbjørn Mjåtveit. *Small scale wind power to heat storage*. en. Tech. rep. NTNU, Dec. 2022.
- [8] Alexander Peter Olsen. *Design and testing of a natural circulating heat storage for cooking*. en. Tech. rep. June 2022, p. 155. URL: <https://ntnuopen.ntnu.no/ntnu-xmlui/handle/11250/3023803>.
- [9] Andreas Bjørshol and Gunn Helen Nylund. *Single Tank Oil Based Heat Storage for Cooking*. en. Tech. rep. June 2021, p. 167. URL: <https://ntnuopen.ntnu.no/ntnu-xmlui/handle/11250/2787173>.
- [10] Trond Toftevaag. *Personal communication*. NTNU, Mar. 2023.
- [11] Yahia Baghzouz. *Synchronous generators 1&2*. UNLV, 2012. URL: <http://www.ee.unlv.edu/~eebag/EE%5C%20340%5C%20Sync%5C%20Generators%5C%20I.pdf>.
- [12] Stephen Chapman. *Chapman, 5e «Electric machinery fundamentals*. en. 5th ed. McGraw Hill International Edition. 2012.
- [13] National high magnetic field Laboratory. *Permanent Magnet Definition - MagLab*. en. URL: <https://nationalmaglab.org/about-the-maglab/around-the-lab/maglab-dictionary/permanent-magnet/> (visited on 03/13/2023).
- [14] Gordon Slemon. *Electric generator — instrument — Britannica*. en. Feb. 2023. URL: <https://www.britannica.com/technology/electric-generator> (visited on 03/13/2023).
- [15] Dura Magnetics. *Top Causes of Demagnetization of Permanent Magnets — Dura Magnetics*. en-US. Jan. 2022. URL: <https://www.duramag.com/techtalk/magnet-design/causes-demagnetization-permanent-magnets/> (visited on 05/29/2023).
- [16] Colin Bayliss and Brian Hardy. *Chapter 23. Distribution Planning — Elsevier Enhanced Reader*. en. DOI: 10 . 1016 / B978 - 0 - 08 - 096912 - 1 . 00023 - X.

- URL: <https://reader.elsevier.com/reader/sd/pii/B978008096912100023X?token=1BFBCC91B14B62DF5573F73B3EDD160F4816F6E56CE5B7819F451DEDCC194FC28690B5481E54A6D6CAA0C4473201E7E0&originRegion=eu-west-1&originCreation=20230321074908> (visited on 03/21/2023).
- [17] The editors of encyclopaedia Britannica. *Engineering — Definition, History, Functions, & Facts — Britannica*. en. URL: <https://www.britannica.com/technology/reactance> (visited on 03/21/2023).
- [18] Electrical volt. *Losses and Efficiency of an Alternator*. URL: <https://www.electricalvolt.com/2023/01/losses-and-efficiency-of-an-alternator/> (visited on 04/26/2023).
- [19] Manish Kumar Saini. *Losses and Efficiency of an Alternator*. en-US. URL: <https://www.tutorialspoint.com/losses-and-efficiency-of-an-alternator> (visited on 04/26/2023).
- [20] Cirris. *Temperature Coefficient of Copper*. URL: <https://www.cirris.com/learning-center/general-testing/special-topics/177-temperature-coefficient-of-copper> (visited on 03/20/2023).
- [21] A. McDonald and J. Carroll. *8 - Design of generators for offshore wind turbines — Elsevier Enhanced Reader*. en. DOI: 10.1016/B978-0-08-100779-2.00008-8. URL: <https://reader.elsevier.com/reader/sd/pii/B9780081007792000088?token=DCC41B64D3FEE5D54E90F729F3079277B643E85DF2478495F757D0269D4721CB2F893CB532C354E356BB081DCC887D14&originRegion=eu-west-1&originCreation=20230320161804> (visited on 03/20/2023).
- [22] Electrical deck. *Types of Losses in a Transformer - Iron & Copper Losses*. URL: <https://www.electricaldeck.com/2020/12/types-of-losses-in-transformer.html> (visited on 03/20/2023).
- [23] Jan A. Melkebeek. “Rectifier”. en. In: *Electrical Machines and Drives: Fundamentals and Advanced Modelling*. Ed. by Jan A. Melkebeek. Power Systems. Cham: Springer International Publishing, 2018, pp. 233–261. ISBN: 978-3-319-72730-1. DOI: 10.1007/978-3-319-72730-1_7. URL: https://doi.org/10.1007/978-3-319-72730-1_7 (visited on 11/04/2022).
- [24] Wayne Storr. *Rectification of a Three Phase Supply using Diodes*. en. June 2018. URL: <https://www.electronics-tutorials.ws/power/three-phase-rectification.html> (visited on 03/14/2023).
- [25] Thieu Ngô. “RASHID, M. H. (2001) Power Electronics Handbook”. en. In: (). URL: https://www.academia.edu/9565229/RASHID_M_H_2001_Power_Electronics_Handbook (visited on 04/24/2023).
- [26] Safiullah Faqirzay and H. D. Patel. “Maximum Power Extraction from Wind Generation System Using MPPT Control Scheme through Power Electronics Converters”. en. In: *IJIREEICE* (Mar. 2015), pp. 141–146. ISSN: 23212004. DOI: 10.17148/IJIREEICE.2015.3332. (Visited on 04/13/2023).
- [27] J. N. Sørensen, V. Okulov, and N. Ramos-García. “Analytical and numerical solutions to classical rotor designs”. en. In: *Progress in Aerospace Sciences* 130 (Apr. 2022), p. 100793. ISSN: 0376-0421. DOI: 10.1016/j.paerosci.2021.100793. URL:

- <https://www.sciencedirect.com/science/article/pii/S0376042121000956> (visited on 03/29/2023).
- [28] Ibrahim Al-Bahadly. “Building a wind turbine for rural home”. en. In: *Energy for Sustainable Development* 13.3 (Sept. 2009), pp. 159–165. ISSN: 0973-0826. DOI: 10.1016/j.esd.2009.06.005. URL: <https://www.sciencedirect.com/science/article/pii/S0973082609000489> (visited on 12/04/2022).
- [29] Office of energy efficiency and renewable energy. *How Do Wind Turbines Work?* en. URL: <https://www.energy.gov/eere/wind/how-do-wind-turbines-work> (visited on 09/21/2022).
- [30] Abhishiktha Tummala et al. “A review on small scale wind turbines”. en. In: *Renewable and Sustainable Energy Reviews* 56 (Apr. 2016), pp. 1351–1371. ISSN: 1364-0321. DOI: 10.1016/j.rser.2015.12.027. URL: <https://www.sciencedirect.com/science/article/pii/S1364032115014100> (visited on 11/03/2022).
- [31] M. A. Abdullah et al. “A review of maximum power point tracking algorithms for wind energy systems”. en. In: *Renewable and Sustainable Energy Reviews* 16.5 (June 2012), pp. 3220–3227. ISSN: 1364-0321. DOI: 10.1016/j.rser.2012.02.016. URL: <https://www.sciencedirect.com/science/article/pii/S1364032112001098> (visited on 04/17/2023).
- [32] inc. Analog devices. *Definition of Buck-Boost Converter — Analog Devices*. URL: <https://www.analog.com/en/design-center/glossary/buck-boost.html> (visited on 05/24/2023).
- [33] M. Narayana et al. “Generic maximum power point tracking controller for small-scale wind turbines”. en. In: *Renewable Energy* 44 (Aug. 2012), pp. 72–79. ISSN: 0960-1481. DOI: 10.1016/j.renene.2011.12.015. URL: <https://www.sciencedirect.com/science/article/pii/S096014811200002X> (visited on 12/06/2022).
- [34] Ababacar Ndiaye et al. “Development of a Charge Controller Dedicated to the Small Wind Turbine System”. In: *Energy and Environment Research* Vol. 4 (Oct. 2014), pp. 68–77. DOI: 10.5539/eer.v4n3p68.
- [35] Henry A. Catherino, Fred F. Feres, and Francisco Trinidad. “Sulfation in lead–acid batteries”. en. In: *Journal of Power Sources*. Selected papers presented at the conference High Energy Density Electrochemical Power Sources 129.1 (Apr. 2004), pp. 113–120. ISSN: 0378-7753. DOI: 10.1016/j.jpowsour.2003.11.003. URL: <https://www.sciencedirect.com/science/article/pii/S0378775303010681> (visited on 04/20/2023).
- [36] N. Gautam and A. Kumar. “Simulation of wind only system with battery energy storage and dump load”. In: *2015 2nd International Conference on Recent Advances in Engineering & Computational Sciences (RAECS)*. Dec. 2015, pp. 1–6. DOI: 10.1109/RAECS.2015.7453384.
- [37] JLC Electromet. *Designing heating elements*. en. URL: <https://www.heating-element-alloy.com/> (visited on 09/14/2022).
- [38] Dogan Ibrahim. “Chapter 8 - Advanced PIC32 Projects”. en. In: *Designing Embedded Systems with 32-Bit PIC Microcontrollers and MikroC*. Ed. by Dogan

- Ibrahim. Oxford: Newnes, Jan. 2014, pp. 359–442. ISBN: 978-0-08-097786-7. DOI: 10.1016/B978-0-08-097786-7.00008-7. URL: <https://www.sciencedirect.com/science/article/pii/B9780080977867000087> (visited on 05/16/2023).
- [39] N. Achaibou, M. Haddadi, and A. Malek. “Modeling of Lead Acid Batteries in PV Systems”. en. In: *Energy Procedia*. Terragreen 2012: Clean Energy Solutions for Sustainable Environment (CESSE) 18 (Jan. 2012), pp. 538–544. ISSN: 1876-6102. DOI: 10.1016/j.egypro.2012.05.065. URL: <https://www.sciencedirect.com/science/article/pii/S1876610212008351> (visited on 04/20/2023).
- [40] David A. J. Rand and Patrick T. Moseley. “Chapter 13 - Energy Storage with Lead–Acid Batteries”. en. In: *Electrochemical Energy Storage for Renewable Sources and Grid Balancing*. Ed. by Patrick T. Moseley and Jürgen Garche. Amsterdam: Elsevier, Jan. 2015, pp. 201–222. ISBN: 978-0-444-62616-5. DOI: 10.1016/B978-0-444-62616-5.00013-9. URL: <https://www.sciencedirect.com/science/article/pii/B9780444626165000139> (visited on 05/15/2023).
- [41] Ibrahim Dincer and Marc A. Rosen. *Thermal Energy Storage: Systems and Applications*. en. Google-Books-ID: 4SY9EAAAQBAJ. John Wiley & Sons, Sept. 2021. ISBN: 978-1-119-71315-9.
- [42] Hydratech. *What are Heat Transfer Fluids?* en. URL: <https://www.hydratech.co.uk/news-thoughts-blog/What-are-Heat-Transfer-Fluids/41> (visited on 10/11/2022).
- [43] Byju Raveendran. *Convection Currents - Definition and Examples — How Convection Current Works*. en. June 2020. URL: <https://byjus.com/physics/convection-currents/> (visited on 05/15/2023).
- [44] Theodore Bergman and Adrienne Lavine. *Fundamentals of heat and mass transfer*. 8th ed. Wiley, Dec. 2018. URL: <http://bcs.wiley.com/he-bcs/Books?action=index&itemId=1119320429&bcsId=10769>.
- [45] Duratherm. *Thermal Fluid That’s Long-Lasting, Economical, and Safe: Duratherm 630*. URL: <https://durathermcanada.ca/products/duratherm-630> (visited on 10/04/2022).
- [46] Kaushikk Ravender Iyer et al. “A novel approach for direct conversion of wind energy to heat utilizing a hydraulic medium for domestic heating applications”. en. In: *Energy Reports* 8 (Nov. 2022), pp. 11139–11150. ISSN: 2352-4847. DOI: 10.1016/j.egypr.2022.08.255. URL: <https://www.sciencedirect.com/science/article/pii/S2352484722017000> (visited on 11/01/2022).
- [47] Roustiam Chakirov and Yuriy Vagapov. “Direct Conversion of Wind Energy into Heat Using Joule Machine”. en. In: (), p. 6. URL: https://www.researchgate.net/publication/265796144_Direct_conversion_of_wind_energy_into_heat_using_Joule_machine.
- [48] Kris De Decker. *Heat your House with a Mechanical Windmill*. en. Feb. 2019. URL: <https://solar.lowtechmagazine.com/2019/02/heat-your-house-with-a-water-brake-windmill.html> (visited on 04/24/2023).
- [49] Lei Chen et al. “Investigation of a Novel Mechanical to Thermal Energy Converter Based on the Inverse Problem of Electric Machines”. en. In: *Energies* 9.7 (July 2016),

- p. 518. ISSN: 1996-1073. DOI: 10.3390/en9070518. URL: <http://www.mdpi.com/1996-1073/9/7/518> (visited on 10/19/2022).
- [50] Ali Khanjari et al. “Direct heat energy harvesting from wind by a permanent magnet eddy currents heater with different magnet arrangements”. en. In: *Energy Science & Engineering* 11.2 (2023). eprint: <https://onlinelibrary.wiley.com/doi/pdf/10.1002/ese3.1324>, pp. 929–951. ISSN: 2050-0505. DOI: 10.1002/ese3.1324. URL: <https://onlinelibrary.wiley.com/doi/abs/10.1002/ese3.1324> (visited on 04/24/2023).
- [51] Muhammad Mujtaba et al. “Throttle Valve as a Heating Element in Wind Hydraulic Thermal System”. en. In: *Journal of Advance Research in Mechanical & Civil Engineering* 5.2 (Feb. 2018). Number: 2, pp. 01–08. ISSN: 2208-2379. DOI: 10.5355/5/nnmce.v5i2.304. URL: <http://nnpub.org/index.php/MCE/article/view/304> (visited on 10/19/2022).
- [52] Tadas Ždankus et al. “Wind Energy Usage for Building Heating Applying Hydraulic System”. en. In: *Journal of Sustainable Architecture and Civil Engineering* 25.2 (July 2019), pp. 63–70. ISSN: 2029-9990. DOI: 10.5755/j01.sace.25.2.21542. URL: <http://sace.ktu.lt/index.php/DAS/article/view/21542> (visited on 10/19/2022).
- [53] Dave Murden. *Lead Acid vs. Lithium Batteries - Which One Utilize the Better Technology*. en-GB. June 2022. URL: <https://ecotreelithium.co.uk/news/lead-acid-vs-lithium-batteries/> (visited on 04/24/2023).
- [54] Lawrie Swinfen-Styles, Seamus D. Garvey, and Donald Giddings. “Combining Wind-Driven Air Compression with Underwater Compressed Air Energy Storage”. In: *2019 Offshore Energy and Storage Summit (OSES)*. July 2019, pp. 1–8. DOI: 10.1109/OSES.2019.8867344.
- [55] A. F. Serov et al. “Experimental investigation of energy dissipation in the multi-cylinder Couette-Taylor system with independently rotating cylinders”. en. In: *Applied Energy* 251 (Oct. 2019), p. 113362. ISSN: 0306-2619. DOI: 10.1016/j.apenergy.2019.113362. URL: <https://www.sciencedirect.com/science/article/pii/S0306261919310360> (visited on 10/31/2022).
- [56] Jagath Sri Lal Senanayaka, Hamid Reza Karimi, and Kjell G. Robbersmyr. “Sensorless small wind turbine with a sliding-mode observer for water heating applications”. In: *IECON 2015 - 41st Annual Conference of the IEEE Industrial Electronics Society*. Nov. 2015, pp. 000863–000868. DOI: 10.1109/IECON.2015.7392207.
- [57] Hailong Li et al. “Feasibility study about using a stand-alone wind power driven heat pump for space heating”. en. In: *Applied Energy* 228 (Oct. 2018), pp. 1486–1498. ISSN: 0306-2619. DOI: 10.1016/j.apenergy.2018.06.146. URL: <https://www.sciencedirect.com/science/article/pii/S030626191831016X> (visited on 10/24/2022).
- [58] Qingsong Ji et al. “Design and evaluation of a wind turbine-driven heat pump system for domestic heating in Scotland”. en. In: *Sustainable Energy Technologies and Assessments* 52 (Aug. 2022), p. 101987. ISSN: 2213-1388. DOI: 10.1016/j.seta.

- 2022.101987. URL: <https://www.sciencedirect.com/science/article/pii/S21313882200039X> (visited on 10/24/2022).
- [59] R. Sebastián and R. Peña Alzola. *Flywheel energy storage systems Review and simulation for an isolated wind power system — Elsevier Enhanced Reader*. en. DOI: 10.1016/j.rser.2012.08.008. URL: <https://reader.elsevier.com/reader/sd/pii/S1364032112004777?token=DE5FA1271CA57B149B7DA1932F4C0CF96F885C76E02A7D7C91781832FEAEAECE84E529B71D85CABCC0A3050A92B71DCB&originRegion=eu-west-1&originCreation=20230424070518> (visited on 04/24/2023).
- [60] Andrew Hutchinson and Daniel T. Gladwin. “Optimisation of a wind power site through utilisation of flywheel energy storage technology”. en. In: *Energy Reports*. 4th Annual CDT Conference in Energy Storage & Its Applications 6 (May 2020), pp. 259–265. ISSN: 2352-4847. DOI: 10.1016/j.egyr.2020.03.032. URL: <https://www.sciencedirect.com/science/article/pii/S2352484720302055> (visited on 04/24/2023).
- [61] Kavian Kazemi et al. “Micro-scale heat and electricity generation by a hybrid solar collector-chimney, thermoelectric, and wind turbine”. en. In: *Sustainable Energy Technologies and Assessments* 53 (Oct. 2022), p. 102394. ISSN: 2213-1388. DOI: 10.1016/j.seta.2022.102394. URL: <https://www.sciencedirect.com/science/article/pii/S2213138822004465> (visited on 04/24/2023).
- [62] Leybold. *Electrical drives*. en. Dec. 2013. URL: <https://www.merazet.pl/wp-content/uploads/img/573883b0.pdf>.
- [63] Hyttetorget. *Air Nordic 400W 24V — Hyttetorget*. nb. URL: <https://www.hyttetorget.no/vindturbin-24v-400w-m-regulator> (visited on 10/10/2022).
- [64] Qeed. *Qeed QI-POWER-485*. en-GB. URL: <https://qeed.it/en/prodotti/network-analysers/single-phase-network-analysers/qi-power-485-2/> (visited on 05/11/2023).
- [65] Artisan. *Yokogawa 253313 3-Phase, 4 Wire (AC) Digital Power Meter - Price, Specs*. en. URL: <https://www.artisan-tg.com/TestMeasurement/91637-1/Yokogawa-253313-3-Phase-4-Wire-AC-Digital-Power-Meter> (visited on 04/18/2023).
- [66] Element14. *72-13210 - DC Electronic Load, 300 W, Programmable, 0 V, 120 V, 30 A*. en. URL: <https://sg.element14.com/tenma/72-13210/dc-electronic-load-prog-30a-120v/dp/2848407> (visited on 03/30/2023).
- [67] *242.36NOK 34% OFF—Waterproof Wind Generator Charge Controller Regulator Fw12/24 Wind Controller Wind Generator Controller - Alternative Energy Generators - AliExpress*. en. URL: https://www.aliexpress.com/item/33023719912.html?src=ibdm_d03p0558e02r02&sk=&aff_platform=&aff_trace_key=&af=&cv=&cn=&dp= (visited on 04/18/2023).
- [68] Vishay Intertechnology. *Three phase bridge rectifier*. en. URL: https://www.vishay.com/docs/93565/vs-36mtseries.pdf?fbclid=IwAR2eLq_Csn1oib5X7wa1061vpEeyzRTOH1VuyY3FFx8T5oaEbUQbc6FQW08 (visited on 12/17/2022).

- [69] Morningstar. *TriStar Installation, Operation and Maintenance Manual*. URL: <https://www.morningstarcorp.com/wp-content/uploads/operation-manual-tristar-en.pdf>.
- [70] Pete Thompson. *Tristar controller*. en. Apr. 2023.
- [71] pico technology. *TC-08, 8-channel thermocouple data logger*. en. URL: https://www.elfadistrelec.no/Web/Downloads/_t/ds/Pico-TC-08_eng_tds.pdf.

A Python code

Load and battery voltage plotted against duty cycle for 6Ω dump load

```
import pandas as pd
import matplotlib.pyplot as plt
import numpy as np

# Load the Excel file into a pandas DataFrame
df = pd.read_excel('data.xlsx', usecols="A:C", nrows=770, sheet_name='PWM Tristar')

fig, ax1=plt.subplots()
ax2 = ax1.twinx()
ax1.plot(df['PWM'], df['Load voltage'],'-k', label='Load voltage ', linewidth=2.5)
ax2.plot(df['PWM'], df['Battery voltage'],'-c',label='Battery voltage')

ax1.set_xlabel('Duty cycle [%]', size=12)
ax1.set_ylabel('Load voltage [V]', size=12)
ax2.yaxis.set_label_coords(1.125, 0.5)
ax2.set_ylabel('Battery voltage [V]', size=12)
ax1.set_ylim(0, 30)
ax2.set_ylim(25.75, 28)

leg = ax1.legend(loc='upper center', bbox_to_anchor=(.17,1.01), ncol=2);
leg2 =ax2.legend(loc='upper center', bbox_to_anchor=(.5,1.01), ncol=2)

plt.show()
```

B Duratherm 630 info brochure



DURATHERM
Heat Transfer Fluids

DURATHERM 630

A high performance, efficient and environmentally friendly thermal fluid engineered for applications requiring high temperature stability to 332°C (630°F). Offering precise temperature control it's a great alternative to aromatic/synthetic fluids, at a fraction of the cost.

It is ideal for a wide range of applications including, high temperature batch processing, chemical reactions, pharmaceutical and resin manufacturing among others.

APPLICATION

Duratherm 630 is a high performance, efficient and environmentally friendly fluid engineered for applications requiring high temperature stability to 332°C (630°F). Offering precise temperature control it's a great alternative to high temperature aromatic fluids, at a fraction of the cost.

It is ideal for a wide range of applications including, high temperature batch processing, chemical reactions, pharmaceutical and resin manufacturing among others.

THE DIFFERENCE

Our exclusive additive package, including a proprietary dual stage anti-oxidant, ensures long trouble free operation. Duratherm 630 also incorporates metal deactivators, a seal and gasket extender, de-foaming and particle suspension agents.

LASTS LONGER

Oxidation can cripple your system. Left unchecked, it will ultimately cause catastrophic failure and costly downtime. That's why Duratherm 630 offers unsurpassed levels of protection against oxidation, and a service life that other fluids simply can't match.

RUNS CLEANER

Duratherm 630 delivers superior resistance to sludging, a problem plaguing most other fluids. That makes it the best defense against extreme oxidation found in many of today's demanding manufacturing environments.

ENVIRONMENTAL

Duratherm 630 is environmentally friendly, non-toxic, non-hazardous and non-reportable. It poses no ill effect to worker safety and does not require special handling. After its long service life, Duratherm 630 can easily be disposed of with other waste oils.

SYSTEM CLEANING

If your existing fluid has let you down and left you with a system full of sludge or carbon, we've developed a full line of heat transfer system cleaners to get your system back to like-new condition. Contact us for complete details.

1 800 446 4910

www.durathermfluids.com

DURATHERM 630

- Maximum temperature: 332°C / 630°F
- Flash point 229°C / 444°F
- Alternative to chemical aromatic fluids
- Non-toxic/non-hazardous
- Includes free fluid analysis and tech support



1 800 446 4910

www.durathermfluids.com

TEMPERATURE RATINGS

Maximum Bulk/Use Temp.	332°C	630°F
Maximum Film Temp.	354°C	670°F
Pour Point ASTM D97	-18°C	-1°F

SAFETY DATA

Flash Point ASTM D92	229°C	444°F
Fire Point ASTM D92	244°C	472°F
Autoignition ASTM E-659-78	368°C	693°F

THERMAL PROPERTIES

Thermal Expansion Coefficient	0.1011 %/°C	0.0562 %/°F
Thermal Conductivity	W/m K	BTU/hr F ft
38°C / 100°F	0.143	0.083
260°C / 500°F	0.131	0.076
316°C / 600°F	0.128	0.074
332°C / 630°F	0.127	0.073
Heat Capacity	kJ/kg K	BTU/lb F
38°C / 100°F	1.991	0.475
260°C / 500°F	2.724	0.650
316°C / 600°F	2.908	0.694
332°C / 630°F	2.962	0.707

PHYSICAL PROPERTIES

Appearance: colorless, clear and bright liquid		
Viscosity ASTM D445		
cSt at 40°C / 104°F	42.31	
cSt at 100°C / 212°F	6.82	
cSt at 316°C / 600°F	0.79	
cSt at 332°C / 630°F	0.74	
Density ASTM D1298	kg/m ³	lb/ft ³
38°C / 100°F	853.39	53.29
260°C / 500°F	702.45	43.85
316°C / 600°F	665.74	41.50
332°C / 630°F	652.5	40.79
Vapor Pressure ASTM D2879	kPa	psi
38°C / 100°F	0.00	0.00
260°C / 500°F	2.28	0.33
316°C / 600°F	9.75	1.40
332°C / 630°F	14.2	2.04
Distillation Range ASTM D2887	10%	383°C (721°F)
	90%	494°C (921°F)
Average Molecular Weight	395	

The values quoted are typical of normal production. They do not constitute a specification.

DURATHERM 630

PROPERTY VS. TEMPERATURE CHART METRIC

TEMPERATURE (Celsius)	DENSITY (kg/m ³)	KINEMATIC VISCOSITY (Centistoke)	DYNAMIC VISCOSITY (Centipoise)	THERMAL CONDUCTIVITY (W/m-K)	HEAT CAPACITY (kJ/kg-K)	VAPOR PRESSURE (kPa)
-5	882.63	683.16	602.98	0.146	1.849	0.00
5	875.83	307.70	269.49	0.145	1.882	0.00
15	869.03	156.16	135.71	0.145	1.915	0.00
25	862.23	87.38	75.34	0.144	1.948	0.00
35	855.43	52.97	45.31	0.144	1.981	0.00
45	848.63	34.31	29.11	0.143	2.014	0.00
55	841.84	23.47	19.76	0.142	2.047	0.00
65	835.04	16.81	14.04	0.142	2.080	0.00
75	828.24	12.51	10.37	0.141	2.113	0.00
85	821.44	9.62	7.90	0.141	2.146	0.00
95	814.64	7.60	6.19	0.140	2.179	0.00
105	807.84	6.15	4.97	0.140	2.212	0.00
115	801.04	5.08	4.07	0.139	2.245	0.01
125	794.24	4.26	3.39	0.138	2.278	0.01
135	787.44	3.64	2.86	0.138	2.311	0.02
145	780.64	3.14	2.45	0.137	2.344	0.03
155	773.84	2.75	2.13	0.137	2.377	0.05
165	767.04	2.43	1.86	0.136	2.410	0.08
175	760.24	2.16	1.65	0.135	2.443	0.12
185	753.45	1.95	1.47	0.135	2.476	0.18
195	746.65	1.76	1.32	0.134	2.509	0.26
205	739.85	1.61	1.19	0.134	2.542	0.38
215	733.05	1.47	1.08	0.133	2.575	0.54
225	726.25	1.36	0.99	0.133	2.608	0.77
235	719.45	1.26	0.91	0.132	2.641	1.06
245	712.65	1.17	0.84	0.132	2.674	1.45
255	705.85	1.10	0.78	0.131	2.707	1.96
265	699.05	1.03	0.72	0.130	2.740	2.60
275	692.25	0.97	0.67	0.130	2.773	3.44
285	685.45	0.92	0.63	0.129	2.806	4.49
295	678.65	0.87	0.59	0.129	2.839	5.82
305	671.86	0.83	0.56	0.128	2.872	7.47
315	665.06	0.79	0.53	0.128	2.905	9.51
325	658.26	0.76	0.50	0.127	2.938	12.00
332	653.39	0.74	0.48	0.126	2.960	15.03

The values quoted are typical of normal production.
They do not constitute a specification.

1 800 446 4910 | www.durathermfluids.com

DURATHERM 630

PROPERTY VS. TEMPERATURE CHART STANDARD

TEMPERATURE (Fahrenheit)	DENSITY (lb/ft ³)	KINEMATIC VISCOSITY (Centistoke)	DYNAMIC VISCOSITY (Centipoise)	THERMAL CONDUCTIVITY (BTU/hr-F-ft)	HEAT CAPACITY (BTU/lb-F)	VAPOR PRESSURE (Psia)
15	55.29	1018.91	902.98	0.084	0.438	0.00
25	55.06	621.05	548.04	0.084	0.443	0.00
35	54.82	395.64	347.63	0.084	0.447	0.00
45	54.58	262.15	229.35	0.084	0.451	0.00
55	54.35	179.91	156.72	0.084	0.456	0.00
65	54.11	127.41	110.51	0.084	0.460	0.00
75	53.88	92.80	80.14	0.083	0.464	0.00
85	53.64	69.32	59.60	0.083	0.469	0.00
95	53.40	52.97	45.34	0.083	0.473	0.00
105	53.17	41.31	35.20	0.083	0.478	0.00
115	52.93	32.81	27.83	0.083	0.482	0.00
125	52.70	26.49	22.38	0.082	0.486	0.00
135	52.46	21.72	18.26	0.082	0.491	0.00
145	52.23	18.04	15.10	0.082	0.495	0.00
155	51.99	15.18	12.65	0.082	0.499	0.00
165	51.75	12.91	10.71	0.082	0.504	0.00
175	51.52	11.09	9.16	0.082	0.508	0.00
185	51.28	9.62	7.91	0.081	0.513	0.00
195	51.05	8.42	6.89	0.081	0.517	0.00
205	50.81	7.42	6.04	0.081	0.521	0.00
215	50.57	6.59	5.34	0.081	0.526	0.00
225	50.34	5.88	4.75	0.081	0.530	0.00
235	50.10	5.29	4.25	0.080	0.534	0.00
245	49.87	4.78	3.82	0.080	0.539	0.00
255	49.63	4.34	3.46	0.080	0.543	0.00
265	49.40	3.97	3.14	0.080	0.548	0.00
275	49.16	3.64	2.87	0.080	0.552	0.00
285	48.92	3.35	2.63	0.080	0.556	0.00
295	48.69	3.09	2.42	0.079	0.561	0.01
305	48.45	2.87	2.23	0.079	0.565	0.01
315	48.22	2.67	2.06	0.079	0.569	0.01
325	47.98	2.49	1.92	0.079	0.574	0.01
335	47.75	2.33	1.79	0.079	0.578	0.02
345	47.51	2.19	1.67	0.079	0.583	0.02
355	47.27	2.06	1.56	0.078	0.587	0.02
365	47.04	1.95	1.47	0.078	0.591	0.03
375	46.80	1.84	1.38	0.078	0.596	0.03
385	46.57	1.74	1.30	0.078	0.600	0.04
395	46.33	1.66	1.23	0.078	0.604	0.05
405	46.09	1.58	1.16	0.077	0.609	0.06
415	45.86	1.50	1.10	0.077	0.613	0.08
425	45.62	1.43	1.05	0.077	0.618	0.08
435	45.39	1.37	1.00	0.077	0.622	0.11
445	45.15	1.31	0.95	0.077	0.626	0.13
455	44.92	1.26	0.91	0.077	0.631	0.15
465	44.68	1.21	0.87	0.076	0.635	0.19
475	44.44	1.17	0.83	0.076	0.639	0.22
485	44.21	1.12	0.80	0.076	0.644	0.26
495	43.97	1.08	0.76	0.076	0.648	0.31
505	43.74	1.05	0.73	0.076	0.653	0.36
515	43.50	1.01	0.71	0.076	0.657	0.42
525	43.26	0.98	0.68	0.075	0.661	0.48
535	43.03	0.95	0.65	0.075	0.666	0.56
545	42.79	0.92	0.63	0.075	0.670	0.66
555	42.56	0.89	0.61	0.075	0.674	0.76
565	42.32	0.87	0.59	0.075	0.679	0.87
575	42.09	0.84	0.57	0.074	0.683	1.00
585	41.85	0.82	0.55	0.074	0.688	1.14
595	41.61	0.80	0.53	0.074	0.692	1.31
605	41.38	0.78	0.52	0.074	0.696	1.49
615	41.14	0.76	0.50	0.074	0.701	1.69
625	40.91	0.74	0.49	0.074	0.705	1.92
630	40.79	0.74	0.48	0.073	0.707	2.04

The values quoted are typical of normal production.
They do not constitute a specification.

1 800 446 4910 | www.durathermfluids.com

C Tristar controller operation manual

TRISTAR™

Solar Charging System Controller

Installation, Operation and Maintenance Manual

For the most recent manual revisions, see the version at:
www.morningstarcorp.com



.....
Solar Battery Charging
.....
Load Control
.....
Diversion Control

 **MORNINGSTAR**
PROFESSIONAL SERIES
World's Leading Solar Controllers & Inverters
www.morningstarcorp.com

MODELS

**TS-45
TS-60
TS-60M**

**This page inside front
COVER 2
(Please do not print this copy)**

Table of Contents

Important Safety Instructions..... 1

1.0 TriStar Description 7

 1.1 Versions and Ratings..... 7

 1.2 Operating Modes 7

 1.3 Adjustability 8

 1.4 General Use..... 8

 1.5 Safety and Regulatory Information..... 10

 1.6 Optional Accessories..... 11

2.0 Installation..... 12

 2.1 General Information..... 12

 2.2 Installation Overview..... 13

 2.3 Installation Steps..... 14

 1. Remove the Cover..... 15

 2. Mounting..... 15

 3. Adjust DIP Switches 16

 4. Remote Temperature Sensor 21

 5. Battery Voltage Sense..... 22

 6. System Wiring and Power-up 23

 7. RS-232 Adjustments 26

 8. Finish Installation 26

3.0 Operation 27

 3.1 Operator's Tasks..... 27

 3.2 Push-button..... 27

 3.3 LED Indications 28

 3.4 Protections and Fault Recovery 29

 3.5 Data-Logging..... 32

 3.6 Inspection and Maintenance 32

4.0 Solar Battery Charging..... 34

 4.1 PWM Battery Charging 34

 4.1.1 Four Stages of Solar Charging..... 34

 4.1.2 Battery Charging Notes..... 34

 4.2 Standard Battery Charging Programs..... 35

 4.3 Temperature Effects & Battery Voltage Sense..... 36

 4.3.1 Remote Temperature Sensor (RTS)..... 36

 4.3.2 Battery Voltage Sense..... 37

 4.4 Equalization..... 38

 4.4.1 Standard Equalization Programs..... 39

 4.4.2 Typical equalizations..... 39

 4.4.3 Preparation for equalization..... 40

 4.4.4 When to Equalize..... 40

 4.4.5 Equalize a Sealed Battery?..... 40

 4.5 Float..... 41

(continued)

5.0	Load & Lighting Control	42
5.1	General Load & Lighting Control Notes.....	42
5.1.1	Inductive Loads.....	42
5.1.2	Parallel TriStars.....	42
5.1.3	Reverse Polarity.....	42
5.2	Load Control Settings.....	42
5.3	LVD Warning.....	44
6.0	Diversion Charge Control	44
6.1	Diversion Charge Control.....	44
6.2	Diversion Current Ratings	45
6.3	Standard Diversion Battery Charging Programs.....	45
6.3.1	Battery Charging References.....	46
6.4	Selecting the Diversion Load.....	47
6.4.1	Suitable Loads for Diversion.....	47
6.4.2	Defintion of Terms.....	47
6.4.3	Load Power Ratings.....	48
6.4.4	Maximum Diversion Load.....	48
6.4.5	Minimum Diversion Load.....	49
6.5	NEC Requirements.....	50
6.5.1	Second Independent Means.....	50
6.5.2	150 Percent Rating.....	50
6.6	Additional Information.....	50
7.0	Custom Settings with PC Software.....	51
7.1	Connection to a Computer.....	51
7.2	Using the PC Software.....	51
7.3	Changing Set-points.....	52
7.4	Finish.....	52
8.0	Self-Test / Diagnostics.....	53
8.1	General Troubleshooting.....	53
8.2	Troubleshooting Solar Charging.....	54
8.3	Troubleshooting Load Control.....	54
8.4	Troubleshooting Diversion Control.....	54
9.0	Battery Information (reference).....	55
9.1	Sealed Batteries.....	55
9.2	Flooded Batteries.....	56
9.3	L-16 Cells.....	57
10.0	Warranty.....	58
11.0	Specifications.....	59
	Appendix 1 - Load and Lighting Control DIP Switch Settings.....	61
	Appendix 2 - Diversion Charge Control DIP SwitchSettings.....	66
	Appendix 3 - LED Indications.....	70
12.0	Certifications.....	73

IMPORTANT SAFETY INSTRUCTIONS

SAVE THESE INSTRUCTIONS.

This manual contains important safety, installation, operating and maintenance instructions for the TriStar-PWM solar controller.

The following symbols are used throughout this manual to indicate potentially dangerous conditions or mark important safety instructions:



WARNING: Indicates a potentially dangerous condition. Use extreme caution when performing this task.



CAUTION: Indicates a critical procedure for safe and proper operation of the controller.



NOTE: Indicates a procedure or function that is important to the safe and proper operation of the controller.

CONSIGNES IMPORTANTES DE SÉCURITÉ

CONSERVEZ CES INSTRUCTIONS.

Ce manuel contient des instructions importantes de sécurité, d'installations et d'utilisation du contrôleur solaire, TriStar-PWM. Les symboles suivants sont utilisés dans ce manuel pour indiquer des conditions potentiellement dangereuses ou des consignes importantes de sécurité.



AVERTISSEMENT: Indique une condition potentiellement dangereuse. Faites preuve d'une prudence extrême lors de la réalisation de cette tâche.



PRUDENCE: Indique une procédure critique pour l'utilisation sûre et correcte du contrôleur.



REMARQUE: Indique une procédure ou fonction importante pour l'utilisation sûre et correcte du contrôleur.

Safety Information

- Read all of the instructions and cautions in the manual before beginning installation.
- There are no user serviceable parts inside the TriStar-PWM. Do not disassemble or attempt to repair the controller.

continued...



WARNING: RISK OF ELECTRICAL SHOCK.

NO POWER OR ACCESSORY TERMINALS ARE ELECTRICALLY ISOLATED FROM DC INPUT, AND MAY BE ENERGIZED WITH HAZARDOUS SOLAR VOLTAGE. UNDER CERTAIN FAULT CONDITIONS, BATTERY COULD BECOME OVER-CHARGED. TEST BETWEEN ALL TERMINALS AND GROUND BEFORE TOUCHING.

- External solar and battery disconnects are required.
- Disconnect all sources of power to the controller before installing or adjusting the TriStar-PWM.
- There are no fuses or disconnects inside the TriStar-PWM. Do not attempt to repair.

Informations de Sécurité

- Lisez toutes les instructions et les avertissements figurant dans le manuel avant de commencer l'installation.
- Le TriStar-PWM ne contient aucune pièce réparable par l'utilisateur. Ne démontez pas ni ne tentez de réparer le contrôleur.



AVERTISSEMENT: RISQUE DE CHOC ÉLECTRIQUE. NON ALIMENTATION OU AUX BORNES D'ACCESSOIRES SONT ISOLÉS ÉLECTRIQUEMENT DE L'ENTRÉE DE C.C ET DOIT ÊTRE ALIMENTÉS À UNE TENSION DANGEREUSE SOLAIRE. SOUS CERTAINES CONDITIONS DE DÉFAILLANCE, LA BATTERIE POURRAIT DEVENIR TROP CHARGÉE. TEST ENTRE TOUTES LES BORNES ET LA MASSE AVANT DE TOUCHER.

- External solaire et la batterie se déconnecte sont nécessaires.
- Déconnectez toutes les sources d'alimentation du contrôleur avant d'installer ou de régler le TriStar-PWM.
- Le TriStar MPPT ne contient aucun fusible ou interrupteur. Ne tentez pas de réparer.
- Installez des fusibles/cope-circuits externes selon le besoin.

Installation Safety Precautions



WARNING: *This unit is not provided with a GFDI device. This charge controller must be used with an external GFDI device as required by the Article 690 of the National Electrical Code for the installation location.*

- Mount the TriStar-PWM indoors. Prevent exposure to the elements and do not allow water to enter the controller.
- Install the TriStar-PWM in a location that prevents casual contact. The TriStar-PWM heatsink can become very hot during operation.
- Use insulated tools when working with batteries.
- Avoid wearing jewelry during installation.

- The battery bank must be comprised of batteries of same type, make, and age.
- IEC 62109 certified for use in negative ground or floating systems only
- Do not smoke near the battery bank.
- Power connections must remain tight to avoid excessive heating from a loose connection.
- Use properly sized conductors and circuit interrupters.
- The grounding terminal is located in the wiring compartment and is identified by the symbol below:



Ground Symbol

- This charge controller is to be connected to DC circuits only. These DC connections are identified by the symbol below:



Direct Current Symbol

The TriStar-PWM controller must be installed by a qualified technician in accordance with the electrical regulations of the country where the product is installed. A means of disconnecting all power supply poles must be provided. These disconnects must be incorporated in the fixed wiring.

A permanent, reliable earth ground must be established with connection to the TriStar-PWM wiring compartment ground terminal.

The grounding conductor must be secured against any accidental detachment. The knock-outs in the TriStar-PWM wiring compartment must protect wires with conduit or rubber rings.

Précautions de Sécurité D'installation



AVERTISSEMENT: *L'appareil n'est pas fourni avec un dispositif GFDI. Ce contrôleur de charge doit être utilisé avec un dispositif GFDI externe tel que requis par l'Article 690 du Code électrique national de l'emplacement de l'installation.*

- Montez le TriStar-PWM à l'intérieur. Empêchez l'exposition aux éléments et la pénétration d'eau dans le contrôleur.
- Installez le MPPT ProStar dans un endroit qui empêche le contact occasionnel. Le dissipateur de chaleur TriStar-PWM peut devenir très chaud pendant

le fonctionnement.

- Utilisez des outils isolés pour travailler avec les batteries.
- Évitez le port de bijoux pendant l'installation.
- Le groupe de batteries doit être constitué de batteries du même type, fabricant et âge.
- UL/IEC 62109 certifié pour utilisation au négatif à la masse ou les systèmes flottants seulement.
- Ne fumez pas à proximité du groupe de batteries.
- Les connexions d'alimentation doivent rester serrées pour éviter une surchauffe excessive d'une connexion desserrée.
- Utilisez des conducteurs et des coupe-circuits de dimensions adaptées.
- La borne de mise à la terre se trouve dans le compartiment de câblage et est identifiée par le symbole ci-dessous:



- Ces connexions CC sont identifiées par le symbole ci-dessous:



WARNING: A battery can present a risk of electrical shock or burn from large amounts of short-circuit current, fire, or explosion from vented gases. Observe proper precautions.



AVERTISSEMENT: Une batterie peut présenter a risque de choc électrique ou de brûlure de grandes quantités de court-circuit courtoeur, incendie ou explosion de ventilé gaz. Observer précautions appropriées.



WARNING: Risk of Explosion.
Proper disposal of batteries is required. Do not dispose of batteries in fire. Refer to local regulations or codes for requirements.



AVERTISSEMENT: Risque d'Explosion.
Au rebut des piles est nécessaire. Ne pas jeter les piles dans le feu. Se référer aux réglementations locales ou des codes pour les exigences.



CAUTION: When replacing batteries, use properly specified number, sizes, types, and ratings based on application and system design.



PRUDENCE: Lorsque le remplacement des piles, utilisez correctement nombre spécifié, tailles, types et les évaluations basées sur conception de système et d'application.



CAUTION: Do not open or mutilate batteries. Released electrolyte is harmful to skin, and may be toxic.



PRUDENCE: Ne pas ouvrir ou mutiler les piles. L'électrolyte est nocif pour la peau et peut être toxique.

- Servicing of batteries should be performed, or supervised, by personnel knowledgeable about batteries, and the proper safety precautions.
- Be very careful when working with large lead-acid batteries. Wear eye protection and have fresh water available in case there is contact with the battery acid.
- Remove watches, rings, jewelry and other metal objects before working with batteries.
- Wear rubber gloves and boots
- Use tools with insulated handles and avoid placing tools or metal objects on top of batteries.
- Disconnect charging source prior to connecting or disconnecting battery terminals.
- Determine if battery is inadvertently grounded. If so, remove the source of contact with ground. Contact with any part of a grounded battery can result in electrical shock. The likelihood of such a shock can be reduced if battery grounds are removed during installation and maintenance (applicable to equipment and remote battery supplies not having a grounded supply circuit).
- Carefully read the battery manufacturer's instructions before installing / connecting to, or removing batteries from, the TriStar-PWM.
- Be very careful not to short circuit the cables connected to the battery.
- Have someone nearby to assist in case of an accident.
- Explosive battery gases can be present during charging. Be certain there is enough ventilation to release the gases.
- Never smoke in the battery area.
- If battery acid comes into contact with the skin, wash with soap and water. If the acid contacts the eye, flood with fresh water and get medical attention.
- Be sure the battery electrolyte level is correct before starting charging. Do not attempt to charge a frozen battery.
- Recycle the battery when it is replaced.

- Entretien des batteries devrait être effectué ou supervisé, par un personnel bien informé sur les piles et les précautions de sécurité appropriées.
- Soyez très prudent quand vous travaillez avec des grandes batteries au plomb. Portez des lunettes de protection et ayez de l'eau fraîche à disposition en cas de contact avec l'électrolyte.
- Enlevez les montres, bagues, bijoux et autres objets métalliques avant de travailler avec des piles.
- Porter des bottes et des gants de caoutchouc
- Utiliser des outils avec poignées isolantes et évitez de placer des outils ou des objets métalliques sur le dessus de batteries.
- Débrancher la source de charge avant de brancher ou de relier les bornes de la batterie.
- Utilisez des outils isolés et évitez de placer des objets métalliques dans la zone de travail.
- Déterminer si batterie repose par inadvertance. Dans l'affirmative, supprimer la source du contact avec le sol. Contact avec n'importe quelle partie d'une batterie mise à la terre peut entraîner un choc électrique. La probabilité d'un tel choc peut être réduite si des motifs de batterie sont supprimés pendant l'installation et maintentretien (applicable à l'équipement et les fournitures de pile de la télécommande n'ayant pas un circuit d'alimentation mise à la terre).
- Lisez attentivement les instructions du fabricant de la batterie avant d'installer / connexion à ou retrait des batteries du TriStar-PWM.
- Veillez à ne pas court-circuiter les câbles connectés à la batterie.
- Ayez une personne à proximité qui puisse aider en cas d'accident.
- Des gaz explosifs de batterie peuvent être présents pendant la charge. Assurez-vous qu'une ventilation suffisante évacue les gaz.
- Ne fumez jamais dans la zone des batteries
- En cas de contact de l'électrolyte avec la peau, lavez avec du savon et de l'eau. En cas de contact de l'électrolyte avec les yeux, rincez abondamment avec de l'eau fraîche et consultez un médecin.
- Assurez-vous que le niveau d'électrolyte de la batterie est correct avant de commencer la charge. Ne tentez pas de charger une batterie gelée.
- Recyclez la batterie quand elle est remplacée.

1.0 TriStar Description

The TriStar is a technically advanced solar system controller. There are three operating modes programmed into each TriStar. This manual describes solar battery charging, and specific load control or diversion charge control instructions are inserted where required.

This manual will help you to become familiar with the TriStar's features and capabilities. Some of these follow:

- ETL Listed (UL 1741) and cETL Listed (CSA-C22.2 No. 107.1)
- TUV Listed (IEC 62109)
- Complies with the US National Electrical Code
- Complies with the Canadian Electrical Code
- Complies with EMC and LVD standards for CE marking
- Rated for 12, 24, 48 volt systems, and 45 or 60 amps current
- Fully protected with automatic and manual recovery
- Seven standard charging or load programs selected with DIP switches
- Adjustability by means of an RS-232 connection with PC software
- Continuous self-testing with fault notification
- LED indications and push-button functions
- Terminals sized for 35mm² (#2 AWG) wire
- Includes battery voltage sense terminals
- Digital meter options (mounted to TriStar or remote)
- Optional remote battery temperature sensor
- 5-year warranty (see Section 10.0)

1.1 Versions and Ratings

There are two standard versions of TriStar controllers:

TriStar-45:
Rated for maximum 45 amps continuous current
(solar, load or diversion load)
Rated for 12, 24, 48 Vdc systems

TriStar-60:
Rated for maximum 60 amps continuous current
(solar, load or diversion load)
Rated for 12, 24, 48 Vdc systems

TriStar-60M:
Rated for maximum 60 amps continuous current
(solar, load or diversion load)
Rated for 12, 24, 48 Vdc systems
Includes on-board meter display

1.2 Operating Modes

There are three distinct and independent operating modes programmed into each TriStar. Only one mode of operation can be selected for an individual TriStar. If a system requires a charging controller and a load controller, two TriStars must be used.

1.3 Adjustability

Eight DIP switches permit the following parameters to be adjusted at the installation site:


DIP switch	Solar Battery Charging
1	Battery charge control mode
2-3	Select battery voltage
4-6	Standard battery charging programs
7	Manual or automatic equalization
8	PWM charging or on-off charging


DIP switch	Load Control
1	DC load control mode
2-3	Select battery voltage
4-6	Standard low voltage disconnects and reconnects
7	not used for load control
8	not used for load control

DIP switch	Diversion Charge Control
1	DC load control mode
2-3	Select battery voltage
4-6	Standard diversion charge control programs
7	Select diversion charge control mode
8	Manual or automatic equalization

In addition to the DIP switches, the TriStar provides for additional adjustments using a PC program. An RS-232 connection between the TriStar and a personal computer will enable extensive adjustments using PC software from Morningstar's website.

1.4 General Use

 **NOTE:** This manual describes solar battery charging. Specific instructions for the load control and diversion charge control modes are provided as notes throughout this manual.

 **REMARQUE :** Ce manuel décrit la charge de batteries solaires. Des instructions spécifiques aux modes de contrôle du chargement et de contrôle de la charge de diversion figurent en tant que remarques dans ce manuel.

The TriStar is suitable for a wide range of solar applications including homes, telecom and industrial power needs.

TriStar controllers are configured for negative ground systems. There are no parts in the controller's negative leg. The enclosure can be grounded using the ground terminal in the wiring compartment.

The TriStar is protected from faults electronically with automatic recovery. There are no fuses or mechanical parts inside the TriStar to reset or change.

Solar overloads up to 130% of rated current will be tapered down instead of disconnecting the solar. Over-temperature conditions will also taper the solar input to lower levels to avoid a disconnect.

The NEC requires overcurrent protection externally in the system (see Section 2.3 step 6). There are no system disconnects inside the TriStar enclosure.

Any number of TriStars can be connected in parallel to increase solar charging current. TriStars can be paralleled ONLY in the battery charging mode. DO NOT parallel TriStars in the load mode, as this can damage the controller or load.

The TriStar enclosure is rated for indoor use. The controller is protected by conformal coated circuit boards, stainless steel hardware, anodized aluminum, and a powder coated enclosure, but it is not rated for corrosive environments or water entry.

The construction of the TriStar is 100% solid state.

Battery charging is by a series PWM constant current charging, with bulk charging, PWM absorption, float and equalization stages.

The TriStar will accurately measure time over long intervals to manage events such as automatic equalizations or battery service notification.

Day and night conditions are detected by the TriStar, and no blocking diodes are used in the power path.

LEDs, a push-button, and optional digital meters provide both status information and various manual operations.

The date of manufacture can be found on the two bar code labels. One label is on the back of the TriStar, and the other is in the wiring compartment. The year and week of manufacture are the first four digits of the serial number. For example:

year	week	serial #
03	36	0087

1.5 Safety and Regulatory Information



NOTE: This section contains important information for safety and regulatory requirements.



REMARQUE : Cette section contient des informations importantes relatives à la sécurité et aux obligations réglementaires.

The TriStar controller is intended for installation by a qualified technician according to electrical rules of each country in which the product will be installed.

TriStar controllers comply with the following EMC standards:

Immunity: EN 61000-4-3: 2006; EN 61000-4-6: 2009

Emissions: CISPR 22: 2008

Safety: EN60335-1 and EN60335-2-29 (battery chargers)

A means shall be provided to ensure all pole disconnection from the power supply. This disconnection shall be incorporated in the fixed wiring.

Using the TriStar grounding terminal (in the wiring compartment), a permanent and reliable means for grounding shall be provided. The clamping of the earthing shall be secured against accidental loosening.

The entry openings to the TriStar wiring compartment shall be protected with conduit or with a bushing.

FCC requirements:

This device complies with Part 15 of the FCC rules. Operation is subject to the following two conditions: (1) This device may not cause harmful interference, and (2) this device must accept any interference received, including interference that may cause undesired operation.

Changes or modifications not expressly approved by Morningstar for compliance could void the user's authority to operate the equipment.

Note: This equipment has been tested and found to comply with the limits for a Class B digital device, pursuant to Part 15 of the FCC rules. These limits are designed to provide reasonable protection against harmful interference in a residential installation. This equipment generates, uses, and can radiate radio frequency energy and, if not installed and used in accordance with the instruction manual, may cause harmful interference to radio communication. However, there is no guarantee that interference will not occur in a particular installation. If this equipment does cause harmful interference to radio or television reception, which can be determined by turning the equipment on and off, the user is encouraged to try to correct the interference by one or more of the following measures:

- Reorient or relocate the receiving antenna.
- Increase the separation between the equipment and receiver.
- Connect the equipment into an outlet on a circuit different from that to which the receiver is connected.
- Consult the dealer or an experienced radio/TV technician for help.

This Class B digital apparatus complies with Canadian ICES-003.

Cet appareil numérique de la classe B est conforme à la norme NMB-003 du Canada.

1.6 Optional Accessories

Remote Temperature Sensor (RTS)

If the temperature of the system battery varies more than 5°C (9°F) during the year, temperature compensated charging should be considered. Because the battery's chemical reactions change with temperature, it can be important to adjust charging to account for the temperature effects. The RTS will measure the battery temperature, and the TriStar uses this input to adjust the charging as required.

The battery charging will be corrected for temperature as follows:

- 12 V battery – 0.030 Volts per °C (–0.017V per °F)
- 24 V battery – 0.060 Volts per °C (–0.033V per °F)
- 48 V battery – 0.120 Volts per °C (–0.067V per °F)

The RTS should be used only for battery charging and diversion control. Do not use the RTS for load control. The charging parameters that are adjusted for temperature include:

- PWM regulation
- Equalization
- Float
- High Voltage Disconnect

See Installation, Step 4, for connecting the RTS to the TriStar.

Digital Meter Displays

Two digital meters can be added to the TriStar at any time during or after installation. One version is mounted on the controller (TS-M), the other is suitable for remote locations (TS-RM). The manual for installation and operation of the meter displays is included with the meter.

The display is a 2x16 LCD meter with backlighting. Four push-buttons are used to scroll through the displays and to execute manual functions.

There are a series of display screens that provide information such as:

- operating information and data
- operating bar charts (voltage and current)
- alarms and faults
- diagnostics
- settings

In addition, there are various manual functions built into the meter. For example, the meter can be used to reset Ah data or start/stop equalizations.

One of 5 languages can be selected for the meter.

Ethernet Communications Adapter (EMC-1)

This product is an Ethernet gateway that provides web monitoring services, a Modbus TCP/IP server, and a local web page server. End users can collect information about their off-grid PV system remotely. One EMC-1 supports all products with MeterBus ports by bridging MODBUS TCP/IP requests to serve LiveView pages for each product.

USB Communications Adapter (UMC-1)

A modular unit that uses a USB-B plug, usually from a USB A-B computer cable, and an RJ-11 plug to connect with a Morningstar controller's MeterBus port, for monitoring and programming using MSView PC software.

2.0 TriStar Installation

The installation instructions describe solar battery charging. Specific instructions for the load control and diversion modes are provided as notes.

2.1 General Information

The mounting location is important to the performance and operating life of the controller. The environment must be dry and protected as noted below. The controller may be installed in a ventilated enclosure with sealed batteries, but never in a sealed battery enclosure or with vented batteries.

If the solar array exceeds the current rating of the controller, multiple TriStars can be installed in parallel. Additional parallel controllers can also be added in the future. The load controllers cannot be used in parallel. To parallel diversion controllers, refer to Morningstar's website.

If solar charging and load control are both required, two separate controllers must be used.

Stranded wires to be connected to the terminals should be prepared first with e.g. clamped copper heads, etc. to avoid the possibility of one conductor free out of the connection screw, and possible contact with the metal enclosure.

WARNING: Solar and battery fuses or DC breakers are required in the system. These protection devices are external to the controller, and must be a maximum of 70 amps for the TriStar-PWM-45, and 90 amps for the TriStar-PWM-60/M.

AVERTISSEMENT: Solaire et batterie fusibles ou disjoncteurs DC sont nécessaires dans le système. Ces dispositifs de protection sont externes au contrôleur, et doivent être un maximum de 70 ampères pour le TriStar-PWM-45, et 90 ampères pour le TriStar-PWM-60/M.

WARNING: Installation must comply with all US National Electrical Code and Canadian Electrical Code requirements. Breakers and fuses may require lower ratings than referenced above, so as not to exceed any specific wire ampacity.

AVERTISSEMENT: Installation doit être conforme à toutes les requirments US National Electrical Code et Code Canadien d'Electricité. Disjoncteurs et fusibles peuvent exiger des cotes inférieures que mentionnés ci-dessus de manière à ne pas pour dépasser n'importe quel fils particulier admissible.

Maximum battery short-circuit current rating must be less than the interrupt current rating of the battery over-current protection device referenced above.

2.2 Installation Overview

The installation is straightforward, but it is important that each step is done correctly and safely. A mistake can lead to dangerous voltage and current levels. Be sure to carefully follow each instruction in Section 2.3 and observe all cautions and warnings.

The following diagrams provide an overview of the connections and the proper order.

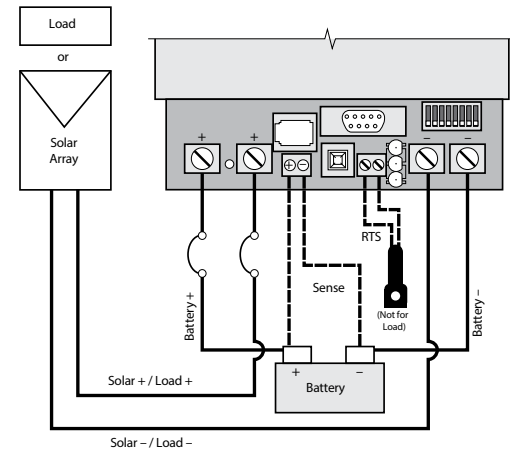


Figure 2.2a Installation Wiring for Solar Charging and Load Control

Step Solar Charging and Load Control

1. Remove the access cover
2. Mount the TriStar using the enclosed template.
3. Adjust the 8 switches in the DIP switch. Each switch must be in the correct position.
4. Attach the RTS if battery charging will be temperature compensated (not for load control).
5. Connect battery voltage sense wires (recommended).
6. Connect the battery power wires to the TriStar. Then connect the solar array wires (or load).
7. Connect a computer to the TriStar if making adjustments with PC software.
8. Replace the cover.

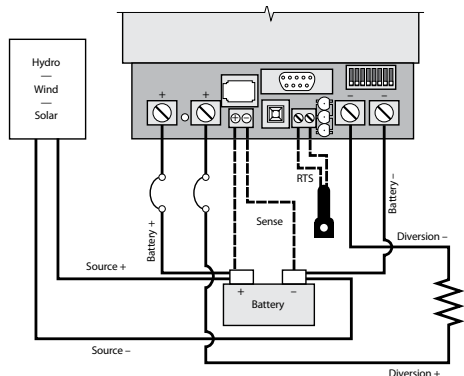


Figure 2.2b Installation Wiring for Diversion Charge Control



NOTE: TriStar negative terminals are common negative.

Steps #3 and #6 are required for all installations.

Steps #4, #5, and #7 are optional.

Step Diversion Charge Control

1. Remove the access cover
2. Mount the TriStar using the enclosed template.
3. Adjust the 8 switches in the DIP switch. Each switch must be in the correct position.
4. Attach the RTS if battery charging will be temperature compensated.
5. Connect battery voltage sense wires (recommended).
6. Connect the battery power wires to the TriStar. Then connect the diversion load wires.

Step Diversion Charge Control (continued)

7. Connect a computer to the TriStar if making adjustments with PC software.
8. Replace the cover.

2.3 Installation Steps

The TriStar controller must be installed properly and in accordance with the local and national electrical codes. It is also important that the installation be done safely, correctly and completely to realize all the benefits that the TriStar can provide for your solar system.

Refer to Sections 4.0 and 9.0 for information about the TriStar's standard battery charging programs and general charging needs for different battery types. Refer to Section 5.0 for load control information, and Section 6.0 for diversion.

Recommended tools:

- wire cutter
- torque wrench (to 50 in-lb)
- phillips screwdrivers
- slotted screw drivers
- wire stripper
- flashlight

Before starting the installation, review these safety notes:

- Do not exceed a battery voltage of 48V nominal (24 cells). Do not use a battery less than 12V (6 cells).
- Do not connect a solar input greater than a nominal 48V array for battery charging. Never exceed a Voc (open-circuit voltage) of 125V.
- Charge only 12, 24, or 48 volt lead-acid batteries when using the standard battery charging programs in the TriStar.
- Verify the nominal charging voltage is the same as the nominal battery voltage.
- Do not install a TriStar in a sealed compartment with batteries.
- Never open the TriStar access cover unless both the solar and battery power has been disconnected.
- Never allow the solar array to be connected to the TriStar with the battery disconnected. This can be a dangerous condition with high open-circuit solar voltages present at the terminals.

Follow the installation steps in order: #1 through #8

Step 1 - Remove the Cover

Remove the 4 screws in the front cover. Lift the cover until the top edge clears the heat sink, and set it aside. If an LCD meter display is attached to the cover, disconnect the RJ-11 connector at the meter for access.



CAUTION: Do not remove the cover if power is present at any of the terminals. Verify that all power sources to the controller are disconnected.



PRUDENCE : N'enlevez pas le couvercle en cas de tension à une des bornes. Vérifiez que toutes les sources d'alimentation au contrôleur sont déconnectées.

Step 2 - Mounting

Locate the TriStar on a wall protected from direct sun, high temperatures, and water. Do not install in a confined area where battery gasses can accumulate.



NOTE: When mounting the TriStar, make sure the air flow around the controller and heat sink is not obstructed. There should be open space above and below the heat sink, and at least 75 mm (3 inches) clearance around the heat sink to allow free air flow for cooling.



REMARQUE : Lors du montage du TriStar, assurez-vous que l'écoulement d'air autour du contrôleur et du puits de chaleur n'est pas obstrué. Un espace doit se trouver au-dessus et en dessous du puits de chaleur et un dégagement de 75 mm (3 po) doit exister autour du puits de chaleur pour permettre l'écoulement de l'air à des fins de refroidissement.

Before starting the installation, place the TriStar on the wall where it will be mounted and determine where the wires will enter the controller (bottom, side, back). Remove the appropriate knockouts before mounting the controller. The knockouts are sized for 1 inch and 1.25 inch conduit.

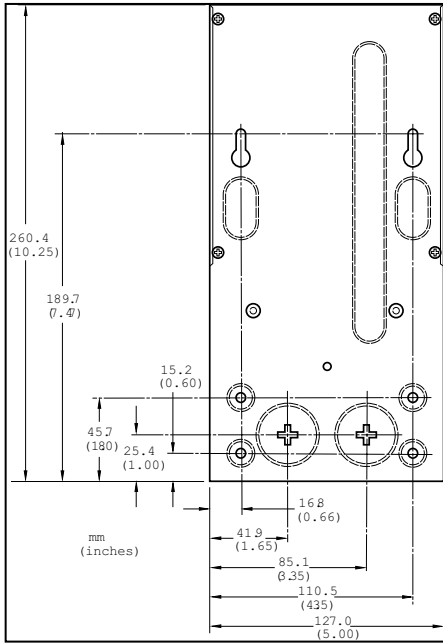


Figure 2.3 - Step 2 Mounting Dimensions

Step 2 - Mounting (continued)

Refer to Figure 2.3. Use the template provided in the shipping carton for locating the mounting holes and for stripping the wires. Use two of the #10 screws provided for the two keyhole slots. Leave the screw heads protruding enough to lock inside the keyhole slots (about 3.8 mm / 0.150 inch). Mount the controller and pull it down to lock the screws into the slots. Use the remaining two screws to fasten the controller to the wall.

Provide for strain relief for the bottom knockouts if conduit will not be used. Avoid excessive pulling forces on the terminals from the wires.

Step 3 - Adjust the DIP Switches

An 8-position DIP switch is used to set-up the controller for its intended use. All major functions can be set with the DIP switches. See Section 7.0 for additional custom settings using PC software.



NOTE: The instructions below are for solar battery charging. Refer to Appendix 1 for Load Control DIP switch settings, and Appendix 2 for Diversion Charge Control DIP switch settings.



REMARQUE : Les instructions ci-dessous concernent la charge de batteries solaires. Reportez-vous à l'Annexe 1 pour les réglages du commutateur DIP de contrôle de charge et à l'Annexe 2 pour les réglages du commutateur DIP de contrôle de charge de diversion.

The DIP switches are located behind the negative power terminals. Each switch is numbered. The solar battery charging functions that can be adjusted with the DIP switches follow:

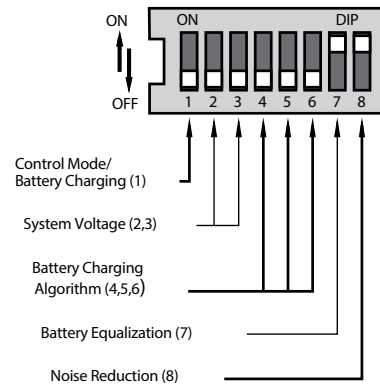


Figure 2.4 - Step 3 DIP Switch Functions

As shown in the diagram, all the positions are in the "OFF" position except switch numbers 7 and 8, which are in the "ON" position.



NOTE: The DIP switches should be changed only when there is no power to the controller. Turn off disconnect switches and remove all power to the controller before changing a DIP switch. A fault will be indicated if a switch is changed while the controller is powered.



REMARQUE : Les commutateurs DIP ne doivent être remplacés que si le contrôleur est hors tension. Mettez tous les interrupteurs sur arrêt et mettez le contrôleur hors tension avant de changer un commutateur DIP. Une panne sera indiquée en cas de changement d'un commutateur alors que le contrôleur est sous tension.



CAUTION: The TriStar is shipped with all the switches in the "OFF" position. Each switch position must be confirmed during installation. A wrong setting could cause damage to the battery or other system components.



PRUDENCE : Le TriStar est expédié avec tous les interrupteurs en position « ARRÊT ». La position de chaque interrupteur doit être confirmée pendant l'installation. Un mauvais réglage peut endommager la batterie ou d'autres composants du système.

The DIP switch settings described below are for Solar Battery Charging only. Load and Diversion switch settings can be found in Appendixes 1 and 2.

The DIP switches are shipped in the OFF position. With the switches in the OFF position, the following functions are present:

Switch	Function
1	Battery charge mode
2, 3	Auto voltage select
4, 5, 6	Lowest battery charging voltage
7	Manual equalization
8	Normal PWM charging mode

To configure your TriStar for the battery charging and control you require, follow the DIP switch adjustments described below. To change a switch from OFF to ON, slide the switch up toward the top of the controller. Make sure each switch is fully in the ON or OFF position.

DIP Switch Number 1 - Control Mode: Solar Battery Charging

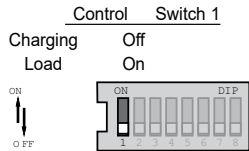


Figure 2.5 - Step 3 DIP Switch #1

For the Solar Battery Charging control mode, leave the DIP switch in the OFF position as shown.

DIP Switches Number 2,3 - System Voltage:

Voltage	Switch 2	Switch 3
Auto	Off	Off
12	Off	On
24	On	Off
48	On	On

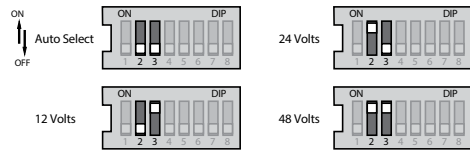


Figure 2.6 - Step 3 DIP Switches # 2,3

The auto voltage selection occurs when the battery is connected and the TriStar starts-up. There should be no loads on the battery that might cause a discharged battery to indicate a lower system voltage.

The DIP switch selectable voltages are for 12V, 24V or 48V lead-acid batteries. Although the "auto voltage" selection is very dependable, it is recommended to use the DIP switches to secure the correct system voltage.

DIP Switches Number 4,5,6 - Battery Charging Algorithm:

Battery Type	PWM	Switch 4	Switch 5	Switch 6
1	14.0	Off	Off	Off
2	14.15	Off	Off	On
3	14.35	Off	On	Off
4	14.4	Off	On	On
5	14.6	On	Off	Off
6	14.8	On	Off	On
7	15.0	On	On	Off
8	Custom	On	On	On

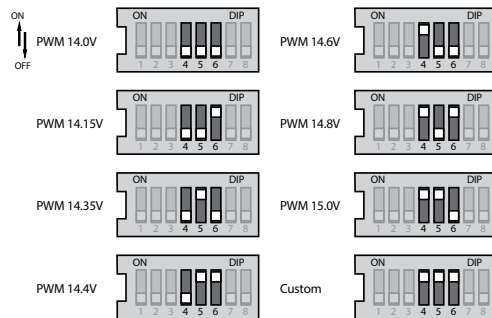


Figure 2.7 - Step 3 DIP Switch # 4,5,6

Select one of the 7 standard battery charging algorithms, or select the "custom" DIP switch for special custom settings using the PC software. Refer to Section 9.0 of this manual for battery charging information. The 7 standard charging algorithms above are described in Section 4.2 - Standard Battery Charging Programs.

DIP Switch Number 7 - Battery Equalization:
Equalize Switch 7
 Manual Off
 Auto On

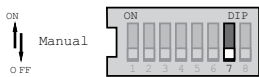


Figure 2.8 - Step 3 DIP Switch # 7

In the Auto Equalization mode (switch #7 On), battery equalization will automatically start and stop according to the battery program selected by the DIP switches 4,5,6 above. See Section 4.0 for detailed information about each standard battery algorithm and the equalization. In the Manual Equalization mode (switch #7 Off), equalization will occur only when manually started with the push-button. Automatic starting of equalization is disabled. The equalization will automatically stop per the battery algorithm selected. In both cases (auto and manual mode), the push-button can be used to start and stop battery equalization.

DIP Switch Number 8 - Noise Reduction:
Charging Switch 8
 PWM Off
 On-Off On

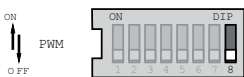


Figure 2.9- Step 3 DIP Switch # 8

The PWM battery charging algorithm is standard for all Morningstar charge controllers. However, in cases where the PWM regulation causes noise interference with loads (e.g. some types of telecom equipment or radios), the TriStar can be converted to an On-Off method of solar charge regulation. It should be noted that the On-Off solar charge regulation is much less effective than PWM. Any noise problem should be suppressed in other ways, and only if no other solution is possible should the TriStar be changed to an On-Off charger.

LOAD CONTROL
 DIP switch settings are in Appendix 1.

DIVERSION CHARGE CONTROL
 DIP switch settings are in Appendix 2.

- NOTE:** Confirm all dip-switch settings before going to the next installation steps.
- REMARQUE :** Confirmez les réglages de tous les commutateurs dip avant de passer aux étapes suivantes d'installation.

Step 4 - Remote Temperature Sensor (RTS)

For solar battery charging and diversion load control, a remote temperature sensor (RTS) is required for temperature-compensated charging. Temperature-compensated charging will not occur without use of an RTS. This remote temperature probe should not be installed for DC load control mode. The optional Morningstar RTS is connected to the 2-position terminal located between the push-button and the LEDs. See the diagram below:

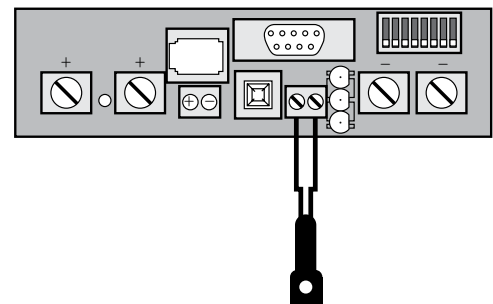


Figure 2.10- Step 4 RTS Connection

The RTS is supplied with 10 meters (33 ft) of 0.34 mm² (22 AWG) cable. There is no polarity, so either wire (+ or -) can be connected to either screw terminal. The RTS cable may be pulled through the conduit with the power wires. Tighten the connector screws with 0.56 Nm (5 in-lb) of torque. Refer to the installation instructions provided with the RTS.

WARNING: Risk of Fire.
 If no Remote Temperature Sensor (RTS) is connected, use the TriStar-PWM within 3m (10 ft) of the batteries. Use of the RTS is strongly recommended.



AVERTISSEMENT: Risque d'incendie.

Si non Capteur de température distant (RTS) est connecté, utilisez le TriStar-PWM moins de 3m (10 pi) de les batteries. Utilisation de la RTS est fortement recommandé.



NOTE: Never place the temperature sensor inside a battery cell. Both the RTS and the battery will be damaged.



REMARQUE : Ne placez jamais la sonde de température dans un élément de batterie. Le RTS et la batterie seraient endommagés.

Step 5 - Battery Voltage Sense Connection

A battery voltage sense connection is not required to operate your TriStar controller, but it is recommended for best performance in all charging and load control modes. The battery voltage sense wires carry almost no current, so the voltage sense input avoids the large voltage drops that can occur in the battery power conductors. The voltage sense connection allows the controller to measure the actual battery voltage under all conditions.

In addition, if a TriStar meter will be added to the controller, the battery voltage sense will ensure that the voltage and diagnostic displays are very accurate.

The two battery voltage sense wires are connected to the TriStar at the 2-position terminal located between the push-button and the positive (+) terminal lug. See the diagram below:

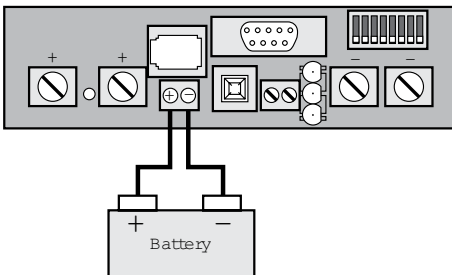


Figure 2.11 - Step 5 Battery Sense Connection

The two voltage sense wires (not provided with the controller) should be cut to length as required to connect the battery to the voltage sense terminal. The wire size can be from 1.0 to 0.25 mm² (16 to 24 AWG). It is recommended to twist the wires together every few feet (twisted pair), but this is not required. The voltage sense wires may be pulled through the conduit with the power wires.

Fuse the positive (+) voltage sense wire as close to the battery as possible. Size the fuse based on wire ampacity - a 1A fuse can be used for #24 wire.

Tighten the connector screws with 0.56 Nm (5 in-lb) of torque.

The maximum length allowed for each battery voltage sense wire is 30 meters (98 ft).

The battery sense terminal has polarity. Be careful to connect the battery positive (+) terminal to the voltage sense positive (+) terminal. No damage will occur if the polarity is reversed, but many functions of the controller can be affected. If a TriStar meter is installed, check the "TriStar Settings" to confirm the Voltage Sense and the RTS (if installed) are both present and "seen" by the controller. The PC software can also be used to confirm the voltage sense is working correctly.

Do not connect the voltage sense wires to the RTS terminal. This may cause an alarm. Review the installation diagram for the correct battery voltage sense connection.

Note that the battery voltage sense connection does not power (start-up) the controller.

Step 6 - System Wiring and Power-Up

To comply with the NEC, the TriStar must be installed using wiring methods in accordance with the latest edition of the National Electric Code, NFPA 70.

Wire Size

The four large power terminals are sized for 35 - 2.5 mm² (2-14 AWG) wire. The terminals are rated for copper and aluminum conductors.

Good system design generally requires large conductor wires for the solar and battery connections that limit voltage drop losses to 3% or less. The following table provides the maximum wire length (1-way distance / 2-wire pair) for connecting the battery, solar array or load to the TriStar with a maximum 3% voltage drop.

Wire Size	60 Amps	45 Amps	30 Amps	15 Amps
95 mm ² (3/0 AWG)	12.86 m (42.2 ft.)	17.15 m (56.3 ft.)	25.72 m (84.4 ft.)	51.44 m (168.8 ft.)
70 mm ² (2/0 AWG)	10.19 m (33.4 ft.)	13.58 m (44.6 ft.)	20.38 m (66.8 ft.)	40.75 m (133.7 ft.)
50 mm ² (1/0 AWG)	8.10 m (26.6 ft.)	10.80 m (35.4 ft.)	16.21 m (53.1 ft.)	32.41 m (106.3 ft.)
35 mm ² (2 AWG)	5.12 m (16.8 ft.)	6.83 m (22.4 ft.)	10.24 m (33.6 ft.)	20.48 m (67.2 ft.)
25 mm ² (4 AWG)	3.21 m (10.5 ft.)	4.27 m (14.0 ft.)	6.41 m (21.0 ft.)	12.82 m (42.1 ft.)
16 mm ² (6 AWG)	2.02 m (6.6 ft.)	2.69 m (8.8 ft.)	4.04 m (13.2 ft.)	8.07 m (26.5 ft.)
10 mm ² (8 AWG)	1.27 m (4.2 ft.)	1.70 m (5.6 ft.)	2.54 m (8.3 ft.)	5.09 m (16.7 ft.)
6 mm ² (10 AWG)		1.06 m (3.5 ft.)	1.60 m (5.2 ft.)	3.19 m (10.5 ft.)
4 mm ² (12 AWG)			1.00 m (3.3 ft.)	2.01 m (6.6 ft.)
2.5 mm ² (14 AWG)				1.26 m (4.1 ft.)

Table 2.3-6a Maximum 1-Way Wire Distance (12 Volts)

NOTES:

- The specified wire length is for a pair of conductors from the solar, load or battery source to the controller (1-way distance).
- Figures are in meters (m) and feet (ft).
- For 24 volt systems, multiply the 1-way length in the table by 2.
- For 48 volt systems, multiply the 1-way length in the table by 4.

The NEC requires that manually operated disconnect switches or circuit breakers must be provided for connections between the TriStar and the battery. If the overcurrent devices being used are not manually operated disconnects, then manual disconnect switches must be added. These manual switches must be rated the same as the overcurrent devices noted above.

- Refer to the NEC for more information.

Minimum Wire Size

The NEC requires that the wires carrying the system current never exceed 80% of the conductors' current rating. The table below provides the minimum size of copper wire allowed by NEC for the TS-45 and TS-60 versions. Wire types rated for 75°C and 90°C are included.

Minimum wire sizes for ambient temperatures to 45°C are provided in the table below:

TS-45	75C Wire	90C Wire	TS-60	75C Wire	90C Wire
≤ 45C	16 mm ² (6 AWG)	10 mm ² (8 AWG)	≤ 45C	25 mm ² (4 AWG)	16 mm ² (6 AWG)

Table 2.3-6b Minimum Wire Size

Both copper and aluminum conductors can be used with a TriStar controller. If aluminum wire is used, the minimum size of the aluminum conductor must be one wire size larger than the minimum wire size specified in the table above.

Ground Connection

Use the grounding terminal in the wiring compartment to connect a copper wire to an earth ground or similar grounding point. The grounding terminal is identified by the ground symbol shown below that is stamped into the enclosure:



Ground Symbol

Per NEC 690.45 (A) and NEC Table 250.122, minimum sizes for copper grounding wire are:

TS-45	10 AWG (5 mm ²)
TS-60/M	8 AWG (8 mm ²)

OR, of the same, or greater, cross-sectional area as the PV wires.

Connect the Power Wires

First, confirm that the DIP switch #1 is correct for the operating mode intended.

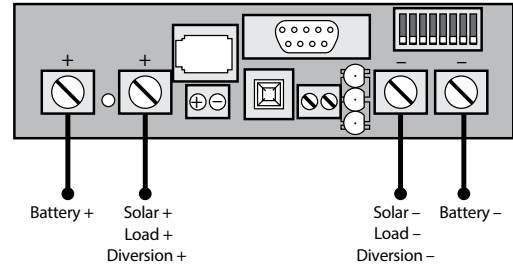


Figure 2.12 - Step 6 Power Wire Connections



CAUTION: The solar PV array can produce open-circuit voltages over 100 Vdc when in sunlight. Verify that the solar input breaker has been opened (disconnected) before installing the system wires (if the controller is in the solar charging mode).



PRUDENCE : Le réseau PV solaire peut produire des tensions de circuit ouvert supérieures à 100 V cc à la lumière du soleil. Vérifiez que le coupe-circuit solaire a été ouvert (déconnexion) avant d'installer les câbles du système (si le contrôleur est en mode de charge solaire).

Using the diagram on the previous page, connect the four power conductors in the following steps:

1. Confirm that the input and output disconnect switches are both turned off before connecting the power wires to the controller. There are no disconnect switches inside the TriStar.
2. Provide for strain relief if the bottom knockouts are used and conduit is not used.
3. Pull the wires into the wiring compartment. The temperature probe wires and battery voltage sense wires can be inside the conduit with the power conductors.
4. Connect the Battery + (positive) wire to the Battery + terminal.
5. Connect the Battery – (negative) wire to a TriStar common – terminal.
6. Connect the Solar + wire (positive) to the Solar + terminal.
(or Load + / Diversion +)
7. Connect the Solar – (negative) wire a TriStar common – terminal.
(or Load – / Diversion –)



NOTE: TriStar negative terminals are common negative.

The CE certification requires that the battery conductors, the battery voltage sense wires, and the remote temperature sensor shall not be accessible without the use of a tool and are protected in the battery compartment.

Do not bend the power wires up toward the access cover. If a TS-M meter is used now or in the future, these large wires can damage the meter assembly when the access cover is attached to the controller.

Torque each of the four power terminals to 5.65 Nm (50 in-lbs).

Power-Up

- Confirm that the solar (or load) and battery polarities are correct.
- Turn the battery disconnect on first. Observe the LEDs to confirm a successful start-up. (LEDs blink Green - Yellow - Red in one cycle)
- Note that a battery must be connected to the TriStar to start and operate the controller. The controller will not operate from a solar input only.
- Turn the solar (or load) disconnect on.

Step 7 - RS-232 Adjustments

The TriStar must be powered from the battery to enable use of the RS-232 / PC computer connection. Refer to Section 7.0 for using the RS-232 and Morningstar's PC software to change set-points or confirm the installation settings.

Step 8 - Finish Installation

Inspect for tools and loose wires that may have been left inside the enclosure.

Check the power conductors to make sure they are located in the lower part of the wiring compartment and will not interfere with the cover or the optional meter assembly.



NOTE: If the power conductors are bent upwards and touch the meter assembly (TS-M option), pressing the cover down on the wires can damage the meter.



REMARQUE : Si les conducteurs d'alimentation sont courbés vers le haut et touche l'ensemble de mesure (option TS-M), la pression du couvercle sur les câbles peut endommager l'appareil de mesure.

Carefully place the cover back on the controller and install the 4 cover screws.

Closely observe the system behavior and battery charging for 2 to 4 weeks to confirm the installation is correct and the system is operating as expected.

3.0 TriStar Operation

The TriStar operation is fully automatic. After the installation is completed, there are few operator tasks to perform. However, the operator should be familiar with the basic operation and care of the TriStar as described below.

3.1 Operator's Tasks

- Use the push-button as needed (see 3.2 below)
- Check the LEDs for status and faults (see 3.3 below)
- Support recovery from a fault as required (see 3.4 below)
- Routine inspection and maintenance (see 3.6 below)

If a TriStar digital meter is installed, please refer to the meter manual.

3.2 Push-button

In the battery charging mode (both solar and diversion), the following functions can be enabled with the push-button (located on the front cover):

PUSH: Reset from an error or fault.

PUSH: Reset the battery service indication if this has been activated with the PC software. A new service period will be started, and the flashing LEDs will stop blinking. If the battery service is performed before the LEDs begin blinking, the push-button must be pushed at the time when the LEDs are blinking to reset the service interval and stop the blinking.

PUSH AND HOLD 5 SECONDS: Begin battery equalization manually. This will begin equalization in either the manual or automatic equalization mode. The equalization will automatically stop per the battery type selected (see Section 4.4).

PUSH AND HOLD 5 SECONDS: Stop an equalization that is in progress. This will be effective in either the manual or automatic mode. The equalization will be terminated.

Note that if two or more TriStars are charging in parallel, the equalization cycles may start on different days for various reasons (such as one controller is disconnected and restarted). If this happens, the push-button on each controller can be used to manually start and then stop an equalization, and this will reset the equalizations to the same schedule.

LOAD & LIGHTING CONTROL

PUSH: Reset from an error or fault.

PUSH AND HOLD 5 SECONDS: After a low voltage disconnect (LVD) of the load, the push-button can be used to reconnect the loads again. The loads will remain on for 10 minutes, and will then disconnect again. The push-button can be used to override the LVD without limit.

NOTE: The purpose of the LVD is to protect the battery. Repeated overrides of an LVD can deeply discharge the battery and may damage the battery.

3.3 LED Indications

Valuable information can be provided by the three LEDs in the front cover. Although there are many different LED indications, they have similar patterns to make it easier to interpret each LED display. Consider as three groups of indications: General Transitions // Battery or Load Status // Faults.

LED Display Explanation:

- G = green LED is lit
- Y = yellow LED is lit
- R = red LED is lit
- G/Y = Green and Yellow are both lit at the same time
- G/Y - R = Green & Yellow both lit, then Red is lit alone
- Sequencing (faults) has the LED pattern repeating until the fault is cleared

1. General Transitions:

- Controller start-up G - Y - R (one cycle)
- Push-button transitions blink all 3 LEDs 2 times
- Battery service is required all 3 LEDs blinking until service is reset

2. Battery Status

- General state-of-charge see battery SOC indications below
- PWM absorption G blinking (1/2 second on / 1/2 second off)
- Equalization state G fast blink (2 to 3 times per second)
- Float state G slow blink (1 second on / 1 second off)

Battery State-of-Charge LED Indications (when battery is charging):

- G on 80% to 95% SOC
- G/Y on 60% to 80% SOC
- Y on 35% to 60% SOC
- Y/R on 0% to 35% SOC
- R on battery is discharging

Refer to the Specifications (Section 11.0) for the State-of-Charge voltages. Another LED chart is provided at the end of this manual (Appendix 3) for easier reference.

Note that because these State-of-Charge LED displays are for all battery types and system designs, they are only approximate indications of the battery charge state.

LOAD & LIGHTING CONTROL

2. Load Status

	12V	24V	48V
LVD+	0.60V	1.20V	2.40V
LVD+	0.45V	0.90V	1.80V
LVD+	0.30V	0.60V	1.20V
LVD+	0.15V	0.30V	0.60V
LVD			

The load status LEDs are determined by the LVD voltage plus the specified transition voltages. As the battery voltage rises or falls, each voltage transition will cause a change in the LEDs.

3. Faults & Alarms

- Short circuit - solar/load R/G - Y sequencing
- Overload - solar/load R/Y - G sequencing
- Over-temperature R - Y sequencing
- High voltage disconnect R - G sequencing
- Reverse polarity - battery no LEDs are lighted
- Reverse polarity - solar No fault indication
- DIP switch fault R - Y - G sequencing
- Self-test faults R - Y - G sequencing
- Temperature probe (RTS) R/Y - G/Y sequencing
- Battery voltage sense R/Y - G/Y sequencing

3.4 Protections and Fault Recovery

The TriStar protections and automatic recovery are important elements of the operating system. The system operator should be familiar with the causes of faults, controller protections, and any actions that may be required.

Some basic fault conditions are reviewed below:

Short circuit:

(R/G-Y sequencing) When a short circuit occurs, the FET switches are opened in micro-seconds. The FETs will probably open before other protective devices in the system can react, so the short circuit may remain in the system. The TriStar will try to reconnect the FETs two times. If the short circuit remains, the LEDs will continue sequencing.

After the short in the system is repaired, there are two ways to restart the controller:

- Power should have been disconnected to repair the short. When power is restored, the TriStar does a normal start-up and will reconnect the solar input or load.
- The push-button can also be used to reconnect the FET switches (if there is battery power to the TriStar).



NOTE: There will always be a 10 second delay between attempts to reconnect the FET switches. Even if power is disconnected, the TriStar will wait for the remainder of the 10 seconds when the power is restored.



REMARQUE : Il existera toujours un délai de 10 secondes entre les tentatives de reconnexion des commutateurs TEC. Même si l'alimentation est déconnectée, le TriStar attend la fin des 10 secondes quand l'alimentation est rétablie.

Solar overload:

(R/Y-G sequencing) If the solar input exceeds 100% of the controller's current rating, the controller will reduce the average current below the TriStar's rating. The controller is capable of managing up to 130% of the rated solar input.

When 130% rated current is exceeded, the solar will be disconnected and a fault will be indicated. The input FET switches will remain open for 10 seconds. Then the switches are closed again and charging resumes. These cycles can continue without limit.

The current overload is reduced to the "equivalent heating" of the rated current input. For example, a 72A solar array (120% overload) will PWM down to 50A, which is equivalent to the heating from a normal 60A solar input.

LOAD & LIGHTING CONTROL

Load overload:

(R/Y-G sequencing) If the load current exceeds 100% of the controller's rating, the controller will disconnect the load. The greater the overload, the faster the controller will disconnect. A small overload could take a few minutes to disconnect.

The TriStar will attempt to reconnect the load two times. Each attempt is at least 10 seconds apart. If the overload remains after 2 attempts, the load will remain disconnected. The overload must be corrected and the controller restarted. The push-button can also be used to reconnect the load.

DIVERSION CHARGE CONTROL

Diversion overload:

(R/Y-G sequencing) If the current to the diversion load exceeds the TriStar rating, the controller will attempt to reduce the load. If the overload is too large, the TriStar will disconnect the diversion load. The controller will continue attempts to reconnect the load.

If the overload LEDs are sequencing, the diversion load is too large for the controller. The size of the load must be reduced.

Reversed polarity:

If the battery polarity is reversed, there will be no power to the controller and no LEDs will light. If the solar is reversed, the controller detects nighttime and there will be no LED indication and no charging. If the load is reversed, loads with polarity will be damaged. Be very careful to connect loads to the controller with correct polarity. See Section 5.4.

DIP switch fault:

(R-Y-G sequencing) If a DIP switch is changed while there is power to the controller, the LEDs will begin sequencing and the FET switches will open. The controller must be restarted to clear the fault.

Solar high temperature:

(R-Y sequencing) When the heatsink temperature limit is reached, the TriStar will begin reducing the solar input current to prevent more heating. If the controller continues heating to a higher temperature, the solar input will then be disconnected. The solar will be reconnected at the lower temperature (see Section 8.0).

LOAD & LIGHTING CONTROL

Load high temperature:

(R-Y sequencing) When the heatsink temperature limit is reached (90°C / 194°F), the TriStar will disconnect the load. The load will be reconnected at the lower temperature setting (70°C / 158°F).

DIVERSION CHARGE CONTROL

Diversion high temperature:

(R-Y sequencing) When the heat sink temperature reaches 80°C, the TriStar will change to an on-off regulation mode to reduce the temperature. If the temperature reaches 90°C, the load will be disconnected. The load is reconnected at 70°C.

Solar high voltage disconnect (HVD):

(R-G sequencing) If the battery voltage continues increasing beyond normal operating limits, the controller will disconnect the solar input (unless the FET switches cannot open due to a failure). See Section 11.0 for the disconnect and reconnect values.

LOAD & LIGHTING CONTROL

Load HVD:

(R-G sequencing) In the Load Control mode, the HVD can only be enabled using the PC software. At the battery voltage value selected in the software, the TriStar will disconnect the load. At the selected lower voltage, the load will be reconnected.

DIVERSION CHARGE CONTROL

Diversion HVD:

In the Diversion mode, an HVD condition will not be indicated with the LEDs, and there is no disconnect. An HVD condition will be indicated on the optional meter.

Battery removal voltage spike:

(no LED indication) Disconnecting the battery before the solar input is disconnected can cause a large solar open-circuit voltage spike to enter the system. The TriStar protects against these voltage spikes, but it is best to disconnect the solar input before the battery.

Very low battery voltage:

(LEDs are all off) Below 9 volts the controller will go into brownout. The controller shuts down. When the battery voltage rises, the controller will restart. In the Load Control mode, the TriStar will recover in the LVD state.

Remote temperature sensor (RTS) failure:


(R/Y-G/Y) If a fault in the RTS (such as a short circuit, open circuit, loose terminal) occurs after the RTS has been working, the LEDs will indicate a failure and the solar input is disconnected. However, if the controller is restarted with a failed RTS, the controller may not detect that the RTS is connected, and the LEDs will not indicate a problem. A TriStar meter or the PC software can be used to determine if the RTS is working properly.

Battery voltage sense failure:

(R/Y-G/Y) If a fault in the battery sense connection (such as a short circuit, open circuit, loose terminal) occurs after the battery sense has been working, the LEDs will indicate a failure. However, if the controller is restarted with the failure still present in the battery sense, the controller may not detect that the battery sense is connected, and the LEDs will not indicate a problem. A TriStar meter or the PC software can be used to determine if the battery sense is working properly.

3.5 Data-Logging

The TriStar records daily records of key system information. Data is stored in all operating modes: Charging, Load/Lighting, Diversion. In Charge mode records are written after dusk each day. In Load and Diversion modes, records are written every 24 hours and may not coincide with the natural day/night cycle. The logged data can be viewed using the TriStar Digital Meter 2 or TriStar Remote Meter 2. Data can also be accessed using MSView™ PC software, which is available for download on our website.

 **NOTE: The Data Logging feature is available in TriStar firmware version v12 and later. Firmware update files and instructions are available on our website.**

3.6 Inspection and Maintenance

 **WARNING: RISK OF ELECTRICAL SHOCK.**

NO POWER OR ACCESSORY TERMINALS ARE ELECTRICALLY ISOLATED FROM DC INPUT, AND MAY BE ENERGIZED WITH HAZARDOUS SOLAR VOLTAGE. UNDER CERTAIN FAULT CONDITIONS, BATTERY COULD BECOME OVER-CHARGED. TEST BETWEEN ALL TERMINALS AND GROUND BEFORE TOUCHING.



AVERTISSEMENT: RISQUE DE CHOC ÉLECTRIQUE.

ON ALIMENTATION OU AUX BORNES D'ACCESSOIRES SONT ISOLÉS ÉLECTRIQUEMENT DE L'ENTRÉE DE C.C ET DOIT ÊTRE ALIMENTÉS À UNE TENSION DANGEREUSE SOLAIRE. SOUS CERTAINES CONDITIONS DE DÉFAILLANCE, LA BATTERIE POURRAIT DEVENIR TROP CHARGÉE. TEST ENTRE TOUTES LES BORNES ET LA MASSE AVANT DE TOUCHER.



WARNING: Shock Hazard

Disconnect all power sources to the controller before removing the wiring box cover. Never remove the cover when voltage exists on the TriStar-PWM power connections.



AVERTISSEMENT: Risque de décharge électrique

Un moyen de déconnexion de tous les poteaux d'alimentation doit être fourni. Ceux-ci se déconnecte doit être intégrée dans le câblage fixe. Ouvrir que toutes les source d'énergie se déconnecte avant de retirer le couvercle de la contrôleur, ou accès au câblage.

The TriStar does not require routine maintenance. The following inspections are recommended two times per year for best long-term performance.

1. Confirm the battery charging is correct for the battery type being used. Observe the battery voltage during PWM absorption charging (green LED blinking 1/2 second on / 1/2 second off). Adjust for temperature compensation if an RTS is used (see Table 4.3).
For load and diversion modes, confirm that the operation is correct for the system as configured.
2. Confirm the controller is securely mounted in a clean and dry environment.
3. Confirm that the air flow around the controller is not blocked. Clean the heat sink of any dirt or debris.
4. Inspect for dirt, nests and corrosion, and clean as required.

4.0 Battery Charging

4.1 PWM Battery Charging

PWM (Pulse Width Modulation) battery charging is the most efficient and effective method for recharging a battery in a solar system. Refer to "Why PWM?" on Morningstar's website for more information.

Selecting the best method for charging your battery together with a good maintenance program will ensure a healthy battery and long service life. Although the TriStar's battery charging is fully automatic, the following information is important to know for getting the best performance from your TriStar controller and battery.

4.1.1 Four Stages of Solar Charging

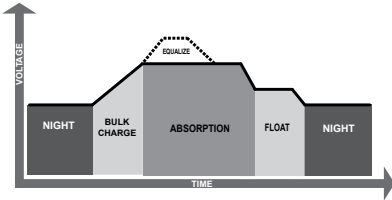


Figure 4.1.1 Solar Charging Stages

- Bulk Charging:** In this stage, the battery will accept all the current provided by the solar system. The LEDs will display an indication of the battery charge state as the battery is being recharged.
- PWM Absorption:** When the battery reaches the regulation voltage, the PWM begins to hold the voltage constant. This is to avoid over-heating and over-gassing the battery. The current will taper down to safe levels as the battery becomes more fully charged. The green LED will blink once per second. See Section 4.2.
- Equalization:** Many batteries benefit from a periodic boost charge to stir the electrolyte, level the cell voltages, and complete the chemical reactions. The green LED will blink rapidly 2-3 times per second. See Section 4.4.
- Float:** When the battery is fully recharged, the charging voltage is reduced to prevent further heating or gassing of the battery. The green LED will blink slowly once every 2 seconds. See Section 4.5.

4.1.2 Battery Charging Notes

The TriStar manages many different charging conditions and system configurations. Some useful functions to know follow below.

Solar Overload: Enhanced radiation or "edge of cloud effect" conditions can generate more current than the controller's rating. The TriStar will reduce this overload up to 130% of rated current by regulating the current to safe levels. If the current from the solar array exceeds 130%, the controller will interrupt charging (see Section 3.4).

Battery Voltage Sense: Connecting a pair of voltage sense wires from the controller to the battery is recommended. This allows a precise battery voltage input to the controller and more accurate battery charging. See Section 4.3 for more information.

Temperature Compensation: All charging set-points are based on 25°C (77°F). If the battery temperature varies by 5°C, the charging will change by 0.15 volts for a 12 volt battery. This is a substantial change in the charging of the battery, and a remote temperature sensor is recommended to adjust charging to the actual battery temperature. See Section 4.3 for more information.

Day-Night Detection: The TriStar will automatically detect day and night conditions. Any functions that require measuring time or starting at dawn, for example, will be automatic.

PWM Noise: In some installations, the PWM charging may cause audible noise in certain equipment. If this occurs, the PWM can be changed to "On-Off" solar charging to reduce the noise. This requires DIP switch number 8 to be turned On. However, it is strongly recommended to try to remedy the noise problem with grounding or filtering first, because the benefits from PWM battery charging are significant.

Battery Types: The TriStar's standard battery charging programs are suitable for a wide range of lead-acid battery types. These standard programs are reviewed in the following Section 4.2. A general review of battery types and their charging needs is provided in Section 9.0.

4.2 Standard Battery Charging Programs

The TriStar provides 7 standard battery charging algorithms (programs) that are selected with the DIP switches (see Step 3 in Installation). These standard algorithms are suitable for lead-acid batteries ranging from sealed (gel, AGM, maintenance free) to flooded to L-16 cells. In addition, an 8th DIP switch provides for custom set-points using the PC software.

The table below summarizes the major parameters of the standard charging algorithms. Note that all the voltages are for 12V systems (24V = 2X, 48V = 4X).

All values are 25°C (77°F).

DIP Switches (4-5-6)	A. Battery Type	B. PWM Absorp. Voltage	C. Float Voltage	D. Equal. Voltage	E. Time in Equal. (hours)	F. Equalize Interval (days)	G. Max Equal. Cycle (hours)
off-off-off	1 - Sealed	14.0	13.4	none	-	-	-
off-off-on	2 - Sealed	14.15	13.4	14.2	1	28	1
off-on-off	3 - Sealed	14.35	13.4	14.4	2	28	2
off-on-on	4 - Flooded	14.4	13.4	15.1	3	28	4
on-off-off	5 - Flooded	14.6	13.4	15.3	3	28	5
on-off-on	6 - Flooded	14.8	13.4	15.3	3	28	5
on-on-off	7 - L-16	15.0	13.4	15.3	3	14	5
on-on-on	8 - Custom		Custom			Custom	

Table 4.2 Standard Battery Charging Programs

A. Battery Type - These are generic lead-acid battery types. See Section 9.0 for more information about battery types and appropriate solar charging.

B. PWM Voltage—This is the PWM Absorption stage with constant voltage charging. The “PWM voltage” is the maximum battery voltage that will be held constant. As the battery becomes more charged, the charging current tapers down until the battery is fully charged.

C. Float Voltage—When the battery is fully charged, the charging voltage will be reduced to 13.4 volts for all battery types. The float voltage and transition values are adjustable with the PC software. See Section 4.5 for more details.

D. Equalization Voltage—During an equalization cycle, the charging voltage will be held constant at this voltage.

E. Time in Equalization—The charging at the selected equalization voltage will continue for this number of hours. This may take more than one day to complete. See Section 4.4.

F. Equalization Interval—Equalizations are typically done once a month. Most of the cycles are 28 days so the equalization will begin on the same day of the week. Each new cycle will be reset as the equalization starts so that a 28 day period will be maintained.

G. Maximum Equalization Cycle—If the solar array output cannot reach the equalization voltage, the equalization will terminate after this many hours to avoid over gassing or heating the battery. If the battery requires more time in equalization, the manual push-button can be used to continue for one or more additional equalization cycles.

These (7) standard battery charging algorithms will perform well for the majority of solar systems. However, for systems with specific needs beyond these standard values, any or all of these values can be adjusted using the PC software. See Section 7.0.

4.3 Temperature Effects & Battery Voltage Sense

4.3.1 Remote Temperature Sensor (RTS)

The RTS is used for temperature compensated battery charging. As the battery gets warmer, the gassing increases. As the battery gets colder, it becomes more resistant to charging. Depending on how much the battery temperature varies, it may be important to adjust the charging for temperature changes.

There are three battery charging parameters that are affected by temperature:

PWM Absorption

This is the most important part of charging that is affected by temperature because the charging may go into PWM absorption almost every day. If the battery temperature is colder, the charging will begin to regulate too soon and the battery may not be recharged with a limited solar resource. If the battery temperature rises, the battery may heat and gas too much.

Equalization

A colder battery will lose part of the benefit of the equalization. A warmer battery may heat and gas too much.

Float

Float is less affected by temperature changes, but it may also undercharge or gas too much depending on how much the temperature changes.

The RTS corrects the three charging set-points noted above by the following values:

- 12 volt battery: -0.030 volts per °C (-0.017 volts per °F)
- 24 volt battery: -0.060 volts per °C (-0.033 volts per °F)
- 48 volt battery: -0.120 volts per °C (-0.067 volts per °F)

Variations in battery temperature can affect charging, battery capacity, and battery life. The greater the range of battery temperatures, the greater the impact on the battery. For example, if the temperature falls to 10°C (50°F) this 15°C (27°F) change in temperature will change the PWM, equalization and float set-points by 1.80V in a 48V system.

If a remote temperature sensor is not used and the temperatures near the battery are stable and predictable, the PWM absorption setting can be adjusted using the PC software per the following table:

Temperature	12 Volt	24 Volt	48 Volt
40°C / 104°F	- 0.45 V	- 0.90 V	- 1.80 V
35°C / 95°F	- 0.30 V	- 0.60 V	- 1.20 V
30°C / 86°F	- 0.15 V	- 0.30 V	- 0.60 V
25°C / 77°F	0 V	0 V	0 V
20°C / 68°F	+ 0.15 V	+ 0.30 V	+ 0.60 V
15°C / 59°F	+ 0.30 V	+ 0.60 V	+ 1.20 V
10°C / 50°F	+ 0.45 V	+ 0.90 V	+ 1.80 V
5°C / 41°F	+ 0.60 V	+ 1.20 V	+ 2.40 V
0°C / 32°F	+ 0.75 V	+ 1.50 V	+ 3.00 V
- 5°C / 23°F	+ 0.90 V	+ 1.80 V	+ 3.60 V
- 10°C / 14°F	+ 1.05 V	+ 2.10 V	+ 4.20 V
- 15°C / 5°F	+ 1.20 V	+ 2.40 V	+ 4.80 V

Table 4.3 Temperature Compensation

The need for temperature compensation depends on the temperature variations, battery type, how the system is used, and other factors. If the battery appears to be gassing too much or not charging enough, an RTS can be added at any time after the system has been installed. See Section 2.3 - Step 4 for installation instructions.

The TriStar will recognize the RTS when the controller is started (powered-up).

4.3.2 Battery Voltage Sense

There can be voltage drops typically up to 3% in the power cables connecting the battery to the TriStar. If battery voltage sense wires are not used, the controller will read a higher voltage at the controller’s terminals than the actual battery voltage while charging the battery.

Although limited to 3% as the generally accepted wiring standard, this can result in a 0.43 voltage drop for 14.4V charging (or 1.72V for a 48 volt nominal system).

These voltage drops will cause some undercharging of the battery. The controller will begin PWM absorption, or limit equalization, at a lower battery voltage because the controller measures a higher voltage at the controller's terminals than is the actual battery voltage. For example, if the controller is programmed to start PWM absorption at 14.4V, when the controller "sees" 14.4V at its battery terminals, the true battery voltage would only be 14.1V if there is a 0.3V drop between the controller and battery.

Two sense wires, sized from 1.0 to 0.25 mm² (16 to 24 AWG), can be used for battery voltage sense. Because these wires carry no current, the voltage at the TriStar will be identical to the battery voltage. A 2-position terminal is used for the connection.

Note that the battery sense wires will not power the controller, and the sense wires will not compensate for losses in the power wires between the controller and the battery. The battery sense wires are used to improve the accuracy of the battery charging.

See Section 2.3 - Step 5 for instructions how to connect the battery sense wires.

4.4 Equalization

Routine equalization cycles are often vital to the performance and life of a battery — particularly in a solar system. During battery discharge, sulfuric acid is consumed and soft lead sulfate crystals form on the plates. If the battery remains in a partially discharged condition, the soft crystals will turn into hard crystals over time. This process, called "lead sulfation," causes the crystals to become harder over time and more difficult to convert back to soft active materials.

Sulfation from chronic undercharging of the battery is the leading cause of battery failures in solar systems. In addition to reducing the battery capacity, sulfate build-up is the most common cause of buckling plates and cracked grids. Deep cycle batteries are particularly susceptible to lead sulfation.

Normal charging of the battery can convert the sulfate back to the soft active material if the battery is fully recharged. However, a solar battery is seldom completely recharged, so the soft lead sulfate crystals harden over a period of time. Only a long controlled overcharge, or equalization, at a higher voltage can reverse the hardening sulfate crystals.

In addition to slowing or preventing lead sulfation, there are also other benefits from equalizations of the solar system battery. These include:

Balance the individual cell voltages.

Over time, individual cell voltages can drift apart due to slight differences in the cells. For example, in a 12 cell (24V) battery, one cell is less efficient in recharging to a final battery voltage of 28.8 volts (2.4 V/c). Over time, that cell only reaches 1.85 volts, while the other 11 cells charge to 2.45 volts per cell. The overall battery voltage is 28.8V, but the individual cells are higher or lower due to cell drift. Equalization cycles help to bring all the cells to the same voltage.

Mix the electrolyte.

In flooded batteries, especially tall cells, the heavier acid will fall to the bottom of the cell over time. This stratification of the electrolyte causes loss of capacity and corrosion of the lower portion of the plates. Gassing of the electrolyte from a controlled overcharging (equalization) will stir and remix the acid into the battery electrolyte.



NOTE: Excessive overcharging and gassing too vigorously can damage the battery plates and cause shedding of active material from the plates. An equalization that is too high or for too long can be damaging. Review the requirements for the particular battery being used in your system.



REMARQUE : Une surcharge excessive et un dégagement gazeux trop vigoureux peuvent endommager les plaques de batteries et provoquer l'élimination du matériau actif des plaques. Une compensation trop élevée ou trop longue peut provoquer des dégâts. Examinez les exigences pour la batterie particulière utilisée dans votre système.

4.4.1 Standard Equalization Programs

Both automatic and manual equalizations can be performed using either the standard charging programs (see 4.2) or a custom program (see 7.0).

Manual Equalization

The TriStar is shipped with the DIP switch set for manual equalization only. This is to avoid an unexpected or unwanted automatic equalization. In the manual mode, the push-button is used to both start or stop a manual equalization. Hold the push-button down for 5 seconds to start or stop an equalization (depending on whether an equalization is in progress or not).

The LEDs will confirm the transition (all 3 LEDs blink 2 times). When the battery charging enters into equalization, the Green LED will start fast blinking 2-3 times per second.

There are no limits to how many times the push-button can be used to start and stop equalizations. Equalizations will be terminated automatically per the charging program selected if the push-button is not used to manually stop the equalization.

Automatic Equalization

If the equalization DIP switch is moved to the ON position (see 2.3 - Step 3), the equalizations will begin automatically per the charging program selected. Other than starting, the automatic and manual equalizations are the same and follow the standard charging program selected. The push-button can be used to start and stop equalizations in both the manual and automatic mode.

4.4.2 Typical Equalizations

The automatic equalizations will occur every 28 days (except L-16 cells at 14 days). When an equalization begins (auto or manual), the battery charging voltage increases up to the equalization voltage (Veq). The battery will remain at Veq for the time specified in the selected charging program (see table in 4.2).

If the time to reach Veq is too long, the maximum equalization cycle time will end the equalization. A second manual equalization cycle can be started with the push-button if needed.

If the equalization cannot be completed in one day, it will continue the next day or days until finished. After an equalization is completed, charging will return to PWM absorption.

4.4.3 Preparation for Equalization

First, confirm that all your loads are rated for the equalization voltage. Consider that at 0°C (32°F) the equalization voltage will reach 16.05V in a 12V system (64.2V in a 48V system) with a temperature sensor installed. Disconnect any loads at risk.

If Hydrocaps are used, be sure to remove them before starting an equalization. Replace the Hydrocaps with standard battery cell caps. The Hydrocaps can get very hot during an equalization. Also, if Hydrocaps are used, the equalization should be set for manual only (DIP switch #7 is Off).

After the equalization is finished, add distilled water to each cell to replace gassing losses. Check that the battery plates are covered.

4.4.4 When to Equalize

The ideal frequency of equalizations depends on the battery type (lead-calcium, lead-antimony, etc.), the depth of discharging, battery age, temperature, and other factors.

One very broad guide is to equalize flooded batteries every 1 to 3 months or every 5 to 10 deep discharges. Some batteries, such as the L-16 group, will need more frequent equalizations.

The difference between the highest cell and lowest cell in a battery can also indicate the need for an equalization. Either the specific gravity or the cell voltage can be measured. The battery manufacturer can recommend the specific gravity or voltage values for your particular battery.

4.4.5 "Equalize" a Sealed Battery?

The standard battery charging table (see Section 4.2) shows two sealed batteries with an "equalization" cycle. This is only a 0.05 volt (12V battery) boost cycle to level individual cells. This is not an equalization, and will not vent gas from sealed batteries that require up to 14.4V charging (12V battery). This "boost" charge for sealed cells allows for adjustability with the PC software.

Many VRLA batteries, including AGM and gel, have increased charging requirements up to 14.4V (12V battery). The 0.05V boost shown in the table (Section 4.2) is less than the accuracy range of most charge controllers. Alternatively, for these two sealed battery charging programs you may prefer to consider the PWM absorption stage to be 14.2V and 14.4V (12V battery).

The 14.0, 14.2, and 14.4 volt standard charging programs should be suitable for most sealed batteries. If not optimum for your battery, the PC software can be used to adjust these values. Refer to Section 9.0 for more information about charging sealed batteries.

4.5 Float

When a battery becomes fully charged, dropping down to the float stage will provide a very low rate of maintenance charging while reducing the heating and gassing of a fully charged battery. When the battery is fully recharged, there can be no more chemical reactions and all the charging current is turned into heat and gassing.

The purpose of float is to protect the battery from long-term overcharge. From the PWM absorption stage, charging is dropped to the float voltage. This is typically 13.4V, and is adjustable with the PC software.

The transition to float is based on the previous 24 hour history. Factors include the battery voltage, the state of charge the night before, the battery type, and the PWM duty cycle and stability of the duty cycle. The battery will be charged for part of the day until the transition to float.

If there are loads for various periods of time during float, the TriStar will cancel float and return to bulk charge.

Float is temperature compensated.

5.0 Load and Lighting Control

5.1 General Load & Lighting Control Notes

IMPORTANT:

5.1.1 Inductive loads

Do not connect inductive loads such as inverters, motors, pumps, compressors, generators to the load terminals. Inductive loads can generate large voltage spikes that may damage the controller's lightning protection devices. Connect inductive loads directly to the battery.

If a heavy load must be connected to the TriStar's load terminals e.g. for LVD purposes, contact your dealer or Morningstar Tech Support for a design solution.

5.1.2 Parallel TriStars

Two or more TriStars should never be put in parallel for a large load. The controllers cannot share the load.

5.1.3 Reverse Polarity

If the battery is correctly connected (LEDs are on), the load should be connected very carefully with regard to polarity (+ / -).

If the polarity is reversed, the controller cannot detect this. There are no indications.

Loads without polarity will not be affected.

Loads with polarity can be damaged. It is possible that the TriStar will go into short circuit protection before the load is damaged. If the LEDs indicate a "short", be certain to check for both shorts and reversed polarity connections.

If the controller does not go into short circuit protection, the loads with polarity will be damaged.



CAUTION: Carefully verify the polarity (+ and -) of the load connections before applying power to the controller.



PRUDENCE : Vérifiez avec précaution la polarité (+ et -) des connexions de la charge avant de mettre le contrôleur sous tension.

5.2 Load Control Settings

The primary purpose of a low voltage load disconnect function (LVD) is to protect the system battery from deep discharges that could damage the battery.

In the Load Control mode, the TriStar provides for seven standard LVD settings that are selected by the DIP switches. These are described in the table below. Custom LVD settings are possible using the PC software (see Section 7.0).

DIP Switch	12V LVD	24V LVD	48V LVD	Battery SOC%	12V LVD _s	24V LVD _s	48V LVD _s
off-off-off	11.1	22.2	44.4	8	12.6	25.2	50.4
off-off-on	11.3	22.6	45.2	12	12.8	25.6	51.2
off-on-off	11.5	23.0	46.0	18	13.0	26.0	52.0
off-on-on	11.7	23.4	46.8	23	13.2	26.4	52.8
on-off-off	11.9	23.8	47.6	35	13.4	26.8	53.6
on-off-on	12.1	24.2	48.4	55	13.6	27.2	54.4
on-on-off	12.3	24.6	49.2	75	13.8	27.6	55.2
on-on-on	Custom		Custom		Custom		

Table 5.1

The table above describes the standard selectable LVD battery voltages for 12, 24 and 48 volt systems. The LVD_s values are the load reconnect set-points. The "Battery SOC %" provides a general battery state-of-charge figure for each LVD setting. The actual battery SOC can vary considerably depending on the battery condition, discharge rates, and other specifics of the system.



NOTE: The lowest LVD settings are intended for applications such as telecom that only disconnect the load as a last resort. These lower LVD settings will deeply discharge the battery and should not be used for systems that may go into LVD more than once a year.



REMARQUE : Les réglages les plus bas du disjoncteur basse tension sont prévus pour les applications comme celles de télécom qui ne déconnectent la charge qu'en dernier recours. Ces réglages les plus bas du disjoncteur basse tension déchargent fortement la batterie et ne doivent pas être utilisés avec les systèmes qui risquent de déclencher le disjoncteur basse tension plus d'une fois par an.

The LVD values in table 5.1 above are current compensated. Under load, the battery voltage will be reduced in proportion to the current draw by the load. A short-term large load could cause a premature LVD without the current compensation. The LVD values in the table above are adjusted lower per the following table:

	TS-45	TS-60
12V	-15 mV per amp	-10 mV per amp
24V	-30 mV per amp	-20 mV per amp
48V	-60 mV per amp	-40 mV per amp

As an example, consider a 24V system using a TriStar-60 with a 30 amp load. The LVD will be reduced by 0.02V (per the table above) times 30 amps. This equals -0.6V. A DIP-switch selected LVD of 23.4V would be reduced to 22.8V in this example.

Note that the LEDs are linked to the LVD setting, so the LEDs are also current compensated.

continued...

After an LVD, the load reconnect voltages are 0.25 volts per battery cell higher than the LVD (for example, in a 12V system the LVD_s would be 1.5 volts above LVD). Battery voltages can rise quickly after an LVD, typically from 1.0 to 1.3 volts or more (12V system). The LVD_s value must be high enough to avoid cycling in and out of LVD.

5.3 LVD Warning

When the battery is discharging and the green LED changes to the next state (G-Y LEDs on), there are four remaining transitions to LVD (refer to the LED indications in Section 3.3). Each of these LED displays will serve as a warning of an approaching LVD. The final warning is a blinking red LED state.

The amount of time from the initial G-Y display until the load disconnect will depend on many factors. These include:

- The rate of discharge.
- The health of the battery
- The LVD setting

For a "typical" system with a healthy battery and an LVD setting of about 11.7 volts, there could be approximately 10 hours per LED transition. The LVD would occur about 40 hours from the first G-Y display (under constant load with no charging).

Another significant factor affecting the warning time is the LVD voltage setpoint. Lower LVD voltage settings may result in the battery discharging 70% or 80% of its capacity. In this case, the battery's very low charge state will result in the voltage dropping much faster. At the lowest LVD settings, there could be as little as 2 or 3 hours of warning between LED transitions for a healthy battery.

The amount of time it takes to transition through the LEDs to LVD can vary greatly for different systems. It may be worthwhile to measure the time it takes for your system to transition from one LED state to the next. Do this under "typical" discharging loads.

This will provide a good reference for how long it will take for your system to reach LVD. It can also provide a benchmark for judging the health of your battery over time.

6.0 Diversion Charge Control

The TriStar's third mode of operation is diversion load battery charge control. As the battery becomes fully charged, the TriStar will divert excess current from the battery to a dedicated diversion load. This diversion load must be large enough to absorb all the excess energy, but not too large to cause a controller overload condition.

6.1 Diversion Charge Control

In the diversion mode, the TriStar will use PWM charging regulation to divert excess current to an external load. As the battery becomes fully charged, the FET switches are closed for longer periods of time to direct more current to the diversion load.

As the battery charges, the diversion duty cycle will increase. When fully charged, all the source energy will flow into the diversion load if there are no other loads. The generating source is typically a wind or hydro generator. Some solar systems also use diversion to heat water rather than open the solar array and lose the energy.

The most important factor for successful diversion charge control is the correct sizing of the diversion load. If too large, the controller's protections may open the FET switches and stop diverting current from the battery. This condition can damage the battery.

If you are not confident and certain about the installation, a professional installation by your dealer is recommended.

6.2 Diversion Current Ratings

The maximum diversion load current capability for the two TriStar versions is 45 amps (TS-45) and 60 amps (TS-60/M). The diversion loads must be sized so that the peak load current cannot exceed these maximum ratings.

See section 6.4 below for selecting and sizing the diversion loads.

The total current for all combined charging sources (wind, hydro, solar) should be equal or less than two-thirds of the controller's current rating: 30A (TS-45) and 40A (TS-60/M). This limit will provide a required margin for high winds and high water flow rates as well as a margin for error in the rating and selection of the diversion load. This protects against an overload and a safety disconnect in the TriStar controller, which would leave the battery charging unregulated.



CAUTION: If the TriStar's rating is exceeded and the controller disconnects the diversion load, Morningstar will not be responsible for any damage resulting to the system battery or other system components. Refer to Morningstar's Limited Warranty in Section 10.0.



PRUDENCE : Si la capacité du TriStar est dépassée et que le contrôleur déconnecte la charge de diversion, Morningstar ne sera pas responsable de tout dommage résultant de la batterie du système ou d'autres composants du système. Reportez-vous à la Garantie limitée de Morningstar dans la Section 10.0.

6.3 Standard Diversion Battery Charging Programs

The TriStar provides 7 standard diversion charging algorithms (programs) that are selected with the DIP switches. An 8th algorithm can be used for custom set-points using the PC software.

The table below summarizes the major parameters of the standard diversion battery charging algorithms. Note that all the voltages are for 12V systems (24V = 2X, 48V = 4X).

All values are @25°C (77°F).

	A.	B.	C.	D.	E.	F.	G.
DIP Switches (4-5-6)	PWM Absorp. Voltage	Float Voltage	Time Until Float (hours)	Equalization Voltage	Time in Equal. (hours)	Equalize Interval (days)	Max. Equalize Cycle (hours)
off-off-off	13.8	13.6	4	14.1	3	28	3
off-off-on	14.0	13.6	4	14.3	3	28	3
off-on-off	14.2	13.6	4	14.5	3	28	4
off-on-on	14.4	13.6	4	14.7	4	28	4
on-off-off	14.6	13.7	4	14.9	4	28	5
on-off-on	14.8	13.7	4	15.1	4	28	5
on-on-off	15.0	13.7	4	15.3	4	28	5
on-on-on	Custom			Custom		Custom	

Table 6.1 Standard Diversion Charging Programs

- A. PWM Absorption Voltage** - This is the PWM Absorption stage with constant voltage charging. The PWM absorption voltage is the maximum battery voltage that will be held constant.
- B. Float Voltage** - When the battery is fully charged, the charging voltage will be reduced to the float voltage for all diversion settings. The float voltage and transition values are adjustable with the PC software.
- C. Time Until Float** - This is the cumulative time in PWM before the battery voltage is reduced to the float voltage. If loads are present during the PWM absorption, the time to transition into float will be extended.
- D. Equalization Voltage** - During an equalization cycle, the charging voltage will be held constant at this voltage. Equalizations are manual, and can be selected for automatic (See Section 4.4.1).
- E. Time in Equalization** - Charging at the selected equalization voltage will continue for this number of hours.
- F. Equalization Interval** - Equalizations are typically done once a month. The cycles are 28 days so the equalization will begin on the same day of the week. Each new cycle will be reset as the equalization starts so that a 28 day period will be maintained.
- G. Maximum Equalization Cycle** - If the battery voltage cannot reach the equalization voltage, the equalization will terminate after this number of hours to avoid over gassing or heating the battery. If the battery requires more time in equalization, the manual push-button can be used to continue for one or more additional equalization cycles.

6.3.1 Battery Charging References

The diversion load battery charging is similar to conventional solar charging. Refer to the following sections in this manual for additional battery charging information.

- 4.1 Four stages of charging (applies to diversion)
- 4.3 Temperature Effects and Battery Voltage Sense
- 4.4 Equalization
- 4.5 Float
- 9.0 Battery Information

6.4 Selecting the Diversion Load

It is critical that the diversion load be sized correctly. If the load is too small, it cannot divert enough power from the source (wind, hydro, etc). The battery will continue charging and could be overcharged.

If the diversion load is too large, it will draw more current than the rating of the TriStar. The controller's overload protection may disconnect the diversion load, and this will result in all of the source current going to the battery.



CAUTION: The diversion load must be able to absorb the full power output of the source, but the load must never exceed the current rating of the TriStar controller. Otherwise, the battery can be overcharged and damaged.



PRUDENCE : La charge de diversion doit être capable d'absorber toute la puissance de sortie de la source, mais la charge ne doit jamais dépasser l'intensité nominale du contrôleur TriStar, pour ne pas surcharger et endommager la batterie.

6.4.1 Suitable Loads for Diversion

Water heating elements are commonly used for diversion load systems. These heating elements are reliable and widely available. Heating elements are also easy to replace, and the ratings are stable.



NOTE: Do not use light bulbs, motors, or other electrical devices for diversion loads. These loads will fail or cause the TriStar to disconnect the load. Only heating elements should be used.



REMARQUE : N'utilisez pas d'ampoules, de moteurs ou d'autres appareils électriques pour les charges de diversion. Ces charges ne fonctionneront pas ou provoqueront une déconnexion de la charge par le TriStar. Seuls les éléments de chauffe doivent être utilisés.

Water heating elements are typically 120 volts. Elements rated for 12, 24 and 48 volts are also available, but more difficult to source. The de-rating for 120 volt heating elements is discussed in 6.4.3 below.

6.4.2 Definition of Terms

Maximum Source Current:


This is the maximum current output of all the energy sources (hydro, wind, solar, etc.) added together. This current will be diverted through the TriStar to the diversion load.


Maximum Battery Voltage:

This maximum voltage is the PWM regulation voltage selected with the DIP switches, plus the increase with an equalization, plus the increase due to lower temperatures. The highest battery voltage is commonly 15, 30 and 60 volts for 12-, 24- and 48-volt systems.

Peak Load Current:

At the maximum battery voltage, this is the current the diversion load will draw. This peak load current must not exceed the TriStar's rating.

 **NOTE:** Because the battery can supply any size load, the peak load current is not limited by the source (hydro or wind rating). The diversion load's power rating is the critical specification for reliable battery charging.

 **REMARQUE :** La batterie pouvant fournir une charge de n'importe quelle dimension, le pic d'intensité de la charge n'est pas limité par la source (puissance hydro ou éolienne). La puissance nominale de la charge de diversion constitue la spécification critique pour une charge fiable de la batterie.

6.4.3 Load Power Ratings


The power rating of the diversion load will depend on the voltage of the battery being charged. If the heating element is not rated for the same voltage as the diversion system, the power rating of the load must be adjusted to the diversion system's voltage.


The manufacturers typically rate the heating elements for power at a specified voltage. The peak load current at the load's rated voltage will be the power divided by the rated voltage ($I = P / V$). For example: $2000W / 120V = 16.7$ amps of current.

If the load is being used at a voltage less than the load's rated voltage, the power can be calculated by the ratio of the voltages squared. For example, a 120 volt 1000 watt heating element being used at 60 volts:

$$1000W \times (60/120)^2 = 250 \text{ watts}$$

The 1000W element will only dissipate 250W when being used at 60 volts.

 **NOTE:** The loads (heating elements) can be used at the manufacturer's voltage rating, or at a lower voltage. Do not use the load at a higher voltage than the load's rating.

 **REMARQUE :** Les charges (éléments de chauffe) peuvent être utilisées à la tension nominale du fabricant ou à une tension inférieure. N'utilisez pas la charge à une tension supérieure à la tension nominale.

6.4.4 Maximum Diversion Load

The diversion load should never exceed the TriStar's current rating (45A or 60A). Note that the load is not limited by the source (wind, hydro), and will draw its rated current from the battery.

The following table specifies the absolute maximum diversion loads that can be used with each TriStar version. These loads (heating elements) are rated for the same voltage as the system voltage.

Nominal Voltage	TriStar-45	TriStar-60
48V	2700W at 60V	3600W at 60V
24V	1350W at 30V	1800W at 30V
12V	675W at 15V	900W at 15V

These maximum power ratings are translated to the equivalent at 120 volts in the following table. If using heating elements rated for 120 volts, the power ratings of all the elements can be simply added up and the sum compared with this table and no further math is required.

Nominal Voltage	TriStar-45	TriStar-60
48V	10,800W at 120V	14,400W at 120V
24V	21,600W at 120V	28,800W at 120V
12V	43,200W at 120V	57,600W at 120V

To illustrate the same point from the opposite perspective, a heating element rated for 120 volts will draw reduced load current as indicated by the following table. A standard 2,000 watt / 120 Vac heating element is used as the reference.

Voltage	Power	Current
120V	2000 W	16.7 A
60V (48V nominal)	500 W	8.3 A
30V (24V nominal)	125 W	4.2 A
15V (12V nominal)	31 W	2.1 A

Whether using dc rated loads (the first table) or 120V elements, the total diversion load current must not exceed the current rating of the TriStar.

6.4.5 Minimum Diversion Load

The diversion load must be large enough to divert all the current produced by the source (wind, hydro, etc.). This value is the maximum battery voltage times the maximum source current.

For example, if a hydro source can generate up to 30 amps of current in a nominal 48 volt system (60V maximum), the minimum diversion load size = $60V \times 30A = 1,800$ watts (for loads rated at 60 volts).

General Sizing Example

Consider a 24V system with a wind turbine that is rated to generate 35A of current. A TriStar-45 will not provide the 150% diversion load margin, and the TS-45 is only rated for 30A of source current. The TS-45 will not provide enough margin for wind gusts and overloads, so a TS-60/M should be used.

The diversion load should be sized for 52.5A (150% of the source current) up to 60A (the rating of the TriStar-60). If 55A is selected for the diversion load, the load must be capable of diverting 55A at 30V (maximum battery voltage). If a 30V heating element is used, it would be rated for 1,650 watts (or from 1,575W to 1,800W per the load range noted above).

If a 2,000 watt / 120 volt heating element is used, 13 of these elements in parallel will be required for the diversion load (4.2 amps per element [Table in 6.4.4] $\times 13 = 54.6$ amps).

continued...

The minimum diversion load would be the source output (35A) times the voltage (30V). This would require a 1,050 watt heating element rated at 30 volts. Or if a 2,000W heater element rated for 120 volts is used, 9 heater elements will be required to draw the required minimum diversion load at 30 volts.

6.5 NEC Requirements

To comply with NEC 690.72 (B), the following requirements will apply when the TriStar is being used as a diversion charge controller in a photovoltaic system.

6.5.1 Second Independent Means

If the TriStar is the only means of regulating the battery charging in a diversion charging mode, then a second independent means to prevent overcharging the battery must be added to the system. The second means can be another TriStar, or a different means of regulating the charging.

6.5.2 150 Percent Rating

The current rating of the diversion load must be at least 150% of the TriStar source current rating. Refer to Section 6.2 (Diversion Current Rating). The maximum allowable current ratings for both TriStar versions are summarized below:

	Max. Input Current	Max. Diversion Load Rating
TS-45	30 A	45 A
TS-60/M	40 A	60 A



CAUTION: The NEC requirement that the diversion load must be sized at least 150% of the controller rating does NOT mean the diversion load can exceed the maximum current rating of the TriStar. NEVER size a diversion load that can draw more than the 45 amps or 60 amps maximum rating of the TriStar controllers.



PRUDENCE : L'obligation de la CNE indiquant que la charge de diversion doit être 150 % plus grande que la puissance nominale du contrôleur NE signifie PAS que la charge de diversion peut dépasser l'intensité maximum du TriStar. Ne dimensionnez JAMAIS une charge de diversion qui peut appeler plus de 45 A ou l'intensité maximum de 60 A des contrôleurs TriStar.

6.6 Additional Information

Visit Morningstar's website (www.morningstarcorp.com) for additional diversion charge control information. The website provides expanded technical support for more complex diversion load systems.

7.0 Custom Settings with PC Software

An RS-232 connection between the TriStar and an external personal computer (PC) allows many set-points and operating parameters to be easily adjusted. The adjustments can be simply a small change to one setpoint, or could include extensive changes for a fully customized battery charging or load control program.



CAUTION: Only qualified service personnel should change operating parameters with the PC software. There are minimal safeguards to protect from mistakes. Morningstar is not responsible for any damage resulting from custom settings.



PRUDENCE : Seul le personnel d'entretien qualifié doit modifier les paramètres de fonctionnement avec le logiciel sur ordinateur. Des protections minimales protègent contre les erreurs. Morningstar n'est pas responsable des dommages résultants de réglages personnalisés.

Consult Morningstar's website for the latest TriStar PC software and instructions.

7.1 Connection to a Computer

An RS-232 cable with DB9 connectors (9 pins in 2 rows) will be required.

If the computer will be used to change battery charging or load control set-points, verify that DIP switches 4, 5, 6 are in the custom position (On, On, On) before connecting the TriStar to a computer. The custom position is required to change set-points. See Section 2.3 - Step 3. Disconnect power before changing DIP switches.

7.2 Using the PC Software

Download the TriStar PC software from Morningstar's website. Follow the instructions on the website for installing the software on your computer.

Open the TriStar PC software. This software will make the connection with the TriStar via the RS-232 cable. The TriStar must be powered by the battery or a power supply to complete the connection. If there is a conflict between the TriStar and PC comm ports, the software will provide instructions to resolve the problem.

7.3 Changing Set-points

Follow the instructions in the PC software.



CAUTION: *There are few limits to the changes that can be made. It is the responsibility of the operator to be certain all changes are appropriate. Any damage resulting to the controller or the system from TriStar setpoint adjustments will not be covered under warranty.*



PRUDENCE : *Les modifications pouvant être effectuées sont sujettes à quelques limites. Il incombe à l'opérateur de s'assurer que toutes les modifications sont appropriées. Tout dommage au contrôleur ou au système résultant de réglages des points de consigne du TriStar ne sera pas couvert par la garantie.*

If you are not certain about each of the changes you are making, the software provides for returning to the factory default settings.

7.4 Finish

Confirm that the changes made to the TriStar are as you intended. It is advisable to make a record of the changes for future reference. Observe the system behavior and battery charging for a few weeks to verify that the system is operating correctly and as you intended.

Exit the software. The PC/TriStar connection can either be disconnected or left in place.

8.0 Self-Test / Diagnostics

The TriStar performs a continuous self-test to monitor controller and system operation. Detected problems are classified as either faults or alarms. Typically, faults are problems that stop the normal operation of the controller and require immediate attention. Alarms indicate an abnormal condition, but will not stop the controller's operation.

If a problem is detected, the TriStar will alert the user to an existing fault or alarm. In this situation, the LED indicators will flash a particular sequence. Section 3.3 references these sequences with their associated faults and alarms. Flashing LED sequences can indicate conditions ranging from a simple battery service reminder to an existing short circuit in the system. It is recommended that the user become familiar with the LED indications and their meanings.

If a TriStar meter option has been added, more detailed information concerning faults and alarms will be available. Menus provide text displays of the specific fault as well as indicating on the standard display screens when a problem exists. *Consult the meter manual for further details.*

8.1 General Troubleshooting

TriStar is not powering up

- Confirm that all circuit breakers and switches in the system are closed
- Check all fuses
- Check for loose wiring connections and wiring continuity
- Verify that the battery voltage is not below 9Vdc (*brownout: section 3.4*)
- Verify that the battery power connection is not reversed polarity

Flashing/Sequencing LEDs

- *Reference Section 3.3 for a list of LED indications and their corresponding faults/alarms*

Self-Test Indication (R - Y - G sequencing)

- Self-testing will also detect various system wiring faults outside the TriStar
- Check for both TriStar faults and external system wiring problems

The RTS or Battery Sense is not working properly

- R/Y - G/Y sequencing LEDs indicates an RTS or Sense fault
- Check for a reverse polarity connection on the sense leads
- Verify that the RTS and Sense connections are wired to the correct terminals
- Check for shorts and continuity in the cables
- Verify that good electrical contact is made at the terminals
- Note that if the TriStar is restarted with an RTS or Sense fault present, it will not detect the RTS or Sense connection and the LED indication will stop.

8.2 Troubleshooting Solar Charging

- Over-charging or under-charging the battery
- DIP switch settings may be wrong
- RTS is not correcting for high or low temperatures
- Over-temperature condition is reducing the charging current (heat sink cooling may be blocked — indicated with LEDs)
- Voltage drop between TriStar and battery is too high (connect the battery voltage sense — see Section 2.3 Step 5)
- Battery charging requires temperature compensation (connect a remote temperature sensor)
- Load is too large and is discharging the battery

Not charging the battery

- DIP switch settings may be wrong (check each switch position carefully)
- TriStar has detected a fault (indicated by sequencing LEDs, refer to Section 3.3)
- Solar circuit breaker or disconnect is open
- Reversed polarity connections at the solar terminals (TriStar will not detect the solar array)
- Short circuit in the solar array has eliminated part of the array output
- Solar array is not providing enough current (low sun or fault in the array)
- Battery is failing and cannot hold a charge

8.3 Troubleshooting Load Control

No power to the load

- DIP switch settings may be wrong (check each switch position carefully)
- Controller is in LVD (check the LEDs)
- Load circuit breaker or disconnect may be open
- Check the load cables for continuity and good connection
- An over-temperature condition may have caused the load to be disconnected

8.4 Troubleshooting Diversion Control

- Diversion load is too small so PWM reaches 99%
- Diversion load is burned out so PWM reaches 99%
- Diversion load is too large so TriStar faults on overcurrent
- An overtemperature condition may have caused the load to be disconnected
- The RTS is not correcting for high or low temperatures
- Voltage drops between the TriStar and battery are too high

Still having problems? Point your web browser to <http://www.morningstarcorp.com> for technical support documents, FAQs, or to request technical support.

9.0 Battery Information

The standard battery charging programs in the TriStar controller, as described in Section 4.2, are typical charging algorithms for three battery types:

- sealed (VRLA)
- flooded (vented)
- L-16 group

Other battery chemistries such as NiCad, or special voltages such as 36V, can be charged using a custom charging algorithm modified with the PC software. Only the standard TriStar battery charging programs will be discussed here.



CAUTION: Never attempt to charge a primary (non-rechargeable) battery.



PRUDENCE : N'essayez jamais de charger une batterie primaire (non-rechargeable).

All charging voltages noted below will be for 12V batteries at 25°C.

9.1 Sealed Batteries

The general class of sealed batteries suitable for solar systems are called VRLA (Valve Regulated Lead-Acid) batteries. The two main characteristics of VRLA batteries are electrolyte immobilization and oxygen recombination. As the battery recharges, gassing is limited and is recombined to minimize the loss of water.

The two types of VRLA batteries most often used in solar are AGM and Gel.

AGM:

Absorbed Glass Mat batteries are still considered to be a "wet cell" because the electrolyte is retained in fiberglass mats between the plates. Some newer AGM battery designs recommend constant voltage charging to 2.45 volts/cell (14.7V). For cycling applications, charging to 14.4V or 14.5V is often recommended.

AGM batteries are better suited to low discharge applications than daily cycling. These batteries should not be equalized since gassing can be vented which causes the battery to dry out. There is also a potential for thermal runaway if the battery gets too hot, and this will destroy the battery. AGM batteries are affected by heat, and can lose 50% of their service life for every 8°C (15°F) over 25°C (77°F).

It is very important not to exceed the gas recombination capabilities of the AGM. The optimum charging temperature range is from 5 to 35°C (40 to 95°F).

Gel:


Gel batteries have characteristics similar to AGM, except a silica additive immobilizes the electrolyte to prevent leakage from the case. And like AGM, it


is important to never exceed the manufacturer's maximum charging voltages. Typically, a gel battery is recharged in cycling applications from 14.1V to 14.4V. The gel design is very sensitive to overcharging.

For both AGM and Gel batteries, the goal is for 100% recombination of gases so that no water is lost from the battery. True equalizations are never done, but a small boost charge may be needed to balance the individual cell voltages.

Other Sealed Batteries:

Automotive and "maintenance-free" batteries are also sealed. However, these are not discussed here because they have very poor lifetimes in solar cycling applications.

 **NOTE: Consult the battery manufacturer for the recommended solar charging settings for the battery being used.**

 **REMARQUE : Consultez le fabricant de la batterie quant aux réglages recommandés de charge solaire pour la batterie utilisée.**

9.2 Flooded Batteries

Flooded (vented) batteries are preferred for larger cycling solar systems. The advantages of flooded batteries include:

- ability to add water to the cells
- deep cycle capability
- vigorous recharging and equalization
- long operating life

In cycling applications, flooded batteries benefit from vigorous charging and equalization cycles with significant gassing. Without this gassing, the heavier electrolyte will sink to the bottom of the cell and lead to stratification. This is especially true with tall cells. Hydrocaps can be used to limit the gassing water loss.

Note that a 4% mixture of hydrogen in air is explosive if ignited. Make certain the battery area is well ventilated.

Typical equalization voltages for flooded batteries are from 15.3 volts to 16 volts. However, a solar system is limited to what the solar array can provide. If the equalization voltage is too high, the array I-V curve may go over the "knee" and sharply reduce the charging current.

Lead-Calcium:

Calcium batteries charge at lower voltages (14.2 to 14.4 typically) and have strong advantages in constant voltage or float applications. Water loss can be only 1/10th of antimony cells. However, calcium plates are not as suitable for cycling applications.


Lead-Selenium:


These batteries are similar to calcium with low internal losses and very low water consumption throughout their life. Selenium plates also have poor cycling life.

Lead-Antimony:

Antimony cells are rugged and provide long service life with deep discharge capability. However, these batteries self-discharge much faster and the self-discharging increases up to five times the initial rate as the battery ages. Charging the antimony battery is typically from 14.4V to 15.0V, with a 120% equalization overcharge. While the water loss is low when the battery is new, it will increase by five times over the life of the battery.

There are also combinations of plate chemistries that offer beneficial tradeoffs. For example, low antimony and selenium plates can offer fairly good cycling performance, long life, and reduced watering needs.

 **NOTE: Consult the battery manufacturer for the recommended solar charging settings for the battery being used.**


 **REMARQUE : Consultez le fabricant de la batterie quant aux réglages recommandés de charge solaire pour la batterie utilisée.**


9.3 L-16 Cells

One particular type of flooded battery, the L-16 group, is often used in larger solar systems. The L-16 offers good deep-cycle performance, long life, and low cost.

The L-16 battery has some special charging requirements in a solar system. A study found that nearly half of the L-16 battery capacity can be lost if the regulation voltage is too low and the time between finish-charges is too long. One standard charging program in the TriStar is specifically for L-16 batteries, and it provides for higher charging voltages and more frequent equalizations. Additional equalizations can also be done manually with the push-button.

A good reference for charging L-16 batteries is a Sandia National Labs report (year 2000) titled "PV Hybrid Battery Tests on L-16 Batteries." Website: www.sandia.gov/pv.

 **NOTE: The best charging algorithm for flooded, deep-cycle batteries depends on the normal depth-of-discharge, how often the battery is cycled, and the plate chemistry. Consult the battery manufacturer for the recommended solar charging settings for the battery being used.**

 **REMARQUE : Le meilleur algorithme de charge pour les batteries à électrolyte liquide à décharge poussée dépend de l'amplitude de la décharge, de la fréquence du cycle de batterie et de la composition chimique des plaques. Consultez le fabricant de la batterie quant aux réglages recommandés de charge solaire pour la batterie utilisée.**

10.0 Warranty

LIMITED WARRANTY Morningstar TriStar-PWM

The TriStar-PWM is warranted to be free from defects in material and workmanship for a period of FIVE (5) years from the date of shipment to the original end user. Morningstar will, at its option, repair or replace any such defective products.

WARRANTY EXCLUSIONS AND LIMITATIONS:

This warranty does not apply under the following conditions:

- ◆ Damage by accident, negligence, abuse or improper use
- ◆ PV or load currents exceeding the ratings of the product
- ◆ Unauthorized product modification or attempted repair
- ◆ Damage occurring during shipment
- ◆ Damage results from acts of nature such as lightning and weather extremes

THE WARRANTY AND REMEDIES SET FORTH ABOVE ARE EXCLUSIVE AND IN LIEU OF ALL OTHERS, EXPRESS OR IMPLIED. MORNINGSTAR SPECIFICALLY DISCLAIMS ANY AND ALL IMPLIED WARRANTIES, INCLUDING, WITHOUT LIMITATION, WARRANTIES OF MERCHANTABILITY AND FITNESS FOR A PARTICULAR PURPOSE. NO MORNINGSTAR DISTRIBUTOR, AGENT OR EMPLOYEE IS AUTHORIZED TO MAKE ANY MODIFICATION OR EXTENSION TO THIS WARRANTY.

MORNINGSTAR IS NOT RESPONSIBLE FOR INCIDENTAL OR CONSEQUENTIAL DAMAGES OF ANY KIND, INCLUDING BUT NOT LIMITED TO LOST PROFITS, DOWN-TIME, GOODWILL OR DAMAGE TO EQUIPMENT OR PROPERTY.

R17-8/16

11.0 Technical Specifications

ELECTRICAL

- System voltage ratings 12, 24, 48 Vdc
- Current ratings — **Solar Input**
 - TS-45: 45 A
 - TS-60/M: 60 A
- Current ratings — **Battery Charge Control**
 - TS-45: 45 A
 - TS-60/M: 60 A
- Current ratings — **Load Control**
 - TS-45: 45 A
 - TS-60/M: 60 A
- Current ratings — **Diversion Charge Control**
 - TS-45: 45 A diversion load
 - TS-60/M: 60 A diversion load
- Accuracy
 - 12/24V: $\leq 0.1\% \pm 50$ mV
 - 48V: $\leq 0.1\% \pm 100$ mV
- Min. voltage to operate 9 V
- Max. solar array Voc 125 V
- Max. operating voltage 68 V
- Self-consumption less than 20 mA
- High temp shutdown
 - 95°C disconnect solar
 - 90°C disconnect load / diversion load
 - 70°C reconnect solar / load / diversion load
- Solar high voltage disconnect
 - HVD disconnect highest equalization + 0.2V
 - HVD reconnect 13.0V
- Transient surge protection: 4500 watts
- Pulse power rating response < 5 nanosec

BATTERY CHARGING / RTS

- Charge algorithm: PWM, constant voltage
- Temp comp. coefficient $-5\text{mV}/^\circ\text{C}/\text{cell}$ (25°C ref)
- Temp comp. range: -30°C to $+80^\circ\text{C}$
- Temp comp. set-points PWM, float, equalize, HVD (with RTS option)

BATTERY CHARGING STATUS LEDs

G	13.3 to PWM
G/Y	13.0 to 13.3 V
Y	12.65 to 13.0 V
Y/R	12.0 to 12.65 V
R	0 to 12.0 V

Note: Multiply x 2 for 24V systems, x 4 for 48V systems

Note: The LED indications are for charging a battery. When discharging, the LEDs will typically be Y/R or R.

MECHANICAL

• Dimensions (mm/inch)	H: 260.4 mm / 10.25 inch W: 127.0 mm / 5.0 inch D: 71.0 mm / 2.8 inch
• Weight (kg/lb)	1.6 kg / 3.5 lb
• Power terminals: largest wire smallest wire	compression connector lug 35 mm ² / 2 AWG 2.5 mm ² / 14 AWG
• Terminal wire slot	8.2 mm / 0.324 in wide 9.4 mm / 0.37 in high
• Knockout sizes	1 and 1.25 inch
• Torque terminals	5.65 Nm / 50 in-lb
• RTS / Sense terminals: wire sizes torque	1.0 to 0.25 mm ² / 16 to 24 AWG 0.40 Nm / 3.5 in-lb

ENVIRONMENTAL

• Operating Altitude	Below 2000 meters
• Ambient temperature	-40 to +45°C
• Storage temperature	-55 to +85°C
• Humidity	100% (NC)
• Enclosure	IP20 Type 1 (indoor & vented), powder coated steel

Appendix 1 — Load & Lighting Control DIP Settings

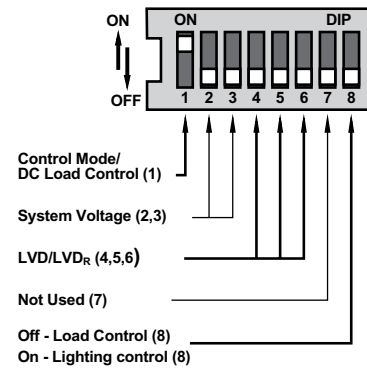


Figure A1-1 - Step 3. Load / lighting DIP Switch Functions



NOTE: The DIP switches should be changed only when there is no power to the controller. Turn off disconnect switches and remove power to the controller before changing a DIP switch. A fault will be indicated if a switch is changed with the controller powered.



REMARQUE : Les commutateurs DIP ne doivent être changés que si le contrôleur est hors tension. Mettez les interrupteurs sur arrêt et mettez le contrôleur hors tension avant de changer un commutateur DIP. Une panne sera indiquée en cas de changement d'un commutateur quand le contrôleur est sous tension.



CAUTION: The TriStar is shipped with all the switches in the "OFF" position. Each switch position must be confirmed during installation. An incorrect setting could cause damage to the load or other system components.



PRUDENCE : Le TriStar est expédié avec tous les interrupteurs en position « ARRÊT ». La position de chaque interrupteur doit être confirmée pendant l'installation. Un mauvais réglage peut endommager la charge ou d'autres composants du système.

The DIP switch settings described below are for **Load and Lighting Control** only. The DIP switches are shipped in the OFF position. The OFF settings will operate as follows:

Switch	Function
1	Must be ON for Load, Lighting or Diversion Control
2, 3	Auto voltage select
4, 5, 6	Lowest LVD = 11.1V
7	Diversion Control mode OFF
8	Lighting Control mode OFF

To configure your TriStar for the Load Control you require, follow the DIP switch adjustments described below. To change a switch from OFF to ON, slide the switch up toward the top of the controller. Make sure each switch is fully in the ON or OFF position.

DIP Switch Number 1 - Control Mode: Load & Lighting Control

Mode	Switch 1
Charging	Off
Load/Lighting	On

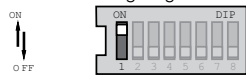


Figure A1-2 - Step 3 DIP Switch #1

For Load or Lighting Control mode, move the DIP switch to the ON position as shown.

DIP Switches Number 2,3 - System Voltage:

Voltage	Switch 2	Switch 3
Auto	Off	Off
12	Off	On
24	On	Off
48	On	On

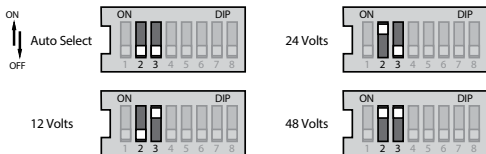


Figure A1-3 - Step 3 DIP Switches # 2,3

The auto voltage selection occurs when the battery is connected and the TriStar starts up. There should be no loads on the battery that might cause a discharged battery to indicate a lower system voltage.

The DIP switch selectable voltages are for 12V, 24V or 48V lead-acid batteries. Although the "auto voltage" selection is very dependable, it is recommended to use the DIP switches to secure the correct system voltage.

DIP Switches Number 4,5,6 - Load Control Algorithm:

For normal Load Control Mode, set the DIP switches 4,5,&6 according to the table below. For Lighting Control, see the table and Figure 2.4 on the next page.

LVD	Switch 4	Switch 5	Switch 6
11.1	Off	Off	Off
11.3	Off	Off	On
11.5	Off	On	Off
11.7	Off	On	On
11.9	On	Off	Off
12.1	On	Off	On
12.3	On	On	Off
Custom	On	On	On

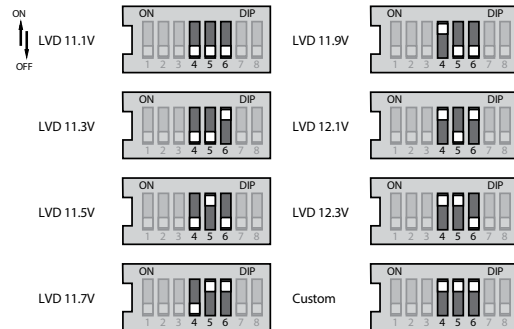


Figure A1-4 - Step 3 DIP Switch # 4,5,6

Select one of the 7 standard load control algorithms, or select the "custom" DIP switch for special custom settings using the PC software.

Refer to Section 5.1 for the 7 standard LVD settings, LVD_R reconnect settings, and current compensation values.

DIP Switches Number 4,5,6 - Lighting Control Algorithm:

For Lighting Control mode, set the DIP switches 4,5,& 6 according to the table below.

hrs after Sunset	hrs before Sunrise	Switch 4	Switch 5	Switch 6
6	0	Off	Off	Off
8	0	Off	Off	On
10	0	Off	On	Off
3	1	Off	On	On
4	2	On	Off	Off
6	2	On	Off	On
Dusk to Dawn		On	On	Off
Custom		On	On	On

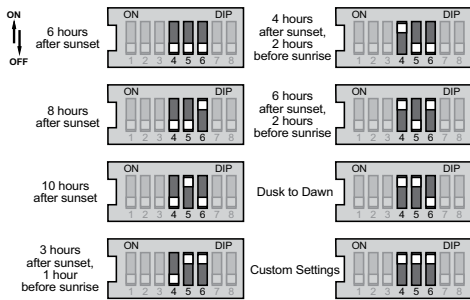


Figure A1-5 - Step 3 DIP Switch # 4,5,6

Select one of the 7 standard Lighting Control algorithms, or select the "custom" DIP switch for special custom settings using the PC software.

The default LVD and LVD reconnect settings for Lighting Control are listed below. These values can be changed in custom settings.

LVD	11.40 Volts
LVDR	13.00 Volts

DIP Switch Number 7 - Must be OFF:

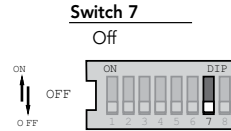


Figure A1-6 - Step 3 DIP Switch # 7

In Load Control and Lighting modes, DIP switch #7 must be in the OFF position.

DIP Switch Number 8 - Lighting Control:

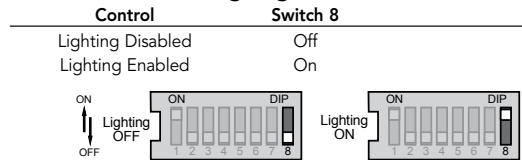


Figure A1-7 - Step 3 DIP Switch # 8

To enable lighting control, DIP switch #8 must be in the ON position.



NOTE: Confirm all dip-switch settings before going to the next installation steps.



REMARQUE : Confirmez les réglages de tous les commutateurs dip avant de passer aux étapes suivantes d'installation.

Appendix 2 - Diversion Charge Control DIP Switch Settings

The Diversion Charge Control DIP function adjustments:

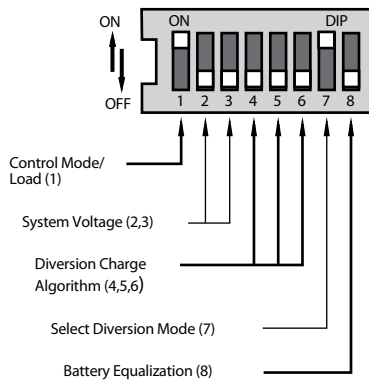


Figure A2-1 - Step 3 (Diversion) DIP Switch Functions

As shown in the diagram, all the positions are in the "OFF" position except switches 1 and 7, which are "ON".

NOTE: The DIP switches should be changed only when there is no power to the controller. Turn off disconnect switches and remove all power to the controller before changing a DIP switch. A fault will be indicated if a switch is changed with the controller powered.

REMARQUE : Les commutateurs DIP ne doivent être changés que si le contrôleur est hors tension. Mettez les interrupteurs sur arrêt et mettez le contrôleur hors tension avant de changer un commutateur DIP. Une panne sera indiquée en cas de changement d'un commutateur quand le contrôleur est sous tension.

CAUTION: The TriStar is shipped with all the switches in the "OFF" position. Each switch position must be confirmed during installation. A wrong setting could cause damage to the battery or other system components.

PRUDENCE : Le TriStar est expédié avec tous les interrupteurs en position « ARRÊT ». La position de chaque interrupteur doit être confirmée pendant l'installation. Un mauvais réglage peut endommager la charge ou d'autres composants du système.

The DIP switch settings described below are Diversion Charge Control only.

The DIP switches are shipped in the OFF position. With switches 1 and 7 in

the ON position, Diversion Charge Control is set. The OFF settings will operate as follows:

Switch	Function
1	Must be ON to set Diversion Control
2, 3	Auto voltage selected
4, 5, 6	Lowest battery charging voltage
7	Must be ON to set Diversion Control
8	Manual Equalization

To configure your TriStar for the diversion battery charging and control you require, follow the DIP switch adjustments described below. To change a switch from OFF to ON, slide the switch up toward the top of the controller. Make sure each switch is fully in the ON or OFF position.

DIP Switch Number 1 - Control Mode: Solar Battery Charging

Control Switch 1

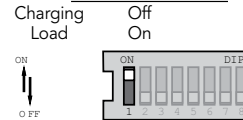


Figure A2-2 - Step 3 DIP Switch #1

For the Diversion Charge Control mode, move the DIP switch to the ON position as shown.

DIP Switches Number 2,3 - System Voltage:

Voltage	Switch 2	Switch 3
Auto	Off	Off
12	Off	On
24	On	Off
48	On	On

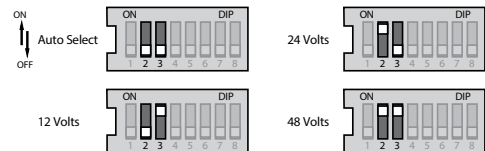


Figure A2-3 - Step 3 DIP Switches # 2,3

The auto voltage selection occurs when the battery is connected and the TriStar starts-up. There should be no loads on the battery that might cause a discharged battery to indicate a lower system voltage.

The DIP switch default voltages are for 12V, 24V or 48V lead-acid batteries. Although the "auto voltage" selection is very dependable, it is recommended to use the DIP switches to secure the correct system voltage.

DIP Switches Number 4,5,6 - Diversion Charge Control:

Battery Type	PWM	Switch 4	Switch 5	Switch 6
1	13.8	Off	Off	Off
2	14.0	Off	Off	On
3	14.2	Off	On	Off
4	14.4	Off	On	On
5	14.6	On	Off	Off
6	14.8	On	Off	On
7	15.0	On	On	Off
8	Custom	On	On	On

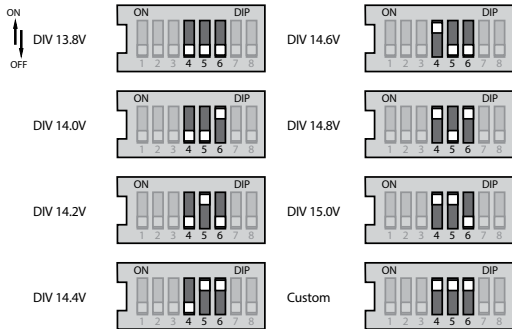


Figure A2-4 - Step 3 DIP Switches # 4,5,6

Select one of the 7 standard diversion charging algorithms, or select the "custom" DIP switch for special custom settings using the PC software.

Refer to Section 6.3 for information describing the 7 standard diversion charging algorithms. Refer to Section 9.0 of this manual for battery charging information.

DIP Switch Number 7 - Select Diversion:

Switch 7

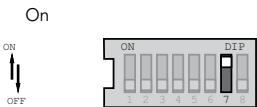


Figure A2-5 - Step 3 DIP Switch # 7

In the Diversion Charge Control mode, DIP switch 7 must be in the ON position.

DIP Switch Number 8 - Battery Equalization:

Equalize Switch 8

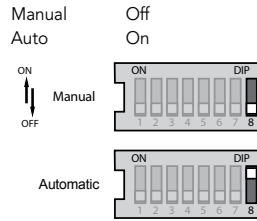


Figure A2-6 - Step 3 DIP Switch # 8

In the Auto Equalization mode (switch 8 On), battery equalization will automatically start and stop according to the battery program selected by the DIP switches 4,5,6 above. See Section 6.0 for detailed information about each standard diversion battery charging algorithm and equalization.

In the Manual Equalization mode (switch # Off), equalization will occur only when manually started with the push-button. Automatic starting of equalization is disabled. The equalization will automatically stop per the battery algorithm selection.

In both cases (auto and manual mode), the push-button can be used to start and stop battery equalization.

NOTE: Confirm all dip-switch settings before going to the next installation steps.

REMARQUE: Confirmez les réglages de tous les commutateurs dip avant de passer aux étapes suivantes d'installation.

Appendix 3 - LED Indications

LED Display Explanation:

- G = green LED is lit
- Y = yellow LED is lit
- R = red LED is lit
- G/Y = Green and Yellow are both lit at the same time
- G/Y - R = Green & Yellow both lit, then Red is lit alone
- Sequencing (faults) has the LED pattern repeating until the fault is cleared

1. General Transitions:

- Controller start-up G - Y - R (one cycle)
- Push-button equalize start G/Y/R - G/Y/R - G (one cycle)
- Push-button equalize stop G/Y/R - G/Y/R - R (one cycle)
- Battery service is required all 3 LEDs blinking until service is reset

2. Battery Status

- General state-of-charge see battery SOC indications below
- PWM absorption G blinking (1/2 second on / 1/2 second off)
- Equalization state G fast blink (2 to 3 times per second)
- Float state G slow blink (1 second on / 1 second off)

Battery State-of-Charge LED Indications (when battery is charging):

- G on 80% to 95% SOC
- G/Y on 60% to 80% SOC
- Y on 35% to 60% SOC
- Y/R on 0% to 35% SOC
- R on battery is discharging

3. Faults & Alarms

- Short circuit - solar/load R/G - Y sequencing
- Overload - solar/load R/Y - G sequencing
- Over-temperature R - Y sequencing
- High voltage disconnect R - G sequencing
- Reverse polarity - battery no LEDs are lighted
- Reverse polarity - solar No fault indication
- DIP switch fault R - Y - G sequencing
- Self-test faults R - Y - G sequencing
- Temperature probe (RTS) R/Y - G/Y sequencing
- Battery voltage sense R/Y - G/Y sequencing

LOAD CONTROL

2. Load Status

		12V	24V	48V
G	LVD+	0.60V	1.20V	2.40V
G/Y	LVD+	0.45V	0.90V	1.80V
Y	LVD+	0.30V	0.60V	1.20V
Y/R	LVD+	0.15V	0.30V	0.60V
R-Blinking	LVD			
R-LVD				

The load status LEDs are determined by the LVD voltage plus the specified transition voltages. As the battery voltage rises or falls, each voltage transition will cause a change in the LEDs.

**THIS PAGE IS
LEFT BLANK
INTENTIONALLY**

12.0 Certifications



- Complies with UL 1741 and CSA-C22.2 No. 107.1
 - FCC & CISPR Class B compliant
 - Installation shall comply with the US National Electrical Code
 - Installation shall comply with the Canadian Electrical Code
- ENs Directives:
Complies with EMI and LVD harmonized standards for CE marking
- Immunity: EN 61000-6-2:2001, EN 61000-4-3, EN 61000-4-6
 - Emissions: CISPR 22
 - Safety: IEC/EN60335-1, IEC/EN60335-2-29, IEC/EN 62109-1

TrisStar™, MeterBus™ are trademarks of Morningstar Corporation

MODBUS™ and MODBUS TCP/IP™ are trademarks of Modbus IDA.

© 2021 Morningstar Corporation. All rights reserved.

MS-001156 v4.6

12.0

D Power meter manual



Q.EED

QUALITY ELECTRONIC DESIGN

www.qeed.it

D.E.M. S.p.A.
WWW.DEM-IT.COM

POWER /ENERGY METER SINGLE PHASE AC/DC TRMS - RS485 MODBUS

QI-POWER-485



POWER SUPPLY 9...30 Vdc, protection against polarity reversal and overtemperature.

ABSORPTION < 1,3 W

MEASUREMENT Irms, Vrms, Watt, Var, Va, Vpk, Ipk, Frequency, Cosφ, Energy bidirectional, THD, min e MAX of each measure

TYPE OF MEASURE TRMS or DC

RANGE

Current: up to 50 A AC/DC

Voltage: up to 800 VAC or 1000 VDC

ACCURACY

Voltage, Current, Active Power: < 0,5% F.S.

Frequency: ± 0,1 Hz

Energy: ± 1% of reading

Vpeak, Ipeak: ± 5% F.S.

OUTPUT RS485 Modbus RTU

BAUDRATE From 1.200 a 115.200 baud

CREST FACTOR 1,8 (on current measurement)

WORKING FREQUENCY DC or 1...400 Hz

SAMPLING RATE 11k samples per second

INPUT IMPEDENCE 1 Mohm ± 1%

STANDARDS CE EN61000-6-4/2006 + A1 2011;

EN64000-6-2/2005; EN61010-1/2010

OVERVOLTAGE CATEGORY Cat III up to 600V;

Cat II up to 1000V

ISOLATION

3 kV on bare wire for Current measure.

4 kV for Voltage measure (reinforced insulation to power supply and serial output)

PROTECTION INDEX IP20

TEMPERATURE COEFFICIENT < 200 ppm/°C

WORKING TEMPERATURE -15...+65°C

STORAGE TEMPERATURE -40°C... +85°C

HUMIDITY 10...90% not condensing

ALTITUDE Up to 2000 m s.l.m.

DIMENSIONS 46,1 x 63 x 26,4 mm (terminal excluded)

TERMINALS Removable terminals 3,5 mm, n°1 of 4 poles, n°2 of 2 poles

WEIGHT 80 g

FILLING Epoxy resin

BOX MATERIAL PBT, grey

LED N°1 yellow, power on fixed, data communication blinking

DIP-SWITCH 2 poles

MOUNTING

Screw predisposition for vertical/horizontal mounting, DIN rail clips (included) for vertical/horizontal mounting.

LEGEND OF SYMBOL ONTO PAD PRINTING

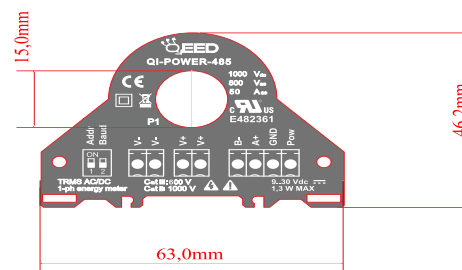
It indicates that all the accessible parts of the object, are separated from the live parts by double or reinforced insulation

High Voltage warning

General warning

Insertion of the cable

The **QI-POWER-485** is a Single-phase Power meter able to measure the **TRMS AC/DC Current and Voltage**. On the RS485 Modbus are available: **Irms, Vrms, Watt, Var, Va, Vpk, Ipk, Frequency, Cosφ, Energy bidirectional and THD**. The device is fully configurable by RS485, DIN rail mounting, 4kV galvanic isolation for Voltage input.



POWER /ENERGY METER SINGLE PHASE
AC/DC TRMS - RS485 MODBUS

STRENGTHS:

- TRMS Measure, THD available;
- 0,5 % Accuracy;
- RS485 Modbus integrated;
- Bidirectional energy metering;
- DIN rail mounting in both side;
- OEM'S design, low cost;
- Fully configurable by free interface software FACILE QI-POWER-485;
- Bootloader for updating firmware;
- Available measure register: MSW first LSW first or hundredts.



ENGLISH

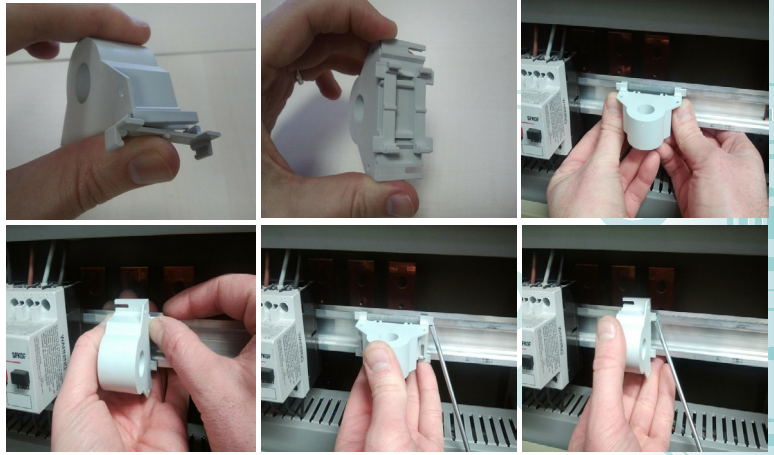
1 09 2022



INSTRUCTION MANUAL

QI-POWER-485

Using a serial link RS485 you can connect the QI-POWER-485 with the interface program FACILE QI-POWER-485. Using this software, allows you to set the Modbus address, baud rate, delay, the TV and TA ratio, to modify a filter in order to have fastest response time instead of a more stable measurement (filter range from 1-speed to 5-accuracy) and to measure frequency on current channel instead of voltage channel. You can download the FACILE QI-POWER-485 free of charge from our website www.qeed.it (section Products / Download Software).



A second way to programming the QI-POWER-485 is by using the **Modbus Register Map** directly. Download it from our website: www.qeed.it (section Download / Documents and Manuals / Network Analyzers / QI-POWER-485 or section Products / Network Analyzers / Single Phase Network Analyzers / QI-POWER-485).

MOUNTING:
the Power Meter QI-POWER-485 can be mounted (see photo below) horizontal or vertical mounting, horizontal or vertical through the two.

- REMARKS:**
- Modbus connections: A+ and B- as per Modbus RTU standards;
 - Modbus Register reference: with reference to the logical address, for ex. 40010, corresponds to physical address n°9 as per Modbus RTU standard;
 - Modbus functions supported: 3 (Read multiple registers, max 100), 6 (Write single), 16 (Write multiple);
 - **Any changes made by dip-switch required to switch off the power supply or sending reset command.**

Energy storage data on flash memory: 4,5 years minimum, 45 years typical.
Minimum Current measurement (cut off): 0 - 1024 mA.
Minimum Power measurement (cut off): 0 - 1024 W.
Measurement refresh: every 50 cycles or 1 second (the faster), programmable by FACILE.

If you want to set the device by FACILE QI-POWER-485 set the dips in 0. If you want to set by RS485 directly, set the first dip to 1 (up) then use the second dip for baudrate setting (0 for 9600 or 1 for 38400). After the settings, please save the configuration by the COMMAND register, then switch off the power supply, before to switch on the power supply set the DIPS in 0.

BAUDRATE SETTING	DIP 1	DIP 2
All setting from EEPROM	0	X
Set address 1 - 9600	1	0
Set address 1 - 38400	1	1

FACILE QI-POWER-485
The free interface program FACILE QI-POWER-485 is the fastest way to configure the device. There is only one configuration screen (see picture shown). The changes made to the program act on the register of the QI-POWER-485, if you want to restore the default configuration, just press the button FACTORY DEFAULT.

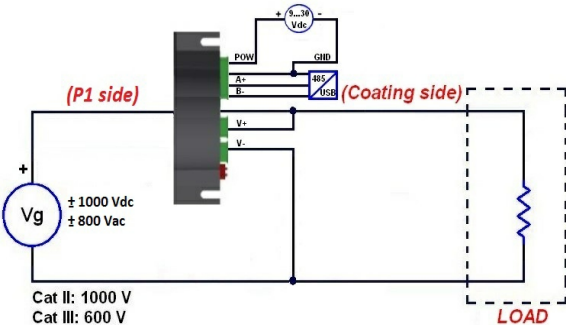
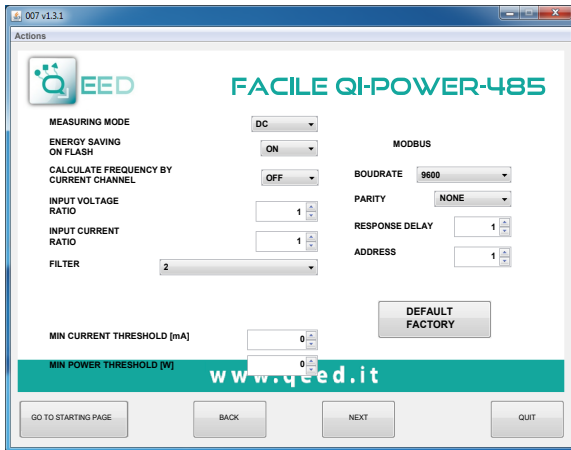
- TYPE OF MEASURE:** allows the selection of the measure RMS or DC only to define the sign, positive or negative, of reading.
- SAVE ON ENERGY FLASH:** it is possible to activate the saving of the counters directly on the device's flash memory.
- REPORT OF TRANSFORMATION:** in case you would use the CT and / or VT, you can define the transformation ratio for the current input and voltage input, the default ratio is 1:1.
- FILTER:** allows you to insert a filter on reading in order to get more speed in responding (value 1) or a more stable and accurate measurement (value 5), by default the value is set to 2. You can choose between intermediate values already set or manually enter the desired filter by choosing the CUSTOM option from the menu, in this case, you can set the following parameters: *filtering in DC, filtering in AC (default value 5), Frequency measurement on Current channel.*

CAUTION: magnetic fields of high intensity can vary the values measured by the transformer. Avoid installation near permanent magnets, electromagnets or iron masses that induce strong changes in the magnetic field. If any irregularity recommend reorient or move the transformer in the area most appropriate.

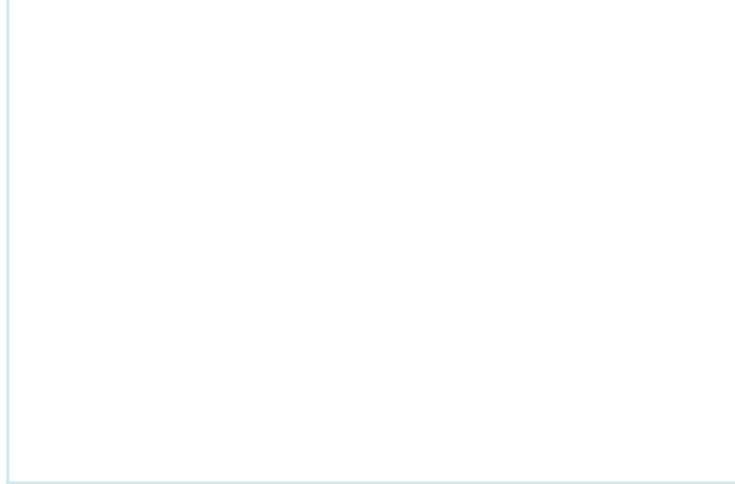
Disposal of Electrical & Electronic Equipment (Applicable throughout the European Union and other European countries with separate collection programs) This symbol, found on your product or on its packaging, indicates that this product should not be treated as household waste when you wish to dispose of it. Instead, it should be handed over to an applicable collection point for the recycling of electrical and electronic equipment. By ensuring this product is disposed of correctly, you will help prevent potential negative consequences to the environment and human health, which could otherwise be caused by inappropriate disposal of this product. The recycling of materials will help to conserve natural resources. For more detailed information about the recycling of this product, please contact your local city office, waste disposal service or the retail store where you purchased this product.

QI-POWER-485

INSTRUCTION MANUAL



! The protection offered by the device can be compromised in the case that it isn't used in accordance with the instructions.



 **NTNU**

Norwegian University of
Science and Technology